Energy and Water Conservation in Biodiesel Purification Processes

Michele Hastie

Thesis submitted to the
Faculty of Graduate and Postdoctoral Studies
In partial fulfillment of the requirements for the degree of

Master of Applied Science
in
Chemical Engineering

Department of Chemical and Biological Engineering
Faculty of Engineering
University of Ottawa

Abstract

Biodiesel purification processes generate wastewater streams that require a large amount of energy when distillation is used as a treatment technology. Process simulation software was used to show that an alternative water treatment process involving ion exchange would require only 31% of the energy used by distillation. Experiments showed that multiple washing stages were required to meet the standard specification for sodium, an impurity present in crude biodiesel, when washing biodiesel made from used frying oil. A comparison was made between washing biodiesel in a cross-current washing configuration and a counter-current configuration. Both configurations met the specification for sodium within three washing stages; however, the counter-current configuration required less water, making it the more efficient process. Lastly, the removal of sodium from wastewater samples using an ion exchange resin was experimentally investigated. The results validated the use of ion exchange to reduce energy consumption in biodiesel purification.

Résumé

Le procédé de purification du biodiésel génère des eaux usées qui nécessitent une grande quantité d'énergie lorsqu'elles sont traitées par distillation. Un logiciel de simulation a été utilisé pour démontrer qu'un processus alternatif de traitement d'eaux impliquant l'échange d'ions nécessiterait seulement 31% de l'énergie requise en utilisant la distillation. Des expériences ont montré que du lavage à plusieurs étapes est nécessaire pour atteindre les spécifications standard pour le sodium, une impureté présente dans le biodiésel brut, lors du lavage du biodiésel fabriqué à partir d'huile de friture usagée. Une comparaison a été faite entre le lavage du biodiésel dans une configuration à courant croisé et une configuration contre-courant. Les deux configurations conforment aux spécifications pour le sodium avec trois étapes de lavage, cependant la configuration à contre-courant nécessite moins d'eau, ce qui rend le processus plus efficace. Enfin, l'enlèvement du sodium à partir d'échantillons d'eaux usées en utilisant une résine d'échange d'ions a été étudiée expérimentalement. Les résultats ont validé l'utilisation de l'échange d'ions pour réduire la consommation d'énergie dans la purification du biodiésel.

Statement of Contributions of Collaborators

I hereby declare that I am the sole author of this thesis. I performed all the experiments, computer simulations, and data analysis. I have written all of the chapters contained in this thesis.

Dr. Marc. A. Dubé and Dr. André Y. Tremblay supervised this thesis project and provided continual guidance and support. They also made editorial comments and corrections to the written work presented.

Acknowledgements

I would like to thank my supervisors, Dr. Marc. A. Dubé and Dr. André Y. Tremblay, for giving me the opportunity to complete this project under their supervision. They gave me guidance and support throughout the completion of this thesis and I appreciate all that I have learned from them.

I would like to thank Dr. Nimal De Silva from the Department of Earth Sciences at the University of Ottawa for the analysis he kindly completed for me.

I would like to thank NSERC for financial support of this project.

I would like to acknowledge the staff of the Chemical Engineering Department: Franco Ziroldo, Gérard Nina, Louis Tremblay, Francine Pértrin, and Sylvie Saindon.

Last but not least, many thanks to all my friends and family for their continued support and encouragement.

Table of Contents

Chapter 3

Chapter 4

Chapter 5

Chapter 6

Chapter 7

Chapter 8

Appendix A

List of Tables

List of Figures

Chapter 1

Introduction

To meet the needs of a growing population, the world energy demand steadily increases with each passing year. In 2008, the world primary energy supply reached a value of 514 EJ (5.14 x 10^{20} J) (IEA, 2010 a). As seen in Figure 1.1 (a), the majority of this energy is provided by non-renewable sources including crude oil, coal, and natural gas. This dependence on non-renewable sources is even more evident when considering the energy used for transportation, shown in Figure 1.1 (b), where 94% is supplied by crude oil.

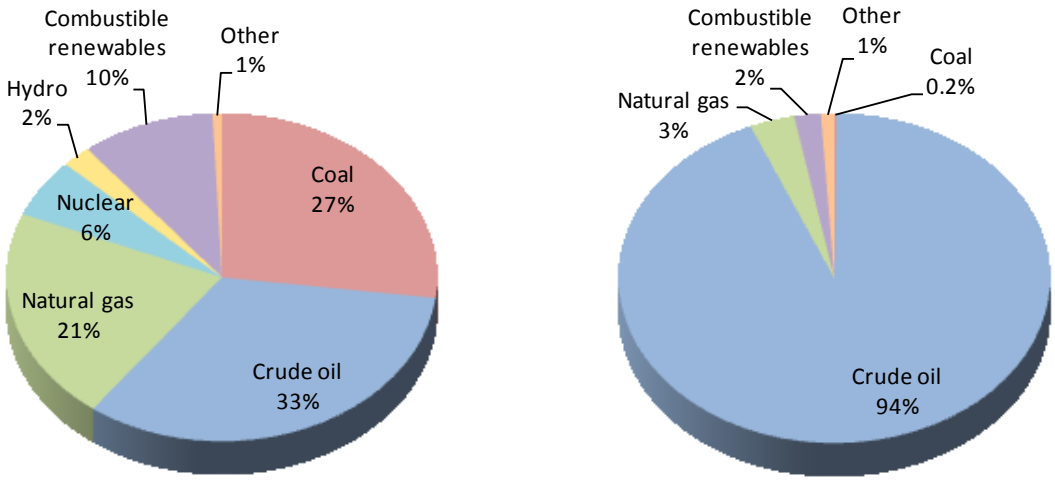

(a) World primary energy supply 514 EJ (2008)

(b) Consumption attributed to transportation 96 EJ (2008)

Figure 1.1 Break down by fuel of (a) the world primary energy supply and (b) consumption attributed to transportation in 2008 (IEA, 2010 a). Other includes geothermal, solar, and wind energy.

The combustion of non-renewable fossil fuels is known to increase the level of carbon dioxide (CO_2) in the atmosphere. Currently, the transportation sector accounts for about 25% of CO_2 emissions and roughly 50% of global oil consumption (IEA, 2010 b). The link between CO_2 emissions and climate change, along with the limited availability of petroleum resources has raised global concerns regarding energy sustainability and security. As a result, biofuels, which are renewable and produce far less net CO_2 emissions than fossil fuels, are receiving more interest for use as transportation fuels.

Biofuels are renewable energy sources produced from biomass. Liquid biofuels such as sugar- or starch-based ethanol and biodiesel made from vegetable oils, animal fats, or waste cooking oil, can replace or be blended with petroleum based fuels. These liquid fuels are especially convenient since they fit into the currently available fuel distribution infrastructure and because they can be used in typical internal combustion engines. Furthermore, due to their closed carbon cycle and renewability, the use of biofuels can reduce CO_2 emissions and contribute toward energy sustainability. As a result, the Government of Canada has made regulations requiring an average renewable fuel content of five per cent in gasoline, which came into effect in December 2010 (EC, 2010).

Biodiesel is produced by chemically converting the triglycerides present in vegetable oils or animal fats. This process forms fatty acid methyl esters (FAME) which have similar properties to petroleum diesel and are compatible with conventional diesel engines. Biodiesel has advantages over petroleum diesel including better lubricity, lower toxicity, improved flash point, biodegradability, negligible sulfur content, and lower overall exhaust emissions (Moser, 2009).

The main drawback of biodiesel is the high cost of production due to the high cost of the vegetable oil feedstock. As a result, commercial production is usually not profitable without government subsidies. The high raw material cost can be circumvented by using cheaper feedstocks such as used frying oils obtained from households or restaurants. Using waste oil also has the added benefit of reusing a waste material that would otherwise need to be disposed of by other means. Unfortunately, used frying oils contain high levels of free fatty acids (FFA), which complicate biodiesel production by adding processing steps and interfering with downstream purification.

Another issue facing biodiesel producers is the large amount of water required to purify crude biodiesel. Typically, per litre of biodiesel produced, between one and three litres of wastewater is produced. This large wastewater stream requires treatment prior to disposal or reuse in the process. The suggested method of water recovery is by distillation, which is an energy intensive process. Therefore, reducing the amount of water required for purification as well as using alternative water treatment methods will improve the energy efficiency of the process. This will increase the energy yield of biodiesel and thus improve the economic viability and sustainability of the fuel.

1.1 Objectives

In this thesis project, it was postulated that the energy efficiency of the biodiesel purification process could be improved by reducing the amount of water used for purification. As a starting point, the process was simulated to determine if the energy required for water treatment could be reduced if ion exchange is used in place of distillation. The simulation would also provide information on the impact that reducing the amount of water used would have on the energy demand of the processes.

To determine the viability of such a process, various experimental works were undertaken. Sodium, a component of the catalyst used to produce biodiesel, is a common impurity found in crude biodiesel that must be removed via water washing. Experiments were carried out to investigate the partitioning behaviour of sodium. Because there is currently a push to move toward the use of waste oil feedstocks, the water washing efficiencies for biodiesel made from refined vegetable (low FFA feedstock) and waste oil feedstocks (high FFA feedstock) were compared.

In multistage liquid-liquid extraction, counter-current contacting schemes are often used to conserve water and produce a more concentrated wastewater stream. Experiments were conducted to compare cross-current and counter-current washing to determine if the same removal efficiency for sodium can be achieved using the counter-current washing scheme. If it can achieve the same level of purification, it would be worthwhile to use the counter-current process since it would result in a more efficient use of water.

Finally, to validate the use of ion exchange for wastewater treatment, the ability of an ion exchange resin to remove salt impurities from the biodiesel wastewater must be tested. With a focus on the removal of sodium, the wastewater generated from previous experiments was treated with ion exchange resins. To determine if the presence of other components in the wastewater would affect the removal capacity of the resin, the removal efficiency was compared to that of prepared sodium chloride solutions.

1.2 Thesis Structure

In Chapter 2, an overview of biodiesel chemistry, production, and purification is presented. The chapter also contains a critical review of current purification techniques, with

a focus on water washing. A review of literature pertaining to treatment options for biodiesel wastewater is also presented.

The experimental methods and analytical techniques used to complete the thesis project are described in Chapter 3.

In Chapter 4, the purification of biodiesel by water washing was simulated using Aspen HYSYS simulation software. Simulations were performed to compare water treatment through distillation to an alternative method using ion exchange. The effect of the amount of water used in the water washing step was also investigated.

The experiments described in Chapter 5 studied the removal of sodium from FAME prepared from both canola oil and waste frying oil. The distribution of sodium between the FAME and water phases in a single water washing step were measured to determine the distribution coefficient. The effect of FFA on sodium removal was also determined.

Chapter 6 describes experiments that compared sodium removal by water washing in a cross-current contacting scheme to that of a counter-current configuration.

In Chapter 7, the wastewater samples obtained from the experiments in Chapter 5 were treated with an ion exchange resin. These results were used to validate the process proposed in Chapter 4 to reduce energy consumption in biodiesel purification.

Lastly, the major conclusions, recommendations, and future work are presented in Chapter 8.

1.3 References

EC, "Government of Canada Releases Final Regulations for Renewable Fuel Content in Gasoline," Environment Canada News Release, Available online: www.ec.gc.ca/default.asp?lang=En&n=714D9AAE-1&news=2D84D5D6-F152-4F5F-A4B9-BE973BE6821B (2010).

IEA, "Key World Energy Statistics," International Energy Agency, Paris, France (2010 a).

IEA, "Sustainable Production of Second-Generation Biofuels," International Energy Agency, Paris, France (2010 b).

Moser, B. R., "Biodiesel production, properties, and feedstocks," In. Vitro Cell. Dev.-Pl. 45, 229-266 (2009).

Chapter 2

Biodiesel Production and Purification

2.1 Introduction

The triglyceride molecule, used to produce biodiesel, is the main component of vegetable oils and animal fats. As shown in Figure 2.1, triglycerides are composed of three fatty acid groups bound to a glycerol molecule through an ester bond. Fatty acids vary in carbon chain length and in number of double bonds. For vegetable oils, the most common fatty acids include oleic (18:1[1]), linoleic (18:2), linolenic (18:3), stearic acid (18:0), and palmitic acid (16:0) (Srivastava and Prasad, 2000).

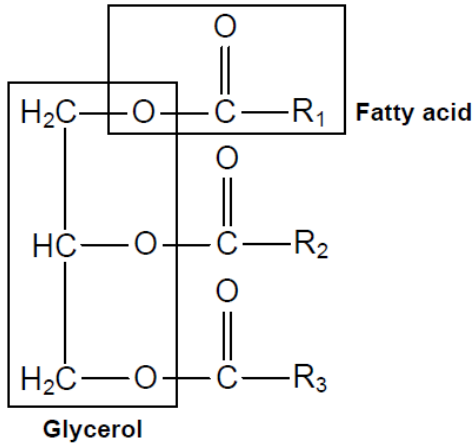

Figure 2.1 Triglyceride molecule.

Due to the large molecular mass and chemical structure of triglycerides, vegetable oils typically have viscosities ten to twenty times higher than that of petroleum diesel (Mittelbach and Remschmidt, 2004). Although the direct use of vegetable oils as fuels for diesel engines has been successfully demonstrated, their high viscosities interfere with the injection process and lead to poor fuel atomization and incomplete combustion (Srivastava and Prasad, 2000). Furthermore, vegetable oils have a high flash point and a tendency for thermal or oxidative polymerization, causing additional engine problems. Consequently, the

[1] First number indicates number of carbons in fatty acid chain; second number indicates number of double bonds

direct use of vegetable oils as a diesel fuel does not represent a commercially viable alternative.

Fortunately, the triglyceride molecule can be modified so that it approximates the properties and performance of petroleum diesel. Transesterification of triglycerides produces fatty acid alkyl esters (FAAE), which have similar properties to petroleum diesel. FAAE is the primary constituent of biodiesel and may be used directly in diesel engines.

In this chapter, the basic reaction chemistry required for producing biodiesel is reviewed along with an overview of the current commercial process for producing biodiesel. The challenges associated with using lower quality feedstocks such as waste frying oil are highlighted. Lastly, a review of current purification techniques, specifically focusing on water washing and treatment of the wastewater, is presented.

2.2 Biodiesel Reaction Chemistry

2.2.1 Transesterification

In the transesterification reaction shown in Figure 2.2, triglycerides are reacted with an alcohol to form three FAAE molecules and glycerol as a by-product. The alcohols most commonly used are methanol and ethanol, but methanol is preferred because it is cheaper and is more easily recovered in downstream operations (Haas et al., 2006). The products formed when using methanol are therefore referred to as fatty acid methyl esters or FAME.

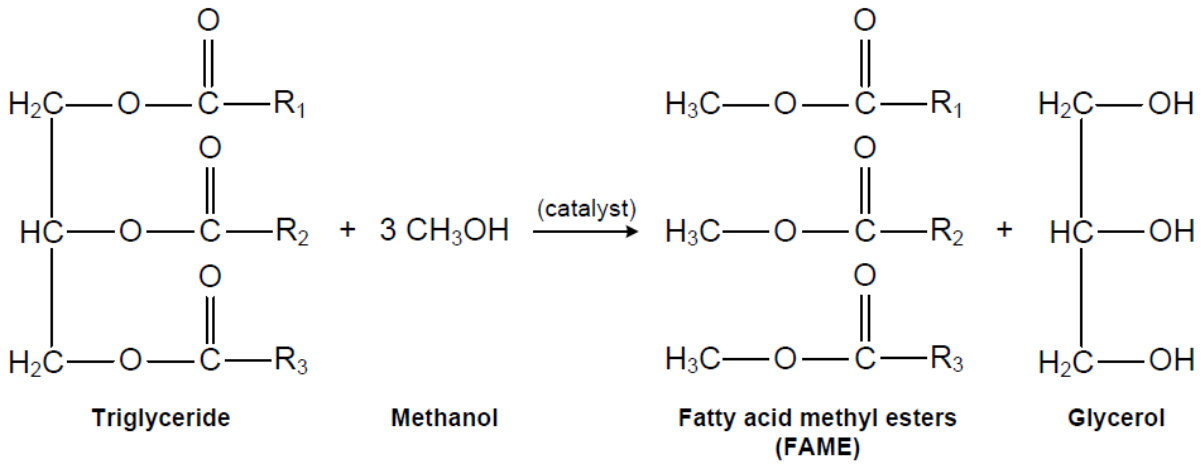

Figure 2.2 Transesterification of a triglyceride molecule with methanol to form fatty acid methyl esters (biodiesel) and glycerol.

Although it is possible for the reaction in Figure 2.2 to proceed without a catalyst, in such a case, very high temperatures (235°C) and pressures (62 bars) are required along with long reaction times (Mittelbach and Remschmidt, 2004). Therefore, to achieve satisfactory yields under mild reaction conditions, the use of a catalyst is required.

2.2.2 Feedstocks

The triglycerides required for the production of biodiesel can be obtained from vegetable oils or animal fats. Currently, more than 95% of biodiesel is prepared from conventionally grown edible oils such as rapeseed, soybean, sunflower, and palm oil (Balat, 2011). However, the cost of biodiesel is higher than that of diesel fuel, and production is usually not profitable without government support (Demirbas and Balat, 2006). The high production cost can be attributed to the high cost of refined vegetable oils. Furthermore, the large scale production of biodiesel from edible fuels raises ethical concerns. These include the competition for the same land and resources as the food industry and the deforestation of land to expand crops and increase production (Gui et al., 2008). As a result, there has been increasing pressure to move towards waste materials and non-edible sources of triglycerides.

One way in which biodiesel production can become more profitable is through the use of used frying oils (also referred to as waste cooking oils) obtained from households or restaurants. The use of these feedstocks not only represents a cost saving, but it provides a viable use for a waste product that would otherwise require treatment before disposal. The amount of available used frying oil is not sufficient to completely replace diesel fuel; however, a substantial amount of biodiesel can be prepared from used frying oil (Kulkarni and Dalai, 2006).

The disadvantage of using waste frying oils is that they contain a large amount of free fatty acids (FFA) which are formed by hydrolysis reactions during the frying process (Encinar et al., 2005). The presence of FFA has a negative effect on biodiesel production by causing an unwanted side reaction and complicating downstream processing. These problems are discussed in further detail below.

Oils can be classified by their FFA content. Refined vegetable oils will typically have very low concentrations of FFA. For example, the FFA content in refined canola oil ranges from 0.4 to 1.2 wt% (Przybylski, 2005). Used oil is classified as yellow grease if its FFA

content is below 15 wt%. Any oil with an even greater FFA concentration is classified as brown grease. The amount of FFA in the waste grease will depend on its previous use. Typically, used cooking oils will contain 2-7 wt% FFA and animal fats will have 5-30 wt% FFA. Some low quality feedstocks, such as trap grease, can have FFA contents that approach 100 wt% (Van Gerpen, 2005).

2.2.3 Catalysts

The catalyst systems currently available for producing biodiesel are summarized in Table 2.1, along with their respective advantages and disadvantages (Lam et al., 2010; Leung et al., 2010).

Table 2.1 Advantages and disadvantages of catalysts available for biodiesel production.

Catalyst	Examples	Advantages	Disadvantages
Homogeneous base	NaOH, KOH, $NaOCH_3$	Mild reaction conditions, high conversions, fast reaction rate	Sensitive to FFA and water content (soap formation), difficult catalyst separation
Homogeneous acid	H_2SO_4, HCl	Insensitive to FFA (no soap formation)	Slow reaction rate, high alcohol requirement and reaction temperature, sensitive to water content, difficult catalyst separation
Heterogeneous base	Zeolites, CaO	Mild reaction conditions, easy catalyst separation, reusable	Sensitive to FFA and water content (soap formation), catalyst leaching, high alcohol requirement, high reaction temperature and pressure
Heterogeneous acid	Ion exchange resins, ZrO_2	Insensitive to FFA (no soap formation), easy catalyst separation, reusable	Slow reaction rate, high alcohol requirement and high reaction temperature
Enzymes	Lipases	No by-product generation, mild reaction conditions, insensitive to FFA	High cost, slow reaction rate, enzyme deactivation
Non-catalytic	Supercritical methanol	Fast reaction rate, no catalyst separation required	High temperature and pressure required

Homogeneous base catalysts such as sodium hydroxide (NaOH) or sodium methoxide ($NaOCH_3$) are currently favoured due to their ability to catalyze the reaction at mild reaction conditions with a high conversion in minimal time. The main disadvantage of base catalysts is the undesired side reaction that produces soap. If water is present in the reaction system, the catalyst will react with the triglyceride to form soap as seen in Figure 2.3. This reaction is referred to as saponification.

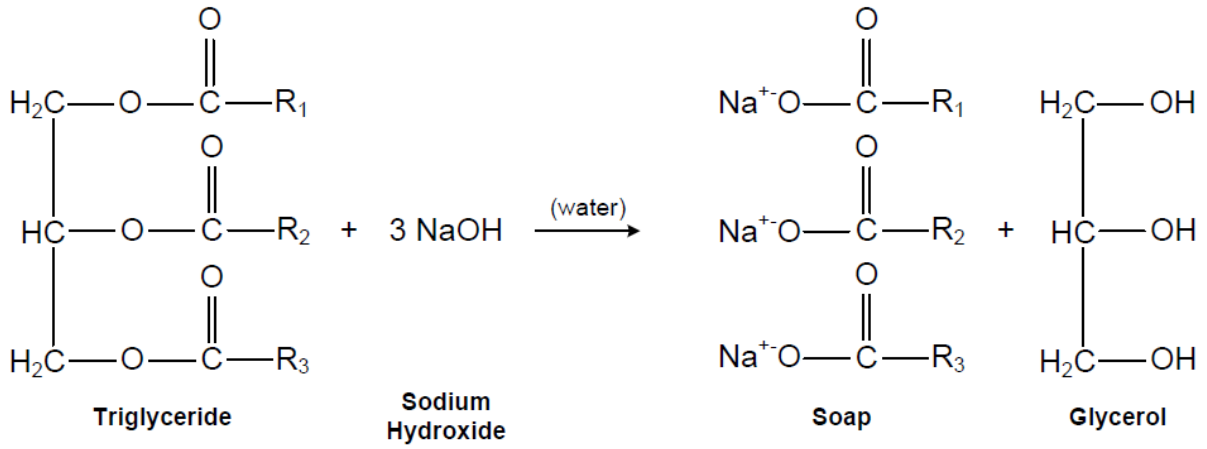

Figure 2.3 Saponification reaction of triglycerides to form soap.

The base catalysts can also form soap by reacting with FFA, as shown in Figure 2.4. This side reaction is undesired because it consumes the catalyst and reduces overall conversion. Furthermore, soap is an emulsifier and its presence complicates downstream purification. As a result, base catalysts are only recommended when using feedstocks with FFA contents between 0.5 to 2 wt% (Lam et al., 2010).

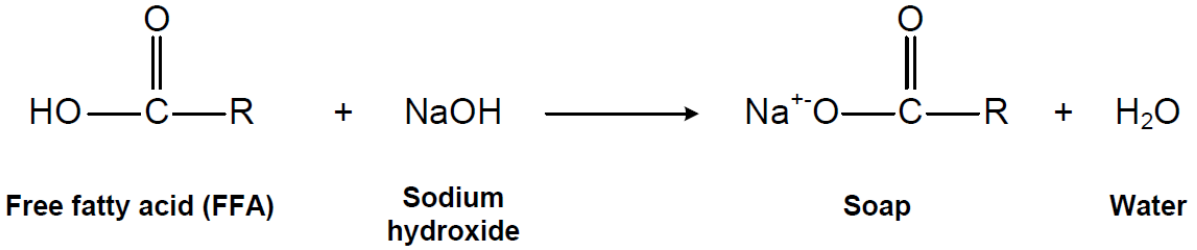

Figure 2.4 Reaction of FFA with base catalyst to form soap.

Homogeneous acid catalysts such as sulphuric acid (H_2SO_4) have the advantage that they can simultaneously catalyze the transesterification reaction (Figure 2.2) and convert FFA to FAME by the esterification reaction shown in Figure 2.5.

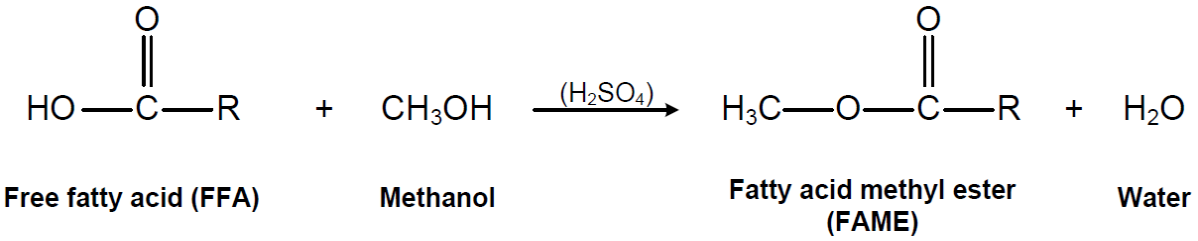

Figure 2.5 Acid esterification of FFA to form FAME.

The disadvantages of using acid catalysts include slower reaction rates and the requirement of a high reaction temperature and a high amount of excess alcohol (Lam et al., 2010). These factors generally make the use of acid catalysts commercially unfavourable.

To combine the advantages of both the base and acid catalyzed processes, a two-step reaction process was suggested by Canakci and Van Gerpen (2001). The high FFA feedstock is first treated with an acid catalyst to convert FFA to FAME by esterification as shown in Figure 2.5. Once the FFA level is reduced below 1 wt%, the transesterification reaction is completed using a base catalyst.

2.3 Reaction Products and Impurities

The mixture of reaction products contains various components, the concentrations of which must meet strict specifications for the product to be classified as biodiesel by ASTM International[2]. The main components of the reaction products mixture are FAME, glycerol, and unreacted methanol. Since FAME and glycerol are only slightly soluble in each other, these three components form two immiscible liquid phases: one rich in FAME and one rich in glycerol. The methanol, which is miscible with both FAME and glycerol, will partition between the two phases.

[2] Formerly known as the American Society for Testing and Materials

The mixture will also contain residual catalyst in the form of salts and soap, as well as water. These polar contaminants tend to partition in the glycerol-rich phase. However, a non-negligible amount will remain in the FAME-rich phase.

If the reaction does not proceed to completion, the mixture will also contain unreacted mono-, di-, and triglycerides. Similarly, FFA not converted by the acid esterification reaction will also be present.

Table 2.2 provides a summary of the negative effects of these components on the properties of the biodiesel and engine performance, along with the limits required by ASTM International (ASTM D6751, 2009).

Table 2.2 Effect of impurities in biodiesel and ASTM concentration limits.

Contaminant	Effect on biodiesel/engine performance	ASTM D6751 limit
Glycerol	Causes injector deposits, clogs fuelling systems, builds up at the bottom of storage and fuelling systems	0.020 % mass
Methanol	Lowers flash point	0.2 % mass
Sodium and potassium (combined)	Contributes to injector, fuel pump, piston and ring wear, creates engine deposits, filter plugging	5 ppm (μg/g)
Calcium and magnesium (combined)	Contributes to injector, fuel pump, piston and ring wear, creates engine deposits, filter plugging	5 ppm (μg/g)
Free fatty acids (FFA)	Increases fuelling system deposits, corrosion	0.50 mg KOH/g (acid value)
Water	Hydrolysis (FFA formation), promotes corrosion, microbiological growth	0.050 % volume
Mono-, di-, and triglycerides	Causes injector deposits, adversely affects cold weather operation, plugs filters	0.240 % mass (includes free glycerol)

The average levels of impurities in the crude, unwashed biodiesel from various authors are presented in Table 2.3 (Berrios and Skelton, 2008; Wang et al., 2009; Gonzalo et al., 2010). It is clear that biodiesel of this grade would not meet the standards required by ASTM and further purification would be required. Although the amount of soap is not

explicitly limited by the ASTM standard, the soap molecule contains both sodium and FFA, and therefore must be within the limits for these two impurities.

Table 2.3 Average level of impurities in crude biodiesel prior to purification.

Impurity	Value	Units
Glycerol	0.13	% mass
Methanol	2.8	% mass
Sodium	227	ppm
Soap	1075	ppm
Water	0.089	% volume
Glycerides	2.4	wt%

2.4 Biodiesel Production Processes

2.4.1 Low FFA Oil Feedstock

A general process for producing biodiesel from refined oil is presented in Figure 2.6. This process is based on the model proposed by Haas et al. (2006). The oil is fed to the reactor along with the methanol and catalyst (sodium methoxide) solution. Methanol is usually present in excess at a molar ratio of 6 to 1 with respect to oil. Catalyst concentration will usually be between 0.5 and 1% by weight of the oil, and the reaction takes place at a temperature of approximately 60°C and close to atmospheric pressure (Meher et al., 2006; Leung et al., 2010).

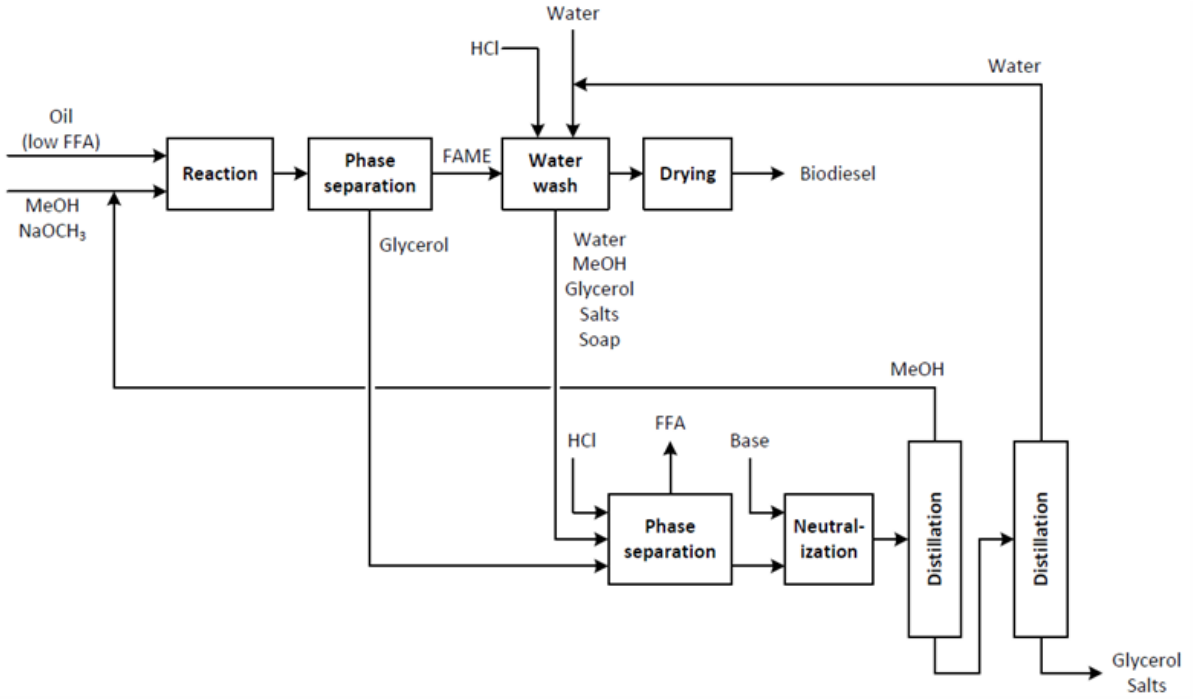

Figure 2.6 Biodiesel production process for low FFA feedstocks.

The reaction products form two immiscible liquid phases that can be separated by centrifugation or gravity settling. The FAME-rich phase is then washed with slightly acidic water with a pH of about 4.5 (Haas et al., 2006). A final drying step removes water to produce ASTM grade biodiesel.

The glycerol-rich phase is combined with the wastewater which is composed of water, methanol, glycerol, salts, and soap. Acid is added to the mixture to convert soaps to FFA, which are not soluble in water and can be removed by centrifugation or settling. The acid is then neutralized with base followed by distillation to recover methanol for recycle to the reactor. Water is recovered by distillation and recycled back to the water washing operation. The crude glycerol stream produced is either further refined or sold to industrial glycerol refiners (Haas et al., 2006).

2.4.2 High FFA Oil Feedstock

The process in Figure 2.6 can only be used for oil feedstocks with a low FFA content, up to about 2 wt%, otherwise significant soap production and its associated challenges will

result. For waste oils such as used frying oil, an acid esterification pre-treatment step, such as the one shown in Figure 2.7, is required to convert FFA to FAME.

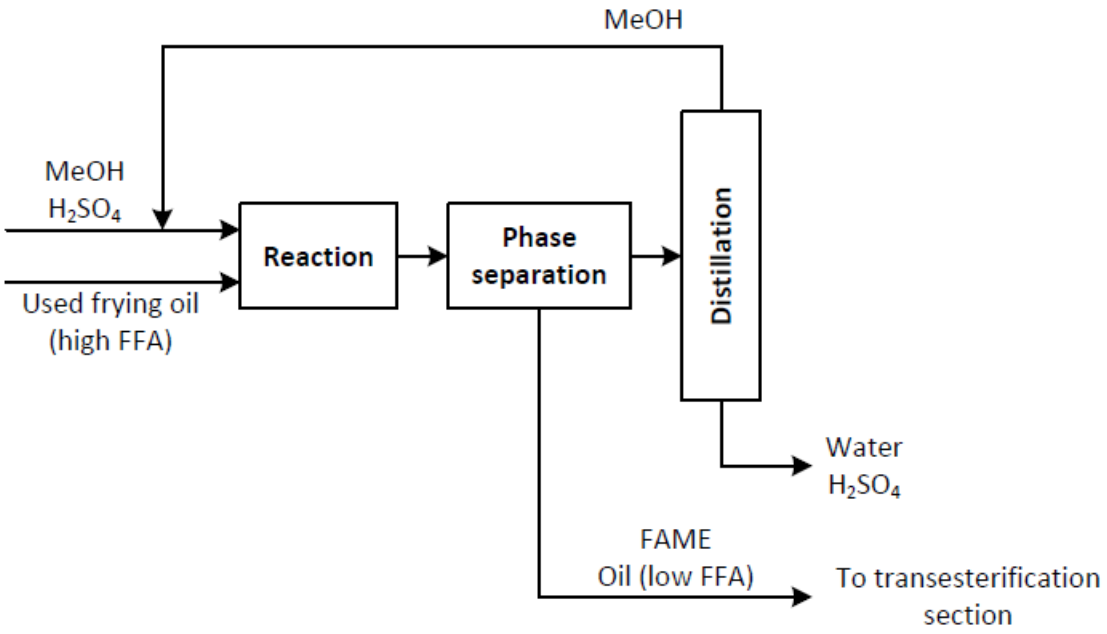

Figure 2.7 Acid esterification pre-treatment for high FFA feedstocks.

In the pre-treatment process, the high FFA used frying oil is fed to the reactor with methanol and sulphuric acid. Typical reaction conditions include a molar ratio of methanol to FFA of 40 to 1, a sulphuric acid concentration of 5% by weight of FFA, and a temperature of 60°C (Canakci and Van Gerpen, 2003). The reaction proceeds until the FFA content of the oil has been reduced below about 1 wt%. Since oil and methanol are immiscible, the reaction mixture forms two liquid phases: one rich in methanol and the other rich in oil. The methanol in the methanol-rich phase can be recovered by distillation and recycled back to the reactor (West et al., 2008). The oil-rich phase now has an FFA content that is low enough that it can be converted into biodiesel using the base catalyzed method. The subsequent process units are therefore identical to those in Figure 2.6.

2.5 Biodiesel Purification Processes

2.5.1 Water Washing

The most common method of purifying the reaction products is to use water washing. Water is an ideal solvent for this purpose since most of the contaminants are polar and therefore have a high solubility in water. Water washing can effectively reduce the amounts of methanol, glycerol, salts, and soap in the crude FAME mixture. A summary of various studies on water washing of crude biodiesel is shown in Table 2.4.

Gonzalo et al. (2010) investigated the water washing step by studying the effect of water amount and washing temperature on biodiesel made from both rapeseed oil and used frying oil. These oils had acid values of 1.1 and 1.3 mg KOH/g, respectively, which correspond to initial FFA concentrations of 0.55 and 0.65 wt%. Using the two-step reaction process of acid esterification and base catalyzed transesterification, the FFA content in the crude FAME product was 0.076 and 0.055 wt%, respectively. They found that the viscosity of the biodiesel increased after water washing, indicating that methanol, which has a lower viscosity than biodiesel, was removed in the washing step. For both biodiesels, the polar compounds (methanol, sodium, and glycerol) were almost completely removed by a single water washing step in the conditions tested and all three impurities were within ASTM specifications. The washing step also resulted in an increase in acidity, which was attributed to the removal of sodium. Prior to washing, the sodium may have neutralized part of the acid present after the reaction, and its removal resulted in an increase in acidity. The concentration of glycerides (mono-, di-, and triglycerides) was not changed significantly.

Significant removal of methanol, sodium, and glycerol was achieved at even the mildest conditions tested using minimum water (30 wt% of biodiesel) and temperature (30°C). This suggests the possibility of using even less water or a lower contacting temperature to achieve the same results.

Despite using a biodiesel made from waste oil, the presence of soap was not detected. This is most likely because the FFA content in the feedstock oil was low. Their work shows that one washing step is sufficient for washing biodiesels with low FFA concentrations, but does not give any information about washing biodiesels with higher FFA contents.

Table 2.4 Summary of studies on water washing of biodiesel.

Author(s)	Oil feedstock	FFA content (wt%)		Washing conditions		
		Oil	FAME	Water to biodiesel volume ratio	Number of washes	Temperature (°C)
Gonzalo et al. (2010)	Rapeseed oil	0.55	0.076	1:3.8 1:1.9 1:1.3	1	40, 50, 60
	Used frying oil	0.65	0.055			
Berrios and Skelton (2008)	Refined cooking oil	np	0.091	1:2 1:1.3 1:1	1	ambient, 60
	Used cooking oil	np	0.12			
Karaosmanoğlu et al. (1996)	Rapeseed oil	0.16	np	1:1	5	50, 65, 80
He et al. (2006)	Soybean oil	np	np	1:1	3	20, 50, 80
Predojević (2008)	Waste sunflower oil	0.936 1.30 1.67	np	1:4.5	up to 10	50
Sabudak and Yildiz (2010)	Waste frying oil	2 4.6	<1	1:1	1	50-60
Rahayu and Mindaryani (2007)	Castor oil	0.1686	np	1:2 1:1 2:1 3:1	1	ambient, 35, 45, 55
Banerjee et al. (2009)	Jatropha oil	np	np	1:5	3	ambient

np: not provided

Berrios and Skelton (2008) compared water washing to purification using ion exchange resins and magnesium silicate. The two biodiesel feedstocks used were made from refined cooking oil and used cooking oil, with acid values of 0.18 and 0.24 mg KOH/g, respectively. Water washing was performed using three water sources: deionised water, town's water, and acidified water (5% phosphoric acid). Two temperatures (ambient and 60°C) were used and three water/oil ratios and two agitator speeds were investigated. Water

washing was the only process that reduced both methanol and free glycerol levels down to those required by the standard. It did not have any effect on glycerides.

The standard was met with a water to biodiesel ratio of 1:2, which was the minimum amount of water tested. They saw no advantage to using deionized or acidified water over town's water. The recommended operating conditions were ambient temperature, town's water, and a water to biodiesel volume ratio of 1:2. There were no measurable differences in treatment efficiencies between the two feedstocks.

Karaosmanoğlu et al. (1996) compared washing with hot distilled water, dissolving the mixture in petroleum ether and then washing it with distilled water, and neutralizing the mixture with sulphuric acid. Of the three temperatures tested, the greatest yield was obtained at the lowest temperature of 50°C. When considering refining yields, water content, and acid values, the recommended method was washing with distilled water at 50°C. The biodiesel was washed in a 1:1 volume ratio of water to biodiesel five times, which represents a relatively high level of wastewater production compared to other studies.

He et al. (2006) compared washing with distilled water, washing with acid (HCl, pH of 1), dissolving and extracting in a solvent, and washing with distilled water with the use of membrane extraction. The properties of the washed biodiesel were similar when washed with distilled water at the three temperatures tested of 20, 50, and 80°C. The highest yield was obtained at 50°C. At 20°C, serious emulsification was encountered and at 80°C, more esters dissolved in the water, resulting in a higher ester loss than at 50°C.

Washing with acid reduced the formation of emulsions and loss of ester than when washing with distilled water. However, the acid value of the biodiesel was slightly higher due to the addition of acid. Agitation greatly affected the process. If the speed was too low, contact between the two phases was insufficient and if the speed was too high, serious emulsification occurred. When using solvent extraction, serious emulsification occurred at the interface and the solvent had to be evaporated out after refining. Both of these factors increased the loss of methyl esters. Although the acid value of the oil feedstock was not given in their study, it was most likely higher than that of the other studies since it is the only study to report the occurrence of serious emulsification.

Predojevic (2008) compared three different methods for the purification of biodiesel made from used frying oils. These methods were washing the mixture with 5% phosphoric

acid and hot distilled water, and contacting with silica gel. The silica gel and phosphoric acid treatments gave the highest yields, while the hot water treatment gave the lowest. This was attributed to the need for excessive washing with water in multiple steps (up to 10) until neutral pH was reached, leading to increased product losses. Using acidified water required up to 7 washes.

Sabudak and Yildiz (2010) compared washing with distilled water, dry wash with magnesium silicate, and using ion-exchange resin to purify biodiesel made from waste frying oils. Washing with water resulted in the lowest yield. Based on this conclusion, the recommended purification method was determined to be ion-exchange. However, a discussion of contaminant removal efficiency was not provided.

Rahayu and Mindaryani (2007) investigated glycerol removal by water washing. Glycerol extraction increases with amount of water used and washing temperature, however glycerol concentration in the biodiesel did not reach standard specifications even at the highest water to biodiesel volume ratio. To achieve the standard requirement, they recommended that the washing should be done in a multistage process.

Banjeree et al. (2009) studied the effect of washing time on the purification of biodiesel made from Jatropha oil. They found that three successive washing steps with distilled water at a water to biodiesel volume ratio of 1:5 at room temperature was sufficient for removing the catalyst from the FAME.

2.5.2 Membrane Technology

He et al. (2006) tested two types of hollow fiber membranes for use in a membrane extraction setup. The membrane materials tested were polysulfone (hydrophilic) and polyacrylonitrile (hydrophobic). The membranes were immersed in a beaker filled with distilled water and the crude biodiesel was pumped into the hollow fiber membrane.

In comparison to the conventional water washing conditions tested, membrane extraction avoided the emulsification problems encountered, thereby decreasing the refining loss. They concluded that polysulfone was the more suitable membrane material, since the polyacrylonitrile membrane resulted in refined biodiesel with a high water content. The purity of the biodiesel refined by polysulfone membrane extraction was the highest (99%)

among all the refining methods tested. The results showed that membranes can be used for water washing in situations that result in a high degree of emulsification.

Wang et al. (2009) compared the use of a ceramic membrane to the traditional water washing step. The membrane effectively separated FAME as permeate from the crude reaction mixture. This was due to the presence of soap existing in a reversed micelle form which bonded to free glycerol, thereby increasing its size so that it did not permeate with the FAME. However, some of the FAME still remained in the retentate, which would require further treatment by water washing to improve the overall yield.

Saleh et al. (2010) studied the use of a hydrophilic polyacrylonitrile membrane for the removal of glycerol from biodiesel. By adding only small quantities of water (0.06 to 0.2 wt%), large particles of a glycerol and water dispersed phase were formed, which were rejected by the membrane. The amount of water required for the process was found to be only 2 g of water per L of treated FAME. In comparison to a typical water washing operation, this represents a significant reduction in wastewater production. Although the results demonstrate the large effect water has on glycerol removal, the presence of methanol and soap were found to negatively impact separation. This suggests that the use of membranes for glycerol removal may not be suitable for the purification of FAME with high levels of contaminants.

2.5.3 Ion Exchange

Berrios and Skelton (2008) tested ion exchange resins from Rohm & Haas (BD10 Dry) and Purolite (PD206). The resins had little effect on methanol removal and no effect on glyceride removal. They did observe a reduction in soap content and concluded that this may indicate a limitation for high soap containing feeds.

Sabudak and Yildiz (2010) purified crude biodiesel using an ion exchange resin from Purolite (PD206). In comparison to water washing and adsorption with magnesium silicate, they concluded that ion exchange was the best purification option because it resulted in the highest yield of biodiesel. The amount of biodiesel purified was only 1.5 times the amount of resin used. Therefore, it is unclear if this method would be efficient on an industrial scale.

2.5.4 Adsorption

Berrios and Skelton (2008) tested the use of magnesium silicate (Magnesol) and observed no significant effect on glyceride (mono-, di-, and triglyceride) removal. There was only a small amount of methanol removal. Reduction in soap value was less than that achieved by the ion exchange resin.

Mazzieri et al. (2008) studied the removal of glycerol from crude biodiesel by adsorption on silica gel. They found that glycerol has a great affinity for silica gel and that it was selectively adsorbed from the biodiesel solutions. They concluded that soaps do not interfere with adsorption. However, adsorption was only tested up to a soap content of 270 ppm. Methanol and monoglycerides produced a decrease of the saturation capacity of the adsorbent. It is therefore unclear if silica gel would be effective when purifying biodiesel with high levels of soap, methanol, and monoglycerides.

2.6 Wastewater

Following the discussion presented in the previous sections, it is clear that presently only water washing has been demonstrated to achieve high purity biodiesel economically. When using water washing as a means of purification, biodiesel production will produce a large wastewater stream. The amount of wastewater produced varies by source, as seen in Table 2.5, ranging from about 0.2 to 4 litres of wastewater for every litre of biodiesel produced. This is most likely due to variability between individual processes and is likely dependent on such process factors as the quality of feedstock, reaction conditions, and method of water contacting. Nonetheless, it is clear that the process produces a relatively large wastewater stream.

Table 2.5 Wastewater generated from biodiesel production by source.

Source	Wastewater generated (L water/L biodiesel)
Chavalparit and Ongwandee (2009)	0.2-1.2
Van Gerpen et al. (2004)	1
Canakci and Van Gerpen (2003)	3
Liu et al. (2009)	3-4

The wastewater will typically contain contaminants including methanol, glycerol, soap, FFA, dissolved and suspended solids, and residual FAME (Boornazian and Smith, 2008). The properties of the wastewater produced from various references are shown in Table 2.6. Chavalparit and Ongwandee (2009) also reported glycerol and methanol concentrations of 1360 and 10,667 mg/L, respectively.

Table 2.6 Properties of biodiesel wastewater by source.

Source	pH	COD (mg/L)	BOD (mg/L)	O&G (mg/L)	Conductivity (µS/cm)
Chavalparit and Ongwandee (2009)	8.9	30,980	np	6020	350
Berrios and Skelton (2008)	6.7	18,362	np	np	1119
Jaruwat et al. (2010)	9.3-10.8	312,000	168,000	18,000	np
Banerjee et al. (2009)	9	684-792	np	1433-1640	np

COD: chemical oxygen demand; BOD: biochemical oxygen demand; O&G: oil and grease
np: not provided

The wastewater is basic with high amounts of oil and grease and low amounts of nitrogen and phosphorus making biological treatment difficult (Chavalparit and Ongwandee, 2009). The water will typically require pre-treatment prior to discharge to a water treatment facility. Some of the treatment methods that have been studied include biological (Suehara et al., 2005), electrocoagulation (Chavalparit and Ongwandee, 2009), electrochemical oxidation (Jaruwat et al., 2010), and adsorption of glycerol (Liu et al., 2009).

The efficient recovery and recycle of this wastewater is an important factor that could help improve the overall environmental impact and economics of biodiesel production. Typical methods of wastewater treatment include distillation, as seen in the process presented in Figure 2.6, or membrane separation (Maliszewski et al., 2008). Distillation is known to be an energy intensive operation, and the energy requirements to recover the water and its impact on the biodiesel process have not been yet been studied.

2.7 Summary

There have been numerous studies that show the effectiveness of using water washing to purify crude biodiesel. In some studies, only one wash was sufficient whereas others

required multiple consecutive washes, up to 10 washes. This indicates that the number of washes required is dependent on the feedstock and may vary from one process to the next.

Gonzalo et al. (2010) and Berrios and Skelton (2008) both concluded that the minimum amount of water they tested was sufficient to achieve effective removal of contaminants. For Gonzalo et al. (2010), this was a water to biodiesel volume ratio of 1 to 3.8, indicating that the amount of water could be further reduced to minimize wastewater generation.

Temperature appears to have opposing effects on purification. Contaminant removal tends to increase with increasing temperature however, product loss also increases. It may therefore be beneficial to use mild temperature conditions since effective contaminant removal can still be achieved while minimizing product loss and process energy requirements.

With respect to initial FFA content, the studies reviewed also only dealt with either refined vegetable oils or used frying oils with a relatively low FFA content. The FFA level of the pre-treated FAME was also very low, always below 1 wt%.

Furthermore, the removal of other contaminants such as methanol and glycerol by water washing has been studied more extensively than the removal of sodium. Gonzalo et al. (2010) concluded that sodium could be easily removed in one washing step. However, the FFA levels in their FAME samples were quite low (0.055 and 0.076 wt%). Sodium is known to interact with FFA to form soap by the saponification reaction. Therefore, its presence may have an effect on the removal efficiency of sodium by water washing.

In these studies, the FAME samples were washed repeatedly with water in consecutive washes ranging up to 10 stages. This represents a cross-current configuration. On an industrial scale, water washing can be performed in a counter-current process to reduce the amount of waste generated and result in a more concentrated waste stream. However, results on such a process have not yet been presented in the literature.

Other purification methods have also been successfully used for biodiesel purification. The advantages of these methods are that they do not produce wastewater and that they have reduced refining losses. However, they have their own disadvantages including interactions with other contaminants or the inability to remove all of the contaminants as effectively as water washing.

The disadvantage of water washing as a means of purification is that it produces a large wastewater stream ranging from 0.2 to 4 litres per litre of biodiesel. This wastewater is generally difficult to treat by conventional methods and may require pre-treatment prior to discharge to a water treatment facility. The water is most commonly recovered by distillation, which is energy intensive and reduces the energy efficiency of biodiesel production. A study on the energy used in recovery of wastewater by distillation is not yet available, and it could prove advantageous to use alternative water treatment methods. For example, the use of ion exchange could help reduce salt levels in the wastewater, making it suitable for recycle back to the process. Its use could also potentially reduce the amount of energy used to treat the wastewater, and result in a more energy efficient process.

2.8 References

ASTM Standard D6751, "Standard specification for biodiesel fuel blend stock (B100) for middle distillate fuels," ASTM International, West Conshohocken, PA (2009).

Balat, M., "Potential alternatives to edible oils for biodiesel production – A review of current work," Energ. Convers. Manage. 52, 1479-1492 (2011).

Banerjee, T., T. K. Bhattacharya, and R. K. Gupta, "Process optimization of catalyst removal and characterization of waste water after alkali-catalyzed transesterification of Jatropha oil," Int. J. Green Energy, 6, 392-400 (2009).

Berrios, M. and R. L. Skelton, "Comparison of purification methods for biodiesel," Chem. Eng. J. 144, 459-465 (2008).

Boornazian, L. Y. and M. T. Smith, "Applicability of Effluent Guidelines and Categorical Pretreatment Standards to Biodiesel Manufacturing," United States Environmental Protection Agency, Office of Water Management, Washington, D.C. (2008).

Canakci, M. and J. Van Gerpen, "Biodiesel production from oils and fats with high free fatty acids," Trans. Am. Soc. Agric. Eng. 44 (6), 1429-1436 (2001).

Canakci, M. and J. Van Gerpen, "A pilot plant to produce biodiesel from high free fatty acid feedstocks," Trans. Am. Soc. Agric. Eng. 46 (4), 945-954 (2003).

Chavalparit, O. and M. Ongwandee, "Optimizing electrocoagulation process for the treatment of biodiesel wastewater using response surface methodology," J. Environ. Sci. 21, 1491-1496 (2009).

Demirbas, M. F. and M. Balat, "Recent advances on the production and utilization trends of bio-fuels: A global perspective," Energ. Convers. Manage. 47, 2371-2381 (2006).

Encinar, J. M., J. F. González, and A. Rodríguez-Reinares, "Biodiesel from used frying oil. Variables affecting the yields and characteristics of the biodiesel," Ind. Eng. Chem. Res. 44 (15), 5491-5499 (2005).

Gonzalo, A., M. García, J. L. Sánchez, J. Arauzo, and J. A. Peña, "Water cleaning of biodiesel. Effect of catalyst concentration, water amount, and washing temperature on biodiesel obtained from rapeseed oil and used oil," Ind. Eng. Chem. Res. 49, 4436-4443 (2010).

Gui, M. M., K. T. Lee, and S. Bhatia, "Feasibility of edible oil vs. non-edible oil vs. waste edible oil as biodiesel feedstock," Energy 33, 1646-1653 (2008).

Haas, M. J., A. J. McAloon, W. C. Yee, and T. A. Foglia, "A process model to estimate biodiesel production costs," Bioresource Technol. 97, 671-678 (2006).

He, H. Y., X. Guo, and S. L. Zhu, "Comparison of membrane extraction with traditional extraction methods for biodiesel production," J. Am. Oil Chem. Soc. 83 (5), 457-460 (2006).

Jaruwat, P., S. Kongjao, and M. Hunsom, "Management of biodiesel wastewater by the combined processes of chemical recovery and electrochemical treatment," Energ. Convers. Manage. 51, 531-537 (2010).

Karaosmanoğlu, F., K. B. Ciğizoğlu, M. Tüter, and S. Ertekin, "Investigation of the refining step of biodiesel production," Energy Fuels, 10, 890-895 (1996).

Kulkarni, M. G. and A. K. Dalai, "Waste cooking oil – An economical source for biodiesel: A review," Ind. Eng. Chem. Res. 45, 2901-2913 (2006).

Lam, M. K., K. T. Lee, and A. R. Mohamed, "Homogeneous, heterogeneous and enzymatic catalysis for transesterification of high free fatty acid oil (waste cooking oil) to biodiesel: A review," Biotechnol. Adv. 28, 500-518 (2010).

Leung, D. Y. C., X. Wu, and M. K. H. Leung, "A review on biodiesel production using catalyzed transesterification," Appl. Energ. 87, 1083-1095 (2010).

Liu S., S. R. Musuku, S. Adhikari, and S. Fernando, "Adsorption of glycerol from biodiesel washwaters," Environ. Technol. 30 (5), 505-510 (2009).

Maliszewski, T. A., D. L. Bunning, D. J. Schreck, L. A. Kapicak, and N. L. Balmer, "Biodiesel production with reduced water emissions," Patent No. WO 2008/091944 A2 (2008).

Mazzieri, V. A., C. R. Vera, and J. C. Yori, "Adsorptive properties of silica gel for biodiesel refining," Energy Fuels, 22, 4281-4284 (2008).

Meher, L. C., D. V. Sagar, and S. N. Naik, "Technical aspects of biodiesel production by transesterification – a review," Renew. Sust. Energ. Rev. 10, 248-268 (2006).

Mittelbach, M. and C. Remschmidt, "Biodiesel - The Comprehensive Handbook," Martin Mittelbach (Publisher), Graz, Austria (2004).

Predojević, Z., "The production of biodiesel from waste frying oils: A comparison of different purification steps," Fuel, 87, 3522-3528 (2008).

Przybylski, R., T. Mag, N. A. M. Eskin, and B. E. McDonald, "Canola Oil," in "Bailey's Industrial Oil and Fat Products," F. Shahidi, Ed., John Wiley & Sons, Inc., Hoboken, NJ (2005).

Rahayu, S. S. and A. Mindaryani, "Optimization of biodiesel washing by water extraction," in "Proc. World Congr. Eng. and Comput. Sci." San Francisco, CA, October 24-26 (2007), pp. 103-107.

Sabudak, T. and M. Yildiz, "Biodiesel production from waste frying oils and its quality control," Waste Manage. 30, 799-803 (2010).

Srivastava, A. and R. Prasad, "Triglycerides-based diesel fuels," Renewable Sustainable Energy Rev. 4, 111-133 (2000).

Saleh, J., A. Y. Tremblay, and M. A. Dubé, "Glycerol removal from biodiesel using membrane separation technology," Fuel 89, 2260-2266 (2010).

Suehara, K., Y. Kawamoto, E. Fujii, J. Kohda, Y. Nakano, and T. Yano, "Biological treatment of wastewater discharged from biodiesel fuel production plant with alkali-catalyzed transesterification," J. Biosci. Bioeng. 100 (4), 437-442 (2005).

Van Gerpen, J., "Biodiesel processing and production," Fuel Process. Technol. 86, 1097-1107 (2005).

Van Gerpen, J., B. Shanks, R. Pruszko, D. Clements, and G. Knothe, "Biodiesel Production Technology," U.S. Department of Energy, National Renewable Energy Laboratory, Golden, CO (2004).

Wang, Y., X. Wang, Y. Liu, S. Ou, Y. Tan, and S. Tang, "Refining of biodiesel by ceramic membrane separation,". Fuel Process. Technol. 90, 422-427 (2009).

West, A. H., D. Posarac, and N. Ellis, "Assessment of four biodiesel production processes using HYSYS.Plant," Bioresource Technol. *99*, 6587-6601 (2008).

Chapter 3

Experimental Design

3.1 Biodiesel Preparation

Crude biodiesel (i.e., fatty acid methyl ester or FAME) was prepared from both canola oil (a low free fatty acid (FFA) feedstock) and used frying oil (a high FFA feedstock). The processes for preparing FAME from each feedstock are described in detail below. Preparation from both feedstocks used the homogenous base catalyzed transesterification method; however, the waste oil feedstock also required an acid esterification pre-treatment. A list of the chemicals used along with suppliers and purities is shown in Table 3.1.

Table 3.1 Chemicals used to prepare FAME.

Chemical	Supplier	Location	Purity (%)
Methanol, Optima Grade	Fisher Scientific	Fair Lawn, NJ	>99.9
Sodium methoxide solution, 25 wt% in methanol	Sigma-Aldrich	Oakville, ON	23.5-26.5
Sulphuric acid, Certified ACS Grade	Fisher Scientific	Ottawa, ON	95.0-98.0
Hydrochloric acid, Certified ACS Grade	Fisher Scientific	Ottawa, ON	36.5-38.0

3.1.1 Canola Oil Feedstock

Spectra Foods brand canola oil (Baie-d'Urfe, QC) was obtained from Tannis Food Distributors (Ottawa, ON) in a 16 L pail. Twelve batches of FAME were produced using a 1 L three-neck, round bottom flask in the reactor set up shown in Figure 3.1. The flask was equipped with a condenser to which cooling water was fed to prevent loss of methanol by evaporation. The flask was suspended in a water bath on a hot plate. The hot plate was equipped with a temperature probe which was immersed in the flask in order to control the flask temperature at 60°C. The hot plate was also equipped with a magnetic stirring mechanism to provide agitation using a magnetic stir bar.

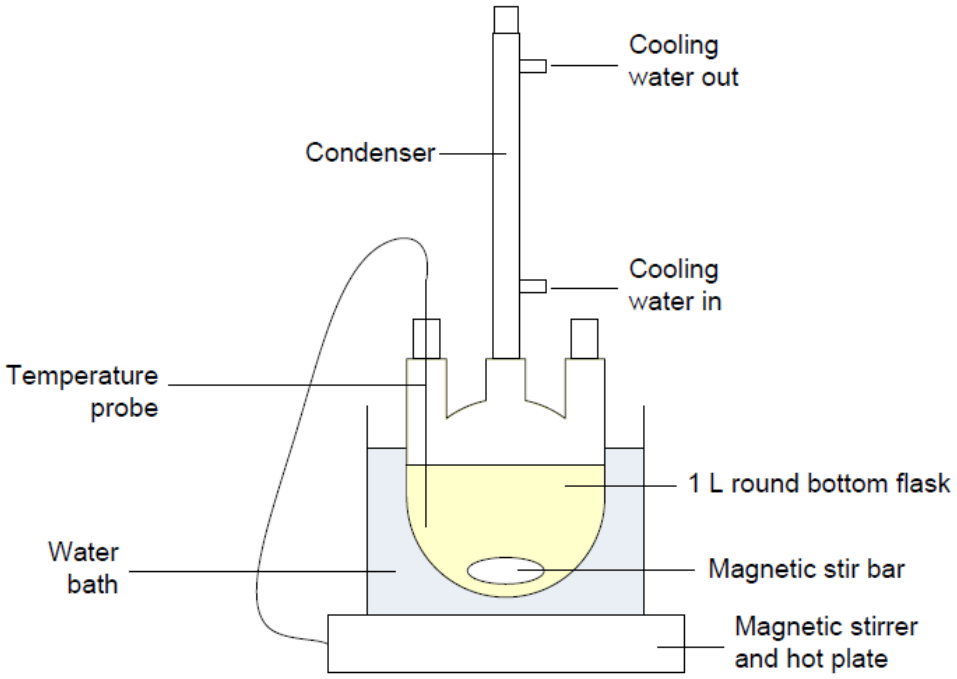

Figure 3.1 Reactor set up for biodiesel preparation.

For each batch, approximately 522 g of oil was used. The reaction conditions included a 6:1 molar ratio of methanol to oil and 0.7 wt% catalyst by weight of oil. The oil was assumed to have a negligible FFA content; therefore, additional catalyst was not required to neutralize FFA. Assuming oil has a molar mass of the triglyceride triolein (885 g/mol), the amounts of methanol and sodium methoxide solution required are shown in Table 3.2. The reaction was completed in two steps using 90% of the methanol and catalyst solution in the first step and the remainder in the second.

Table 3.2 Mass of reactants used for transesterification of canola oil.

Reactant	**Molar mass (g/mol)**	**Mass (g)**	**Moles (mol)**
Oil	885	522	0.590
Methanol	32	102.3	3.20
Sodium methoxide solution:	-	14.6	-
25% $NaOCH_3$	54	3.65	0.068
75% CH_3OH	32	11.0	0.343

The following procedure was used to prepare the first batch of FAME:

1. 523.09 g of oil was added to the reaction flask and placed in the water bath on the hot plate. While the oil was being heated, 92.25 g of methanol and 13.32 g of sodium methoxide solution (0.64 wt% by weight of oil) were combined. Once the oil reached a temperature of 60°C, the methanol and sodium methoxide mixture was added to the reaction flask. The mixture was agitated at 800 rpm for 60 min.
2. The mixture was transferred to a 1 L separatory funnel and allowed to settle for 3 h. Two phases were formed. The bottom, denser phase was rich in glycerol and had a mass of 73.20 g. The top, less dense, phase was rich in FAME and had a mass of 539.17 g. The two phases were separated and the FAME-rich phase was returned to the reaction flask.
3. The mixture in the reaction flask was heated to 60°C. 11.17 g of methanol and 1.47 g of sodium methoxide solution (0.07 wt% by weight of oil) were combined and added to the reaction flask once the temperature reached 60°C. The mixture was agitated at 800 rpm for 60 min.
4. The mixture was transferred back to the 1 L separatory funnel and allowed to settle overnight. Again, two phases were formed. The glycerol rich phase had a mass of 5.42 g and the FAME rich phase had a mass of 541.95 g. The phases were separated and the FAME-rich phase was transferred to a 1 L Erlenmeyer flask.
5. Using pH paper, the pH of the FAME mixture was measured to be between 9 and 10.
6. To neutralize the catalyst, drops of concentrated sulfuric acid (98%) were slowly added while stirring the mixture at low rpm. After each addition of acid, the mixture was allowed to stir for 30 min. This step was repeated until the pH of the mixture was neutral. This required a total of 200 μL of acid.
7. Residual methanol was removed from the neutralized FAME using a rotary evaporator at ~40°C under vacuum. 170.63 g of the mixture was added to a 250 mL evaporating flask. The evaporation process took ~30 min. After removing the flask from the rotary evaporator, the change in mass was found to be 6.55 g.
8. Step 7 was repeated two more times for the remainder of the FAME rich phase. The total amount of methanol removed was 19.49 g.

9. The FAME rich phase was filtered to remove the precipitate formed from the neutralization of catalyst. The filter paper was Fisherbrand Quantitative Grade Circles Q8 with pore size of 20-25 μm.

The final mass of crude, unwashed FAME produced was 410.64 g. The same method described above was used to prepare eleven more batches of FAME. Batches 1 to 7 were combined to create a total of about 3000 g of FAME (or 3.4 L). Batches 8 to 12 were prepared at a later time to complete the experiments described in Chapter 5. The total prepared from Batches 8 to 12 was about 2400 g (or 2.7 L).

3.1.2 Waste Oil Feedstock

Used frying oil was obtained from a cafeteria. The waste oil was dark brown and contained solid particulates left over from the frying process. It also contained water which, as mentioned in Chapter 2, will promote the formation of soap when making biodiesel. To remove water, about 4 L of oil was poured into a deep fryer (Bravetti 4 L deep fryer) and heated until the temperature of the oil was above 100°C (between 100 and 110°C). It was left at this temperature for about 30 min to ensure that most of the water had evaporated from the oil. The oil was then cooled to about 40°C. It was then pumped through two filters to remove solids and water. The filters were a Donaldson brand hydraulic filter (P551553) with a pore size of 25 μm and a Pentek brand water filter. The filtered and dehydrated oil was then stored in a sealed container.

Using the titration method described in Section 3.4, the FFA content was measured to be approximately 9 wt%. The oil therefore required an acid esterification pre-treatment to convert FFA to FAME. Using the reaction conditions of Canakci and Van Gerpen (2003), the molar ratio of methanol to FFA was 40:1 and the catalyst concentration was 6 wt% based on the weight of FFA. Seven batches were produced and for each batch about 466 g of oil was used. Assuming the molar mass of FFA to be that of oleic acid (282 g/mol), the amounts of reactants required are shown in Table 3.3.

Table 3.3 Mass of reactants used for acid esterification of waste oil.

Reactant	Molar mass (g/mol)	Mass (g)	Moles (mol)
Waste oil:	-	466	-
9% FFA	282	41.9	0.149
91% triglycerides	885	424	0.479
Methanol	32	190	5.95
Sulphuric acid	98	2.52	0.0257

Biodiesel production using waste oil was performed in the reaction set up shown in Figure 3.1. The procedure followed for the first batch was as follows:

1. 466.37 g of the waste oil was added to the reaction flask in the hot water bath. Meanwhile, 2.56 g of sulphuric acid was slowly added to 189.30 g of methanol. Once the oil reached a temperature of 60°C, the methanol and acid mixture was added to the reaction flask. The mixture was agitated at 800 rpm for 3 h.
2. The mixture was transferred to a 1 L separatory funnel and allowed to settle for 30 min. Two phases were formed. The top, less dense phase was rich in methanol (135.50 g) and the bottom phase was rich in oil (516.90 g). The two phases were separated. The oil phase was returned to the reaction flask.
3. Using pH paper, the pH was measured to be ~4 due to the presence of sulphuric acid.
4. While gently stirring, 50 µL of 25% sodium methoxide in methanol solution was added to the mixture to neutralize the catalyst. After stirring for 15 min, the pH was measured again. This procedure was repeated until the pH was neutral, which required a total of 300 µL of the sodium methoxide solution.
5. The FFA content in the oil, measured using the titration method described in Section 3.4, was found to be 0.24 wt%.

The mass of reactants required for the transesterification reaction step are shown in Table 3.4. Their amounts resulted in a methanol to oil molar ratio of 6:1 and a sodium methoxide concentration of 0.8 wt% based on the weight of oil.

Table 3.4 Mass of reactants used for transesterification of waste oil.

Reactant	Molar mass (g/mol)	Mass (g)	Moles (mol)
Waste oil:	-	466	-
91% triglycerides	885	424	0.479
Methanol	32	81.8	2.56
Sodium methoxide solution:	-	13.6	-
25% $NaOCH_3$	54	3.39	0.0628
75% CH_3OH	32	10.2	0.318

The procedure for preparing the first batch of FAME continued as follows:

6. The neutralized oil mixture from Step 4 was heated to 60°C in the water bath. Meanwhile, 13.7 g of sodium methoxide solution was added to 81.96 g of methanol.
7. Once the temperature of the oil mixture reached 60°C, the catalyst and methanol solution was added to the reaction flask and the mixture was stirred at 800 rpm for 60 min.
8. The mixture was transferred to the separatory funnel and allowed to phase separate overnight. The bottom glycerol-rich phase (112.74 g) was removed and the top FAME-rich phase (490.94 g) was transferred to a 1 L Erlenmeyer flask.
9. The pH of the FAME-rich phase was ~10.
10. 400 µL of concentrated hydrochloric acid (36%) was added to neutralize the basic catalyst. The mixture was left stirring at low rpm for about 15 min and the pH was ~6. To bring the pH to neutral, 100 µL of sodium methoxide was added. After 15 min of stirring at low rpm, the pH was found to be 7.

Seven batches were produced using the above method. The first three batches were combined for a total of 1500 g (about 1.7 L) and were used for the single stage washing experiments described in Chapter 5. The final four batches were also combined for a total of 2000 g (about 2.2 L) and were used for the counter-current washing experiments described in Chapter 6. The final soap concentration in the FAME was measured to be, on average, 0.36 wt%.

3.2 Water Washing Procedure

For each washing experiment, the apparatus shown in Figure 3.2 was used. 200 mL of FAME was washed with 40 mL of water (i.e., a FAME to water volume ratio of 5:1). Contact between the two phases was accomplished by bubbling air through a fritted glass gas dispersion tube (Pyrex brand, porosity of 40 to 60 μm) suspended in the water phase. This gentle washing method minimized the formation of emulsions while maintaining contact between the phases. Air flow was provided by an aquarium pump (Elite brand, model 802) and was controlled by a clamp.

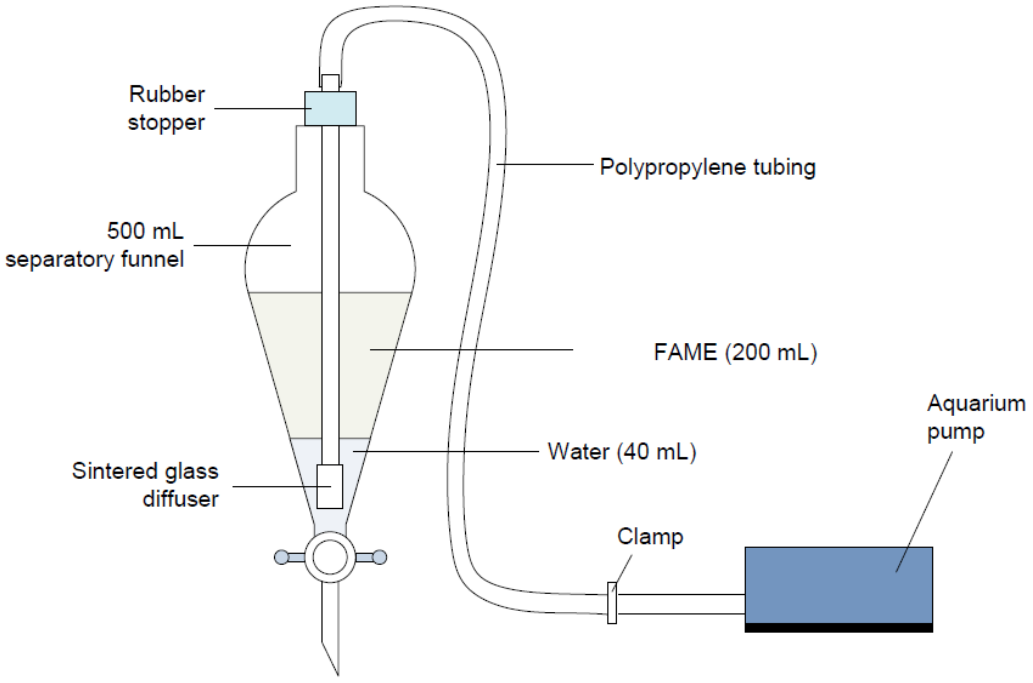

Figure 3.2 Water washing apparatus.

When washing the canola oil derived FAME, the bubble washing lasted 3 h. For the waste oil derived FAME, serious emulsification occurred if the bubbling was left this long. As a result, bubbling was stopped at 2 h.

For the single stage washing experiments of the canola oil derived FAME, the two phases were transferred to a 250 mL centrifuge bottle and centrifuged at 3500 rpm for 10 min. The water phase was then removed by pipette and stored separately from the FAME phase. Unfortunately, the length of centrifugation used was later determined to be much

higher than what would be used in an industrial setting. Acceleration due to centrifugation, *G*, is measured in multiples of earth gravity, *g*, and is determined as follows:

$$\frac{G}{g} = 0.000559 \times \Omega^2 D \tag{3.1}$$

where Ω is the speed of the centrifuge in rpm and *D* is the diameter of the centrifuge bowl in m (Genck, 2008). For a typical commercial centrifuge[3] with an operating speed of 4300 rpm and bowl diameter of 1.1 m, the acceleration experienced by a particle in the centrifuge is 11,370 g. For an operating flowrate of 40 m^3/h (75% of capacity) and bowl volume of 66 L, the particle will experience this gravitational acceleration for about 5.9 s:

$$\frac{h}{40\ m^3} \times 66\ L \times \frac{m^3}{1000\ L} \times \frac{3600\ s}{h} = 5.9\ s \tag{3.2}$$

According to Stokes' law, the settling velocity of a particle is proportional to the gravitational acceleration (Geankoplis, 2003), and thus, the time required to settle is inversely proportional to acceleration. Therefore, to be equivalent to an industrial centrifuge, the time required for the phases to settle under earth gravity, *g*, is:

$$t = \frac{g_c}{g} t_c = \frac{11{,}370\ g}{g} \times 5.9\ s \times \frac{h}{3600\ s} = 18.8\ h \tag{3.3}$$

where *t* is the time required for settling under earth gravity, *g*, g_c is the gravitational acceleration experienced in the centrifuge, and t_c is the time a particle would spend in the centrifuge. Therefore, leaving the phases to settle overnight should be equivalent to an industrial centrifuge operation. Selected runs from the single stage washes of the canola oil derived FAME were repeated and the original centrifugation conditions were not found to have an effect on the results.

For all experiments involving the waste oil derived FAME, after washing was complete, the phases were left to settle overnight. The phases were then separated and stored for analysis.

[3] Alfa Laval, BD 95 High-capacity disc stack centrifuge for biodiesel production

3.3 Analysis for Sodium Concentration

3.3.1 Inductively Coupled Plasma Optical Emission Spectroscopy (ICP-OES)

For the single stage water washing experiments (Chapter 5), the sodium concentration in both the water and FAME phases was determined by Inductively Coupled Plasma Optical Emission Spectroscopy (ICP-OES). The principle behind ICP-OES is that metal atoms, when introduced to a plasma flame, will become excited and emit light at elementally characteristic wavelengths. The analysis was completed in the Department of Earth Sciences at the University of Ottawa (Ottawa, ON) by Dr. Nimal De Silva. Sample preparation was completed by the author.

Sample preparation for the water samples was as follows:

1. 1 mL of the water phase was added to a sample tube. The sample mass was recorded.
2. 1 mL of 10% nitric acid was added to the sample tube.
3. 8 mL of deionized water was added and the final mass was recorded. This sample was submitted for ICP-OES analysis.

Sample preparation for the FAME samples was as follows:

1. 5 mL of the FAME phase was added to a sample tube. The sample mass was recorded.
2. 1 mL of 10% nitric acid was added and the sample was shaken well for ~2 min.
3. The sample was left to settle for 1 h.
4. The sample was centrifuged at 3500 rpm for 30 min.
5. The aqueous phase was then removed by pipette and transferred to a new sample tube. The mass of sample transferred was recorded.
6. Steps 2 to 5 were repeated.
7. 4 mL of deionized water was added to each of the extracted aqueous phases and the mass of each diluted sample was recorded. These samples were submitted for ICP-OES analysis.

The ICP-OES analysis measured the sodium concentration in the diluted aqueous samples. To determine the concentration in the original sample, the following conversion was used:

$$C = \frac{C_{ICP} m_{diluted}}{m_{sample}} \tag{3.4}$$

where C is the sodium concentration in the original water sample in ppm, C_{ICP} is the concentration determined by ICP-OES in the diluted sample in ppm, $m_{diluted}$ is the mass of the diluted sample in g, and m_{sample} is the mass of the original water sample.

For the FAME samples that required two acid extractions, the mass of sodium in each diluted sample were combined before dividing by the original FAME sample mass:

$$C = \frac{(C_{ICP} m_{diluted})_1 + (C_{ICP} m_{diluted})_2}{m_{sample}} \tag{3.5}$$

where *1* and *2* represent the first and second extractions, respectively, and m_{sample} is the mass of the original FAME sample.

3.3.2 Conductivity

The conductivity of an electrolyte solution is measured using a conductivity meter and probe. The probe contains two electrodes and, when placed in contact with the solution, a voltage is applied to the electrodes. The measured current is then converted to conductivity, with units of conductance (Siemens (S)) per unit length of conductor (cm). The conductivity meter used was YSI Model 3200 and the probe had a cell constant of 1.0/cm (model number 3253).

Because the ability of a solution to conduct electric current is dependent on the ions in solution, it can be used as a measure of ionic concentration. For dilute electrolyte solutions, the conductivity is proportional to the concentrations of ions. This trend was observed when the conductivity of prepared sodium sulphate and sodium chloride solutions were measured, as seen in Figure 3.3.

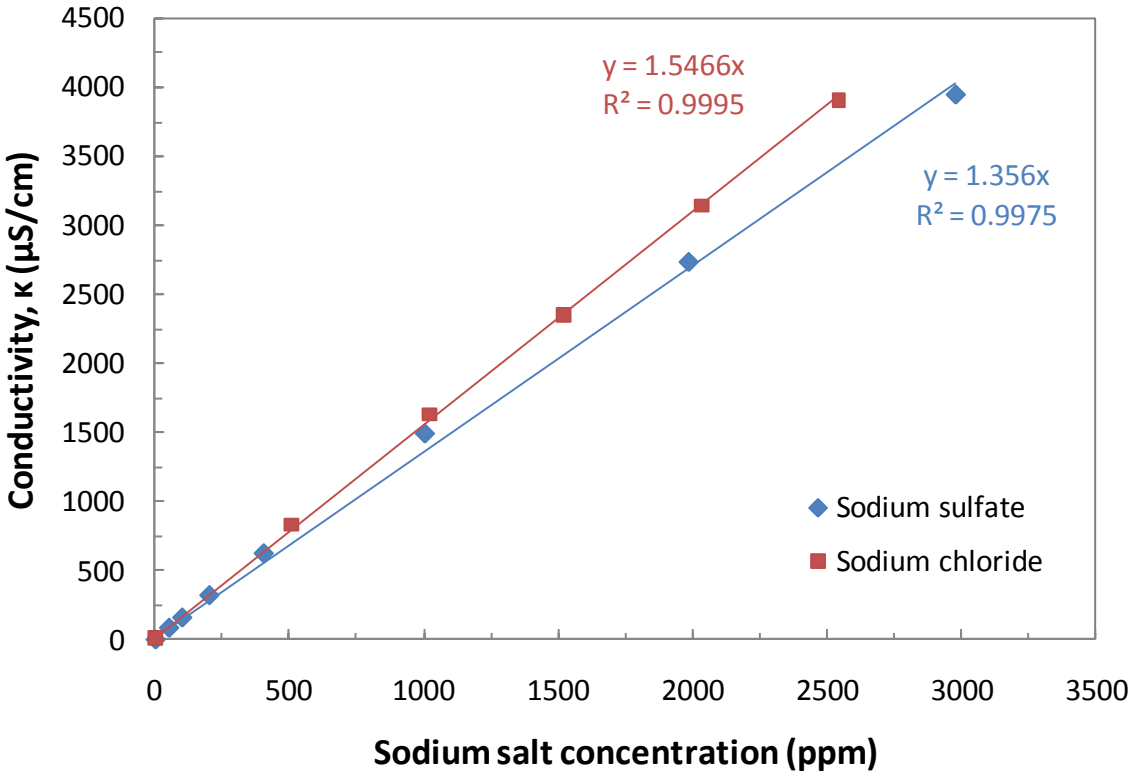

Figure 3.3 Conductivity of sodium sulphate and sodium chloride solutions.

For the counter-current washing experiments described in Chapter 6, conductivity was used to determine the concentration of sodium in the extracted water phases. The calibration curve used is shown in Figure 3.4. It was determined using the ICP-OES results from the single stage washing of waste oil derived FAME, described in Chapter 5. The use of the conductivity meter allowed for quick, real time measurements which made the experiments described in Chapter 6 possible.

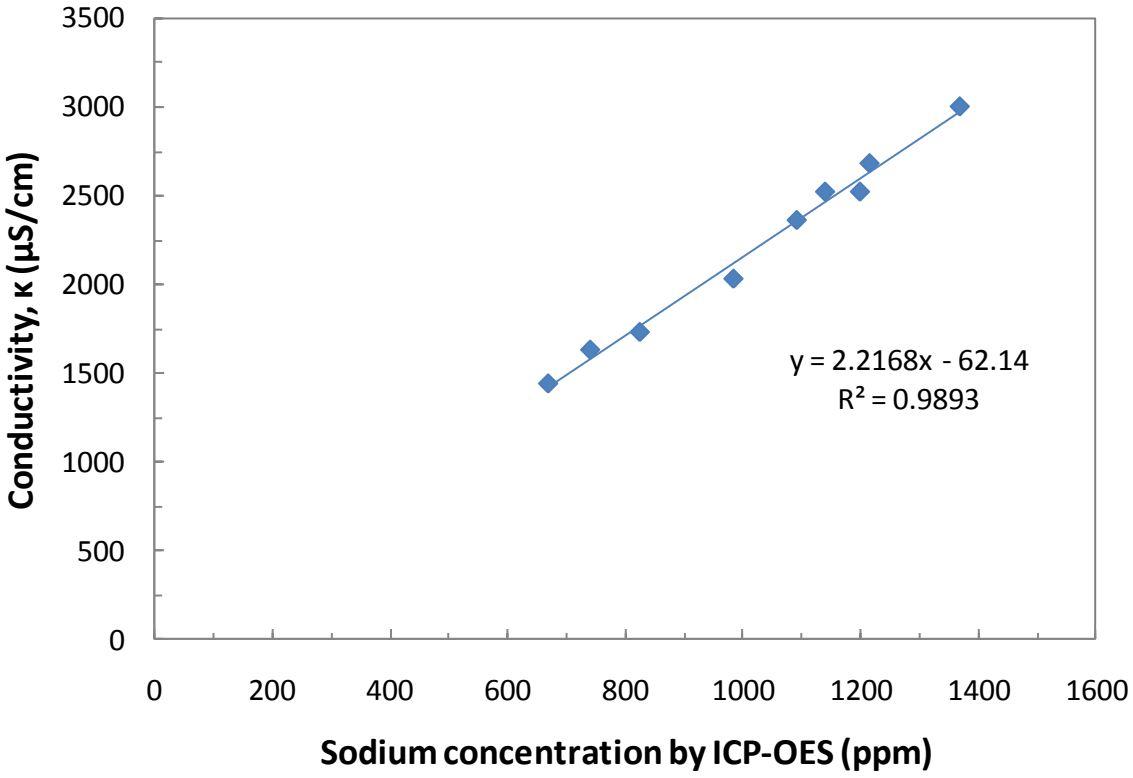

Figure 3.4 Conductivity calibration curve for determining sodium concentration of wastewater samples.

3.4 Analysis for FFA/Soap Concentration

The titration method for measuring the amount of soap or FFA in the FAME samples was based on the modified AOCS method Cc 17-79 presented by Van Gerpen et al. (2004). Potassium hydroxide in isopropanol (0.01 N) and hydrochloric acid in isopropanol (0.01 N) were prepared using the chemicals listed in Table 3.5. The required pH indicators are also listed.

Table 3.5 Chemicals used in titration of FFA/soap.

Chemical	Supplier	Location	Purity (%)
Isopropanol	Fisher Scientific	Fair Lawn, NJ	>95
Potassium hydroxide solution (0.1 N in isopropanol)	Fisher Scientific	Fair Lawn, NJ	0.56
Hydrochloric acid solution (0.1 N in isopropanol)	Fisher Scientific	Fair Lawn, NJ	0.4
Phenolphthalein, Certified ACS Grade	Fisher Scientific	Fair Lawn, NJ	100
Bromophenol blue solution (0.04 wt% in water)	Sigma-Aldrich	Oakville, ON	0.04

The measurement was based on the equilibrium between FFA and soap, shown in Figure 2.4. Under acidic conditions, the FFA is in the protonated FFA form (left side of the equation) whereas under basic conditions, the FFA is in the soap form (right side of the equation).

The concentrations of FFA in the washed FAME and water phases from the single stage washing experiments (Chapter 5) were measured. To determine the distribution of FFA between the phases, measurements were made at the FAME phase, the water phase, and the interface. The procedure used was as follows:

1. 2-3 mL of sample was added to a sample tube. The mass of sample was recorded.
2. About 10 mL of isopropanol was added to the sample tube. The mixture was shaken for ~1 min then left for ~20 min to allow time for the FFA to dissolve in the isopropanol.
3. About 100 µL of 1% phenolphthalein indicator in isopropanol solution was added to the sample. The colour of the sample did not change, indicating that the pH was below the phenolphthalein endpoint of 8.2.
4. The sample was then transferred to a clear, 20 mL, flat bottom vial.
5. A few drops of 0.01 N potassium hydroxide in isopropanol solution was added with a burette. These drops would appear pink once they contacted the sample. The sample was then gently mixed by hand such that any FFA present would react with the potassium hydroxide and the pink colour would disappear.

6. Step 5 was repeated until the colour of the sample remained pink. This indicated that the equilibrium was such that all FFA present was in the soap form. The volume of base added was recorded in mL.
7. About 100 μL of bromophenol blue solution was added to the sample. The solution would turn blue, indicating the pH was above the bromophenol blue endpoint of 4.6.
8. A few drops of 0.01 N hydrochloric acid in isopropanol solution was added to the sample with a burette. The sample was then gently mixed by hand to ensure the soap would react with the acid to form protonated FFA molecules.
9. Step 8 was repeated until the colour of the sample changed from blue to yellow. This indicated that the equilibrium was such that all FFA present was in the protonated FFA form. The volume of acid added was recorded in mL.

The concentration of FFA was then calculated using the following equation:

$$C_{FFA} = \frac{V_{acid} MW_{FFA}}{m_{sample}} \times \left(0.01 \frac{mol}{L}\right) \times \left(\frac{L}{1000\ mL}\right) \times \left(\frac{10^6 \mu g}{g}\right) \tag{3.6}$$

where C_{FFA} is the concentration of FFA in parts per million (ppm), V_{acid} is the volume of acid added in Steps 8 and 9 in mL, MW_{FFA} is the molecular weight of oleic acid (282.5 g/mol), and m_{sample} is the mass of sample measured in Step 1 in g.

3.5 References

Canakci, M. and J. Van Gerpen, "A pilot plant to produce biodiesel from high free fatty acid feedstocks," Trans. Am. Soc. Agric. Eng. 46 (4), 945-954 (2003).

Geankoplis, C. J., "Transport Processes and Separation Process Principles," Pearson Education, Inc., Upper Saddle River, NJ (2003).

Genck, W. J., D. S. Dickey, F. A. Baczek, D. C. Bedell, K. Brown, W. Chen, D. E. Ellis, P. Harriott, T. J. Laros, W. Li, J. K. McGillicuddy, T. P. McNulty, J. Y. Oldshue, F. Schoenbrunn, J. C. Smith, D. C. Taylor, D. R. Wells, and T. W. Wisdom, "Liquid-Solid Operations and Equipment," in "Perry's Chemical Engineers' Handbook," D. W. Green and R. H. Perry, Eds., McGraw-Hill Companies, Inc., New York, NY (2008).

Van Gerpen, J., B. Shanks, R. Pruszko, D. Clements, and G. Knothe, "Biodiesel Analytical Methods," U.S. Department of Energy, National Renewable Energy Laboratory, Golden, CO (2004).

Chapter 4

Simulation of Biodiesel Wastewater Treatment Processes

4.1 Introduction

Because energy production requires large amounts of water and water treatment requires energy, the two can be considered to be closely linked (Elcock, 2010). With the increasing world production of biodiesel, the consumption of water must be considered to ensure efficient use of this valuable resource. Reducing the amount of water used will also reduce the amount of energy used for water treatment, thereby improving the overall energy efficiency of biodiesel fuel.

The purification of crude fatty acid methyl esters (FAME) will typically consume one litre of water per litre of FAME washed (Van Gerpen et al., 2004). Some processes using high free fatty acid (FFA) feedstocks can require up to three litres of water per litre of FAME (Canakci and Van Gerpen, 2003). Depending on municipal disposal requirements, this wastewater will most likely require treatment. Recycling the water will result in cost savings and minimize the environmental impact of the process. Therefore, the best process is one that not only minimizes water use and waste production, but also minimizes the amount of energy required to treat the resulting wastewater.

In this chapter, the purification of biodiesel was modelled using a process simulation software (Aspen HYSYS, 2011) to determine the energy required by the water washing process. The simulated biodiesel was produced from used frying oil by the homogenous alkali-catalyzed reaction with an acid-catalyzed pre-treatment step. Similar simulations have been previously performed to compare different catalyst systems (Zhang et al., 2003; West et al., 2008). However, to our knowledge, simulations have not yet been used to compare wastewater treatment options. A comparison was made between water treatment by distillation as well as by ion exchange, including an evaluation of the effect of reducing the amount of water used for each of the processes.

4.2 Simulation Conditions

4.2.1 Thermodynamic Model

Due to the presence of polar compounds (such as methanol and glycerol), the Non-Random Two Liquid (NRTL) thermodynamic model is most commonly used for biodiesel related simulations (Zhang et al., 2003; West et al., 2008; Gonzalo et al., 2010). Unfortunately, this model is not applicable for electrolytes, such as the catalysts sodium hydroxide and sulphuric acid. Therefore, these components were not included in the simulation. In practice, these components would most likely partition almost completely into the aqueous phase and their presence would not have a large effect on the distillation operations.

4.2.2 Components

For most vegetable oils, including canola oil, the most common fatty acid is oleic acid (Srivastava and Prasad, 2000). Therefore, when simulating the biodiesel process, both Zhang et al. (2003) and West et al. (2008) used triolein as the initial oil feedstock. Further, they modelled FFA as oleic acid and FAME as methyl oleate. The properties of these three components are all present in the Aspen HYSYS component library. Other components used in the process include methanol, glycerol, and water, which are also available in the component library.

4.2.3 Transesterification Reaction Products

Both Zhang et al. (2003) and West et al. (2008) simulated the production of biodiesel from a used frying oil feedstock with 5% FFA (i.e., 95% triolein and 5% oleic acid). Plant production was specified at 8000 metric tonnes of biodiesel per year, which translates to an oil feed of approximately 1000 kg/h. Although both authors modelled various catalyst systems, the simulations presented in this chapter are mainly based on the process presented by West et al. (2008). This process involved an acid esterification pre-treatment (using sulphuric acid as the catalyst) to completely convert oleic acid to methyl oleate followed by transesterification (using sodium hydroxide as catalyst) to convert triolein to methyl oleate.

In order to model the downstream purification operations, only the reaction products from the transesterification step were required, so modelling the reaction itself was not

necessary. West et al. (2008) did not explicitly provide the composition of the reaction product stream, but did give the composition and flows of the oil and methanol feed streams. They also provided the following reaction conditions: a methanol to oil molar ratio of 6 and a reaction conversion of 95%. Using this information, the reaction products were determined and are presented in Table 4.1.

Table 4.1 Molar flows of reactants and products from transesterification.

Component	Molar flows (kmol/h)		
	Oil and FAME	**Methanol**	**Products**
Triolein	1.111	-	0.056
Methyl oleate	0.222	-	3.390
Methanol	-	6.668	3.501
Glycerol	-	-	1.056

These reaction products form two immiscible phases – one rich in FAME and one rich in glycerol. As shown in the process model presented by Haas et al. (2006), these phases are typically separated prior to purification. The liquid-liquid equilibrium of this phase separation was calculated using Aspen HYSYS with the NRTL thermodynamic package. Unknown binary interaction parameters were estimated with the Aspen PLUS Properties V7.2 software, as described by Gonzalo et al. (2010), using the Universal Functional Activity Coefficient (UNIFAC) method. The phase separation was modelled at 25°C and the resulting mass fractions and flows are shown in Table 4.2. The water washing step was then simulated using the streams presented in Table 4.2 along with the subsequent wastewater treatment operations.

Table 4.2 Compositions and mass flows of the two liquid phases formed by the transesterification reaction.

Property	FAME-rich phase	Glycerol-rich phase
Mass flow (kg/h)	1076	188.2
Mass fractions:		
Triolein	0.0461	0.0000
Methyl oleate	0.9341	0.0004
Methanol	0.0197	0.4835
Glycerol	0.0001	0.5161

4.2.4 Manipulated Variable

After phase separation of the reaction products, the FAME-rich phase is contacted with water in a water washing step to remove polar contaminants including methanol, glycerol, and catalyst. This operation was simulated using a counter-current liquid-liquid extraction column.

Typically, the crude FAME is washed with an equal volume of water (Van Gerpen et al., 2004). In this simulation, the mass flow of methyl oleate after phase separation was approximately 1005 kg/h, which corresponds to a volume flow of about 1155 L/h. Therefore a water flow of 1153 kg/h (1155 L/h) was used to simulate the 1 to 1 volume ratio condition as a base case scenario. By changing the amount of inlet fresh water, the volume ratio was varied to determine the effect of the water load on the downstream water treatment operations.

It is important to note that, for all the simulations presented in this chapter, the washed biodiesel met the purity specifications for methanol and glycerol. It would therefore seem obvious that the lowest possible wash water flowrate should be selected. However, as is demonstrated in later chapters, biodiesel with high initial FFA content leads to soap formation and increased salt partitioning. As a result, more wash water is required to meet the specifications for residual salts in the biodiesel. The simulations presented in this chapter are intended to show the increased energy load associated with using larger amounts of wash water.

4.3 Water Treatment by Distillation

The process flow diagram (PFD) for treating the wastewater by distillation is shown in Figure 4.1. The simulated process was based on the model presented by Haas et al. (2006).

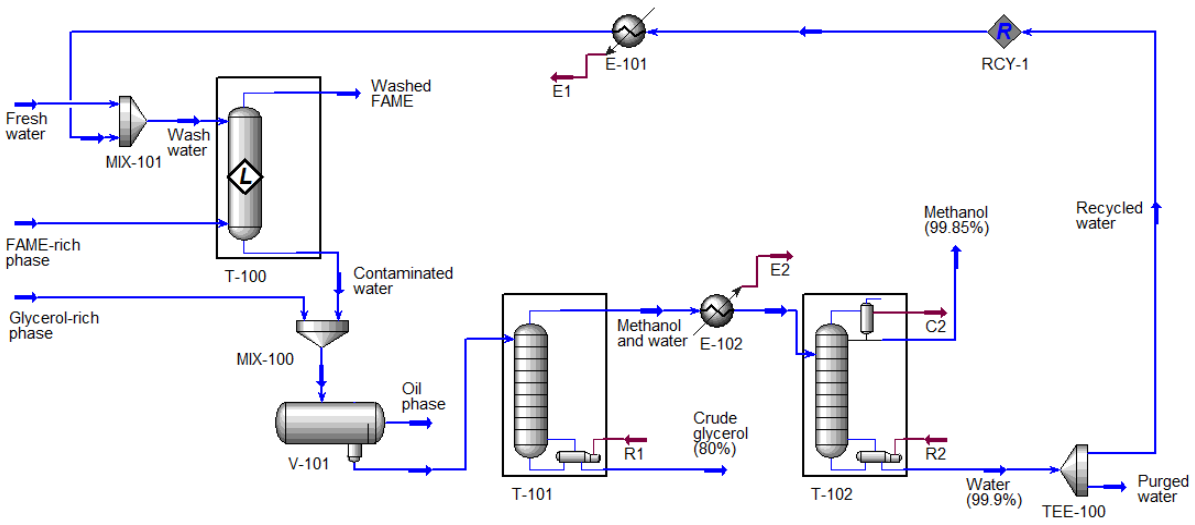

Figure 4.1 Biodiesel purification process with water treatment by distillation.

The "FAME-rich phase" is first contacted with the "Wash water" stream in a liquid-liquid extraction column (T-100). This produces the "Washed FAME" and "Contaminated water" streams. The "Contaminated water" is combined with the "Glycerol-rich phase". After removing the small oil phase in a two phase separator (V-101), this combined stream is then treated by distillation to recover the methanol and water to be recycled back to the process.

4.3.1 Glycerol Purification Column (T-101)

For a three-component mixture, two columns are required to separate the three components (Geankoplis, 2003). Referring to the different boiling points of methanol, water, and glycerol shown in Table 4.3, the first separation is to separate the most volatile components (methanol and water) from the least volatile (glycerol). This is accomplished in the first distillation column (T-101 in Figure 4.1).

Table 4.3 Normal boiling points of the components in the wastewater mixture.

Component	Normal boiling point (°C)
Methanol	65
Water	100
Glycerol	290

For typical biodiesel processes, it is often cost effective to partially purify the glycerol by removing methanol and most of the water and selling the product to glycerol refiners at 80% glycerol by mass (Haas et al., 2006). The specifications for this column were therefore set at a bottoms concentration of 80 wt% glycerol and 20 wt% water. The "Crude glycerol" stream would also contain the salt impurities originating from both the "FAME-rich phase" and the "Glycerol-rich phase".

Because glycerol is much less volatile than the other two components, the distillation operation did not require reflux and the separation was therefore simulated as a stripping-column distillation. The energy required by the reboiler of column T-101 is represented by the energy stream "R1".

4.3.2 Methanol Recovery Column (T-102)

After the methanol and water have been recovered from the crude glycerol steam, the two components must be further purified prior to recycling to the process. The water content in the methanol recycled to the transesterification reactor must be as low as possible to reduce soap formation. Also, the methanol content in the water must be low to reduce the amount that must be purged with the wastewater. The specification for the methanol stream was set at the purity of commercial grade methanol, which is 99.85 wt% (Fiedler et al., 2005). To minimize methanol loss, a purity of 99.9 wt% of water for the water stream was selected.

The "Methanol and water" stream exiting the top of the glycerol purification column (T-101) is first cooled to its dew point by cooler E-102. The energy released is represented by energy stream "E2".

The design of column T-102 was accomplished by optimizing the conditions in Aspen HYSYS. However, as a starting point, the minimum number of stages was estimated using the Fenske equation (Geankoplis, 2003):

$$N_{min} = \frac{log\left[\left(\frac{x_D}{1-x_D}\right)\left(\frac{1-x_B}{x_B}\right)\right]}{log\ \alpha_{avg}} \tag{4.1}$$

where N_{min} is the minimum number of theoretical plates required at total reflux, x_D is the mole fraction of the more volatile component in the distillate, x_B is the mole fraction of the more volatile component in the bottoms, and α_{avg} is the average relative volatility of the more volatile component to the less volatile. The average relative volatility can be estimated as:

$$\alpha_{avg} = \sqrt[3]{\alpha_D \alpha_B \alpha_F} \tag{4.2}$$

where

$$\alpha = \frac{K_i}{K_j} = \frac{(y_i/x_i)}{(y_j/x_j)} \tag{4.3}$$

where α_D is the relative volatility of the distillate, α_B is the relative volatility of the bottoms, α_F is the relative volatility of the feed, i is the more volatile component (i.e., methanol), j is the less volatile component (i.e., water), K is the vapour-liquid distribution coefficient, y is the mole fraction in the vapour, and x is the mole fraction in the liquid. The actual number of trays (N) was then estimated by multiplying N_{min} by 2. Multiplying N_{min} by 2 is approximately equivalent to using a reflux ratio that is 1.3 times R_{min}, which usually represents a nearly optimal column configuration (Seader et al., 2010). This value was used for the number of stages of the simulated distillation column. The feed stage was then selected so that it minimized the reflux ratio required to meet the purity specifications. The energy demand of the reboiler is represented by energy stream "R2" and "C2" represents the energy released by the condenser.

4.3.3 Water Recycle

The "Water" stream exiting the bottom of column T-101 has a purity of 99.9 wt%. A small portion (5%) is purged by TEE-100, and the remainder is recycled to the water washing process. It is first cooled to 25°C by cooler E-101 and the energy released is represented by

stream “E1”. The stream is then combined with “Fresh water” in MIX-101 to form the “Wash water” stream used to wash the crude FAME.

4.3.4 Energy Demand

The overall energy demand of the water treatment by distillation process was determined by summing up all the energy input streams to the column reboilers in Figure 4.1. Cooling streams were not included in this analysis since cooling is usually accomplished using cooling water, which has a minimal impact on overall process energy demand and economics. These column energy streams are summarized in Table 4.4.

Table 4.4 Energy streams for water treatment by distillation process.

Stream		Description
Heating	R1	Reboiler energy for glycerol purification column
	R2	Reboiler energy for methanol recovery column
Cooling	E1	Decreases temperature of recycled water stream to 25°C
	E2	Decreases temperature of methanol/water stream to its dew point
	C2	Condenser energy for methanol recovery column

4.4 Water Treatment by Ion Exchange

An alternative process, shown in Figure 4.2, regenerates the water by ion exchange. As in the distillation process, the “FAME-rich phase” is contacted with the “Wash water” stream in a liquid-liquid extraction column (T-100). Instead of combining the resulting wastewater stream with the “Glycerol-rich phase”, the two streams are kept separate. Methanol is recovered to the same level of purity (99.85%) from the “Contaminated water” stream by distillation in column T-102.

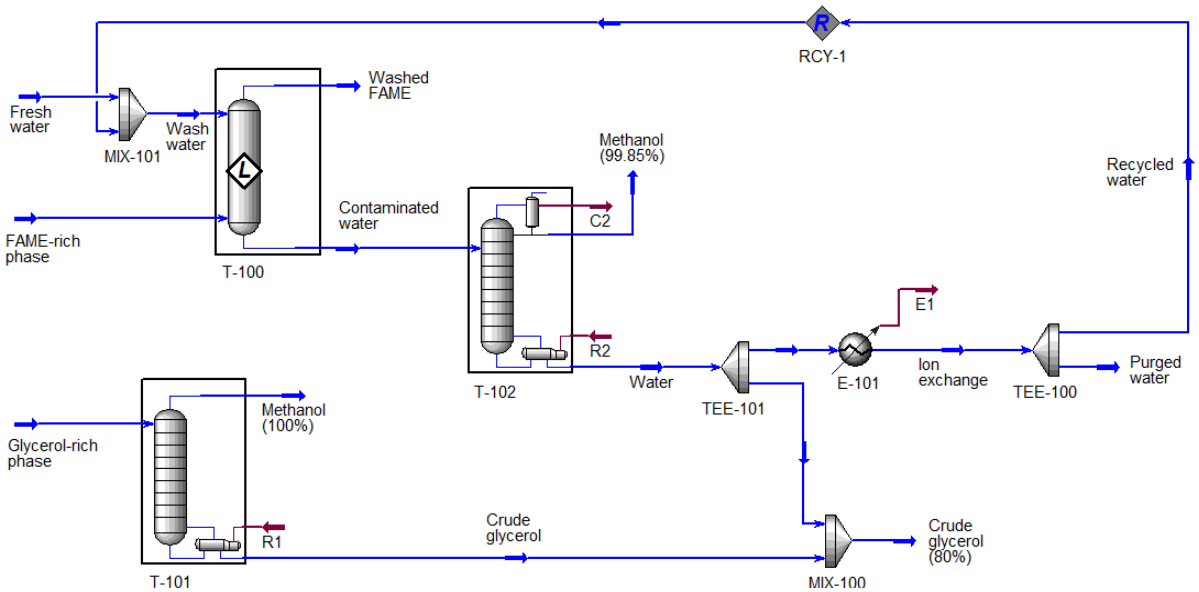

Figure 4.2 Biodiesel purification process with water treatment by ion exchange.

In order for the ion exchange process to be comparable to the distillation process presented in Section 4.3, the "Glycerol-rich phase" requires the same level of purification. First, methanol is recovered by stripping-column distillation (T-101). Some of the "Water" stream leaving the bottom of the methanol recovery column (T-102) was then used to produce crude glycerol at 80 wt% purity.

Although the "Water" stream is now free of methanol, it will still contain the salts washed out of the "FAME-rich phase". The type of salts present in the wastewater will depend on the catalyst and acid used for neutralization. If sodium hydroxide is used as the catalyst followed by neutralization by hydrochloric acid, the majority of the salts present will be sodium chloride. To remove these salts, the remaining water exiting TEE-101 is first cooled to 25°C by cooler E-101 and then contacted with ion exchange resins to remove salts.

Ion exchange operations, which would take place at the "Ion exchange" stream in Figure 4.2, cannot be simulated with Aspen HYSYS. The operation was therefore simulated using the shortcut design calculations described below.

4.4.1 Ion Exchange Columns

The ion exchange operation requires the use of two types of resins: a cation exchanger to exchange sodium (Na^+) ions for hydrogen (H^+) ions and an anion exchanger to exchange chlorine ions (Cl^-) for hydroxide ions (OH^-). Similar to other adsorption processes, ion exchangers are typically used in cyclic operations involving both sorption and desorption steps (LeVan and Carta, 2008). The steps, shown in Figure 4.3, include loading the resin by passing the wastewater through the bed until breakthrough occurs, regeneration to restore the original ionic form of the exchanger, and rinsing to remove regenerant from the void volume and resin pores.

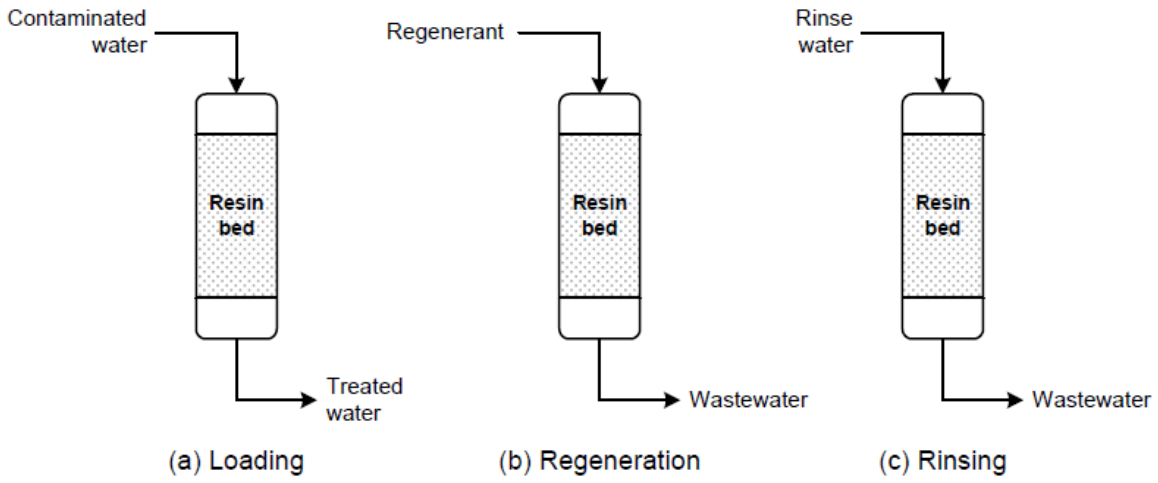

Figure 4.3 Steps involved in a typical ion exchange operation.

For the removal of sodium and chlorine ions from an aqueous solution, strong acid and strong base resins are used. Pertinent properties of two ion exchangers produced by Dow Chemicals are shown in Table 4.5. These values were used in the approximate design of an ion exchange system for the process shown in Figure 4.2.

Table 4.5 Resin properties used to design the ion exchange operation.

Resin property	Strong acid cation exchanger Dowex Marathon C	Strong base anion exchanger Dowex Marathon A
Total exchange capacity	1.8 eq/L	1.0 eq/L
Regenerant	4-5% HCl	2-5% NaOH
Efficiency of regeneration	120-150%	140-220%
Rinse requirement	2-5 bed volumes	3-6 bed volumes

Referring to Table 2.3 in Chapter 2, the average level of sodium in crude, unwashed FAME is about 227 ppm. Assuming hydrochloric acid is used to neutralize the catalyst, this represents a sodium chloride (NaCl) concentration of 577 ppm. It was therefore assumed that when washing FAME in a 1:1 water to FAME volume ratio, the resulting wastewater would have a concentration of 508 ppm NaCl. Note that for lower water amounts, this concentration will increase.

Dow Chemicals recommends using an operational capacity efficiency of 65-90% of the total exchange capacity. Therefore an efficiency of 75% was assumed.

The chemical efficiency of regeneration for an ion exchange resin is defined as:

$$Efficiency = \frac{Amount\ of\ regenerant\ chemical\ added\ (\frac{eq}{L})}{Resin\ operating\ capacity\ (\frac{eq}{L})} \times 100\% \qquad (4.4)$$

The resin usage of the regenerant chemical is non-ideal, therefore the chemical efficiency is always greater than 100% and becomes worse as the value increases (Dow Water and Process Solutions, 2011). This efficiency takes into account the amount of regenerant required in excess in order to achieve sufficient conversion of the resin back to its original form.

Using the above information and the resin properties in Table 4.5, the amount of wastewater that can be treated by each resin and the regeneration and rinsing requirements were calculated for each level of wastewater produced. Sample calculations are shown in Section 4.8.

The regenerant solutions and rinse water streams represent a waste that would require treatment. Therefore, in order for the ion exchange process to be comparable to the

distillation process, the energy required to evaporate the water from these waste streams was also determined. Another option to recover water from the regenerant and rinse solutions would be reverse osmosis. However, evaporation is the most widely used separation method and was therefore used in this study.

4.4.2 Energy Demand

The total energy demand of the process in Figure 4.2 included the reboiler energies required by the two distillation columns as well as the energy required to treat the waste effluent from the ion exchange operations (regeneration and rinsing). The energy streams are summarized in Table 4.6. Note that the energy required for treating the ion exchange waste is not part of the process in Figure 4.2, due to the cyclic nature of ion exchange operations.

Table 4.6 Energy streams for water treatment by ion exchange process.

Stream		Description
Heating	R1	Reboiler energy for glycerol purification column
	R2	Reboiler energy for methanol recovery column
	-	Evaporation of ion exchange waste effluents
Cooling	E1	Decreases temperature of water stream to 25°C
	C2	Condenser energy for methanol recovery column

4.5 Results and Discussion

4.5.1 Water Treatment by Distillation

The energy demand of the water treatment by distillation process per litre of biodiesel produced with respect to the volume ratio in the water washing step is shown in Figure 4.4. Decreasing the amount of water used in the washing step results in a decrease in the amount of energy required to treat the produced wastewater. This is simply because there is less water in the system thereby reducing the load on the distillation columns.

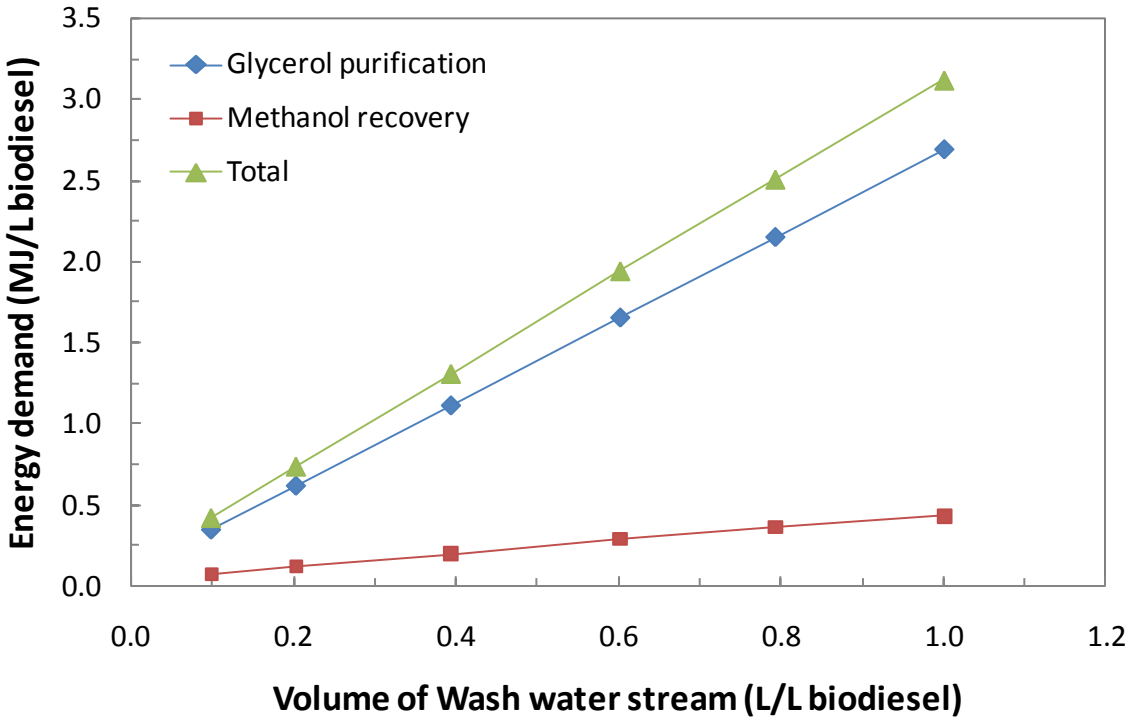

Figure 4.4 Energy demand of water treatment of biodiesel wastewater by distillation.

The separation of methanol and water from glycerol was found to require more energy than the methanol recovery step. This is because a large amount of water must be evaporated from the glycerol, requiring a large amount of energy.

4.5.2 Water Treatment by Ion Exchange

The energy demand of the ion exchange process with respect to the volume of water used is shown in Figure 4.5. As expected, decreasing the amount of water decreases the amount of energy required for water treatment linearly. The energy required for glycerol separation remains constant because it is independent of the water washing steps. The energy demand for treating the ion exchange effluent (from regeneration and rinsing) also remains constant because the volume of effluent generated is constant. Although less wastewater is produced when using lower amounts of water to wash the FAME, it is more concentrated in sodium chloride. These opposing effects cancel each other out and result in a constant volume of ion exchange effluent produced, regardless of the amount of water used to wash the FAME.

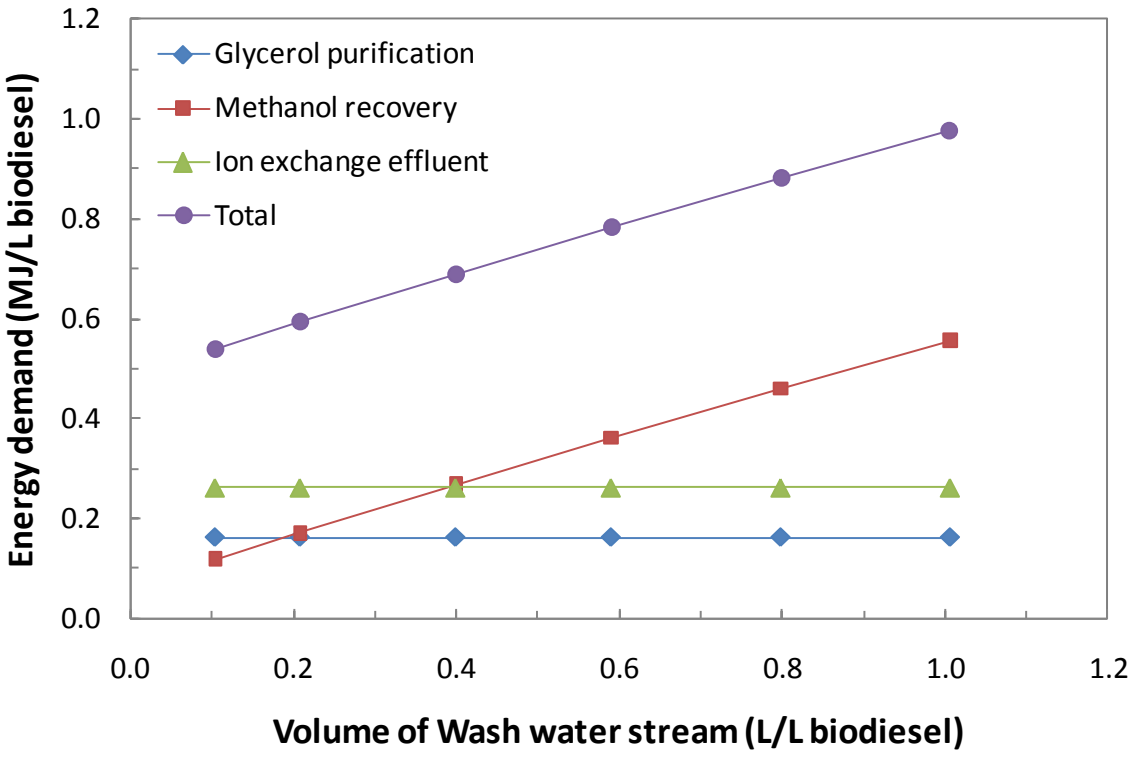

Figure 4.5 Energy demand of water treatment of biodiesel wastewater by ion exchange.

One potential limitation of the ion exchange process is the accumulation of glycerol. Glycerol will be present in the wastewater in small amounts and will not be removed by ion exchange. It would therefore accumulate in the recycled water stream and be fed to the water washing column. The amount of glycerol in the wastewater will typically be in the range of about 0.1 to 0.2 wt%[4]. The presence of small amounts of glycerol in the washing steam is not expected to affect the efficiency of the washing operation. In fact, glycerol has been suggested to be used as the extraction solvent (Bam et al., 1995). However, it could lower the efficiency of phase separation by increasing the viscosity of the washing phase. Therefore, if the accumulation of glycerol does become problematic, it may need to be removed from the recycled wash water periodically by distillation or an alternative method such as adsorption (Liu et al., 2009). Alternatively, a higher purge ratio could be used on the water recycle stream, but this would again increase the fresh water demand.

[4] Chavalparit and Ongwandee (2009) reported a concentration of 0.136 wt% of glycerol

4.5.3 Comparison of Water Treatment Options

A comparison between the total energy required for both the distillation and ion exchange water treatment options is shown in Figure 4.6. The results show that using ion exchange to treat the wastewater results in a decrease in energy requirements of about 69% at a wash water volume ratio of 1:1. The difference between the two treatment options decreases with decreasing water volume. The ion exchange process is more favourable except at water wash volumes less than about 0.15 L per L of biodiesel. This is most likely because the ion exchange resins become less efficient at very high concentrations of sodium chloride.

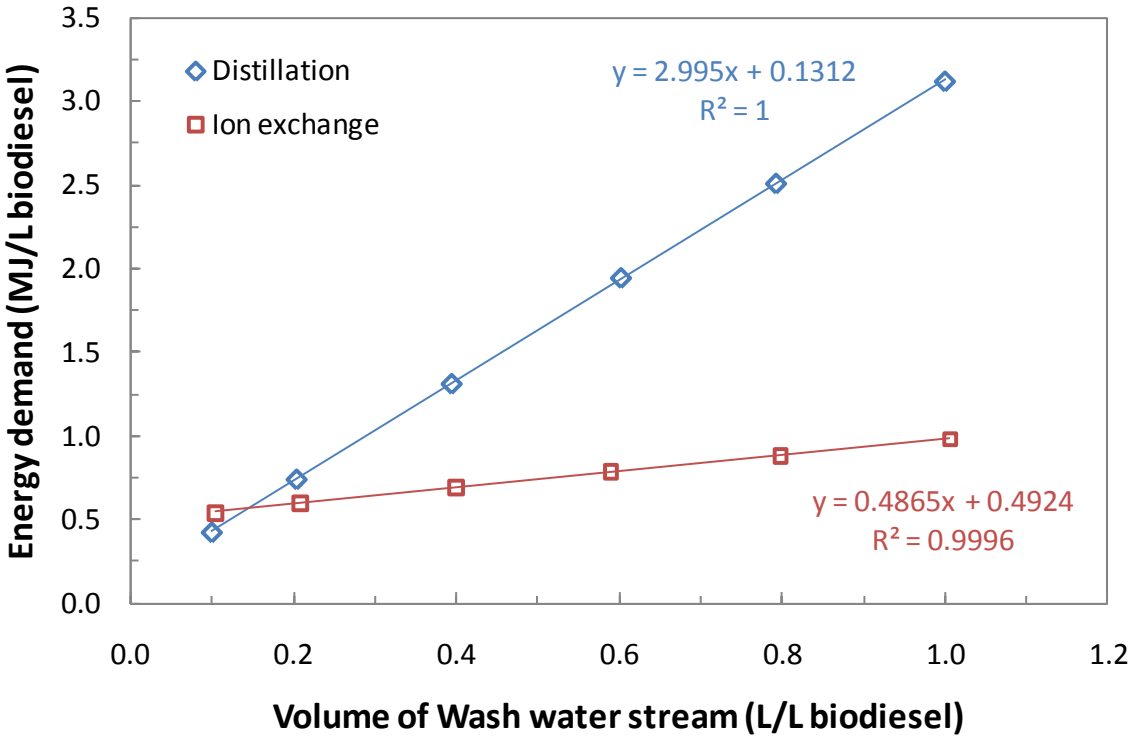

Figure 4.6 Total energy demand of water treatment of biodiesel wastewater.

Biodiesel has a heat of combustion of about 35.2 MJ/L (Mittelbach and Remschmidt, 2004). According to this simulation, at the typical water washing volume ratio of 1:1, the distillation process requires 3.12 MJ of energy for water treatment per litre of biodiesel produced. This is 8.9% of the heat of combustion which represents a reduction in the overall

energy efficiency of the fuel. At the same volume ratio, 0.978 MJ of energy is required to treat each litre of wastewater using the ion exchange process. This represents only 2.8% of the heat of combustion of biodiesel, thereby improving the energy efficiency in comparison to the distillation process.

4.5.4 Effect of Amount of Water

In both processes, reducing the amount of water had a clear impact on the overall energy efficiency of the biodiesel purification process. Both treatment options show a decreasing linear trend with decreasing amounts of wash water. It is clear that the water washing process should be optimized to minimize water and energy requirements. Washing in a counter-current washing configuration as opposed to a cross-current one can reduce the amount of water used in the washing step. The amount of water used in each washing stage must also be chosen such that it optimizes the removal efficiency of the contaminants, while minimizing the amount of wastewater generated.

To optimize the water washing process, the determination of the distribution of impurities between the water and biodiesel phases for all feedstock qualities is important. Such information on the distribution of salts is lacking in the literature and would clearly be useful for process optimization.

4.6 Summary

The treatment and recycle of the wastewater generated by biodiesel production was simulated using Aspen HYSYS process simulation software. By changing the amount of fresh water fed to the process, the effect of the amount of water in the process on the energy requirements of the process was quantified. Furthermore, a comparison between conventional wastewater treatment by distillation and the use of ion exchange resins was made.

Biodiesel production will typically generate about 1 litre of wastewater per litre of biodiesel produced. Under these conditions and using conventional water treatment by distillation, 3.12 MJ of energy are required to purify the wastewater per litre of biodiesel. This represents 8.9% of the heat of combustion of biodiesel, resulting in a reduction in the fuel's overall energy efficiency. The simulations showed that reducing the amount of water

used in the purification process would improve the energy efficiency of the process linearly by reducing the load on the distillation operations.

An alternative process using ion exchange resins was shown to improve the energy efficiency of biodiesel production. This process reduces the amount of purification performed using distillation. After recovering methanol by distillation and removing salt impurities by ion exchange, the wastewater can be directly reused to purify incoming FAME. At the typical water washing ratio of 1:1, the ion exchange process required 0.978 MJ of energy per litre of biodiesel, representing only 2.8% of the heat of combustion of biodiesel. In comparison, to distillation, the ion exchange method reduced the amount of energy by approximately 69%.

The simulation results show the importance of reducing the amount of water used in the purification process. Reducing the amount of energy required for wastewater treatment can represent a cost saving, since it improves the overall energy efficiency of the biodiesel fuel. Also, smaller wastewater streams reduce the size of the required distillation columns, which decreases the capital cost of the plant. If the same degree of purification can be accomplished in a counter-current washing configuration, this would be an ideal way of reducing the amount of wastewater produced.

These results also provide validation for the use of ion exchange for treating the wastewater from a biodiesel process. Further investigation would be required to verify that the resin can effectively and efficiently remove the salt impurities from the wastewater even when other impurities are present. Furthermore, the fate of non-ionic components such as glycerol must also be determined. If the glycerol is not removed prior to recycle, it will accumulate in the recycled wash water stream. Therefore, the limit to which glycerol can be allowed to accumulate would need to be determined. Once these issues have been addressed, the use of ion exchange for wastewater treatment could prove to be a viable, less energy intensive alternative to distillation.

4.7 References

Aspen HYSYS V7.2, Aspen Technology Inc., Cambridge, MA (2011).

Bam, N., D. C. Drown, R. Korus, D. S. Hoffman, T. G. Johnson, and J. M. Washam, "Method for purifying alcohol esters," U. S. Pat. 5,424,467 (1995).

Canakci, M. and J. Van Gerpen, "A pilot plant to produce biodiesel from high free fatty acid feedstocks," Trans. Am. Soc. Agric. Eng. 46 (4), 945-954 (2003).

Chavalparit, O. and M. Ongwandee, "Optimizing electrocoagulation process for the treatment of biodiesel wastewater using response surface methodology," J. Environ. Sci. 21, 1491-1496 (2009).

Dow Water and Process Solutions, "How to Design an Ion Exchange System," Technical information on ion exchange, Accessed in April 2011, Available online: http://www.dowwaterandprocess.com/support_training/literature_manuals/ix_techinfo/designstps_eff.htm.

Elcock, D., "Future U.S. water consumption: The role of energy production," J. Am. Water Resour. Assoc. 46 (3), 447-460 (2010).

Fiedler, E., G. Grossmann, D. B. Kersebohm, G. Weiss, and C. Witte, "Methanol," in "Ullmann's Encyclopedia of Industrial Chemistry," Wiley-VCH, Weinheim, Germany (2005).

Geankoplis, C. J., "Transport Processes and Separation Process Principles," Pearson Education, Inc., Upper Saddle River, NJ (2003).

Gonzalo, A., M. García, J. L. Sánchez, J. Arauzo, and J. A. Peña, "Water cleaning of biodiesel. Effect of catalyst concentration, water amount, and washing temperature on biodiesel obtained from rapeseed oil and used oil," Ind. Eng. Chem. Res. 49, 4436-4443 (2010).

Haas, M. J., A. J. McAloon, W. C. Yee, and T. A. Foglia, "A process model to estimate biodiesel production costs," Bioresource Technol. 97, 671-678 (2006).

LeVan, M. D., G. Carta, "Adsorption and Ion Exchange," in "Perry's Chemical Engineers' Handbook," D. W. Green and R. H. Perry, Eds., McGraw-Hill Companies, Inc., New York, NY (2008).

Liu S., S. R. Musuku, S. Adhikari, and S. Fernando, "Adsorption of glycerol from biodiesel washwaters," Environ. Technol. 30 (5), 505-510 (2009).

Mittelbach, M. and C. Remschmidt, "Biodiesel - The Comprehensive Handbook," Martin Mittelbach (Publisher), Graz, Austria (2004).

Seader, J. D., E. J. Henley, and D. K. Roper, "Separation Process Principles," John Wiley and Sons (2010).

Srivastava, A. and R. Prasad, "Triglycerides-based diesel fuels," Renewable Sustainable Energy Rev. 4, 111-133 (2000).

Van Gerpen, J., B. Shanks, R. Pruszko, D. Clements, and G. Knothe, "Biodiesel Production Technology," U.S. Department of Energy, National Renewable Energy Laboratory, Golden, CO (2004).

West, A. H., D. Posarac, and N. Ellis, "Assessment of four biodiesel production processes using HYSYS.Plant," Bioresource Technol. 99, 6587-6601 (2008).

Zhang, Y., M. A. Dubé, D. D. McLean, and M. Kates, "Biodiesel production from waste cooking oil: 1. Process design and technological assessment," Bioresour. Technol. 89, 1-16 (2003).

4.8 Sample Calculations

Volume of wastewater treated per volume of strong acid cation exchange resin:

$$0.75 \times \frac{1.8\ eq}{L\ resin} \times \frac{mol\ Na^+}{eq} \times \frac{mol\ NaCl}{mol\ Na^+} \times \frac{58.44\ g\ NaCl}{mol\ NaCl} \times \frac{10^6 \mu g}{g} \times \frac{g\ FAME}{577\ \mu g\ NaCl} \times \frac{L\ FAME}{880\ g\ FAME} \times \frac{1\ L\ water}{L\ FAME} = 155\ \frac{L\ water}{L\ resin} \quad (4.5)$$

Volume of wastewater treated per volume of strong base anion exchange resin:

$$0.75 \times \frac{1.0\ eq}{L\ resin} \times \frac{mol\ Cl^-}{eq} \times \frac{mol\ NaCl}{mol\ Cl^-} \times \frac{58.44\ g\ NaCl}{mol\ NaCl} \times \frac{10^6 \mu g}{g} \times \frac{g\ FAME}{577\ \mu g\ NaCl} \times \frac{L\ FAME}{880\ g\ FAME} \times \frac{1\ L\ water}{L\ FAME} = 86.3\ \frac{L\ water}{L\ resin} \quad (4.6)$$

Volume of 4.5% HCl regenerant solution per volume of strong acid cation exchange resin:

$$1.35 \times 0.75 \times \frac{1.8\ eq}{L\ resin} \times \frac{mol\ H^+}{eq} \times \frac{mol\ HCl}{mol\ H^+} \times \frac{36.46\ g\ HCl}{mol\ HCl} \times \frac{100\ g\ regenerant}{4.5\ g\ HCl} \times \frac{L\ regenerant}{1000\ g\ regenerant} = 1.48 \frac{L\ regenerant}{L\ resin} \quad (4.7)$$

Volume of 3.5% NaOH regenerant solution per volume of strong base anion exchange resin:

$$1.80 \times 0.75 \times \frac{1.0\ eq}{L\ resin} \times \frac{mol\ OH^-}{eq} \times \frac{mol\ NaOH}{mol\ OH^-} \times \frac{40.00\ g\ NaOH}{mol\ NaOH} \times \frac{100\ g\ regenerant}{3.5\ g\ HCl} \times \frac{L\ regenerant}{1000\ g\ regenerant} = 1.54 \frac{L\ regenerant}{L\ resin} \quad (4.8)$$

Volume flow of regenerant and rinse water for strong acid cation exchange resin:

$$\frac{1138\ L\ wastewater}{h} \times \frac{L\ resin}{155\ L\ wastewater} \times \left(\frac{1.48\ L\ regenerant}{L\ resin} + \frac{3.5\ L\ rinse\ water}{L\ resin}\right) = 36.6 \frac{L}{h} \quad (4.9)$$

Volume flow of regenerant and rinse water for strong base anion exchange resin:

$$\frac{1138\ L\ wastewater}{h} \times \frac{L\ resin}{86.3\ L\ wastewater} \times \left(\frac{1.54\ L\ water}{L\ resin} + \frac{4.5\ L\ rinse\ water}{L\ resin}\right) = 79.6 \frac{L}{h} \quad (4.10)$$

Total volume flow of regenerant and rinse water:

$$36.6 \frac{L}{h} + 79.6 \frac{L}{h} = 116.2 \frac{L}{h} \quad (4.11)$$

Chapter 5

Sodium Distribution between Water and FAME Phases

5.1 Introduction

Water washing is used to remove unwanted polar components from the crude biodiesel (i.e., fatty acid methyl ester or FAME) including the catalyst which is, depending on the catalyst used, in the form of a sodium salt. The separation is based on the component's relative solubility between the two immiscible phases, i.e., the water phase and the FAME phase. Due to the partition that is formed, multiple wash stages are often required to reduce the component's concentration to an acceptable level. Investigation of the distribution in a single stage is important because it can help predict the behaviour in a multistage operation.

The objective of these experiments was to investigate the removal of sodium from FAME in a single water washing step. Specifically, the distribution of sodium between the two liquid phases was measured to determine the distribution coefficient for both FAME derived from refined canola oil (low free fatty acid (FFA) feedstock) and waste frying oil (high FFA feedstock). For the waste oil derived FAME, the amount of FFA in each phase was also measured to determine its effect on sodium partitioning.

5.2 Experimental Design

5.2.1 Canola Oil Derived FAME

Canola oil was used to produce FAME, as described in Chapter 3 (Section 3.1.1). Samples of FAME were then washed with water containing varying amounts of sodium. The conditions for these washing experiments are shown in Table 5.1. The sodium sulfate concentration of the water phase ranged from 0 to 3000 ppm which corresponded to sodium concentrations up to about 1000 ppm.

Table 5.1 Run conditions for single stage washing of canola oil derived FAME.

Run	Sodium sulfate (Na_2SO_4) concentration (ppm)	Sodium (Na) concentration (ppm)
1	0	0
10	0	0
2	50.0	16.2
6	50.5	16.3
3	99.1	32.1
5	200	64.7
4	402	130
7	1002	324
8	1980	641
11	1984	642
9	2976	963

The order in which the runs were conducted was randomized. Replicate runs were performed at sodium concentrations of 0, 16, and 640 ppm (Runs 1 and 10, 2 and 6, and 8 and 11).

5.2.2 Waste Oil Derived FAME

The run conditions for the waste oil derived FAME are shown in Table 5.2. The range of conditions investigated was the same as for the canola oil derived FAME, however the sodium salt was sodium chloride instead of sodium sulfate. This was to remain consistent with the acid used to neutralize the catalyst, which was sulfuric acid for the canola oil FAME and hydrochloric acid for the waste oil FAME (see Chapter 3, Section 3.1.2).

Table 5.2 Run conditions for single stage washing of waste oil derived FAME.

Run	Sodium chloride (NaCl) concentration (ppm)	Sodium (Na) concentration (ppm)
1	0	0
9	0	0
2	510	201
3	1020	401
8	1503	591
4	1536	604
6	2035	801
5	2037	801
7	2545	1001

Three sets of replicate runs were performed at sodium concentrations of 0, 600, and 800 ppm (Runs 1 and 9, 4 and 8, and 5 and 6). The order in which the runs were conducted was randomized.

5.2.3 Initial Sodium Conductivity

Prior to contacting the water phase with FAME, the conductivity of the water phase was measured to confirm the concentration of sodium salt. The conductivities with respect to initial salt concentration are shown in Figure 3.3 in Chapter 3 and indicate a linear relationship between conductivity and concentration.

5.2.4 Method

For each run condition, 40 mL of the salt solution was contacted with 200 mL of FAME in a 500 mL separatory funnel at ambient temperature using the washing method described in Chapter 3 (Section 3.2). This represented a 5:1 FAME to water volume ratio. These conditions reflect the results of Gonzalo et al. (2010) who performed washing experiments at a 4:1 FAME to water volume ratio and 40°C. Because polar contaminants were reduced to a very low level at these conditions, they recommended using a lower amount of water and a lower washing temperature to improve the economy of the process.

For the waste oil derived FAME runs, slightly acidic water (pH of 4.5) was used by adding hydrochloric acid to the salt solutions. Using acidic water is recommended to help reduce foaming and the formation of emulsions caused by the presence of FFA (Haas et al., 2006).

After the phases were separated, the concentration of sodium was measured in both phases by Inductively Coupled Plasma Optical Emission Spectroscopy (ICP-OES).

5.2.5 Determination of Error

The error bars shown in the figures below represent two standard deviations (95% confidence interval) which were determined using the replicate data.

5.2.6 Initial Concentrations in FAME

The initial concentrations of sodium (Na) were measured by ICP-OES in both unwashed FAME sources and are presented in Table 5.3.

Table 5.3 Initial sodium concentrations in FAME.

Sample	Sodium (Na) concentration (ppm)
Canola oil derived FAME (Batches 1-7)	58.7
Canola oil derived FAME (Batches 8-12)	89.7
Waste oil derived FAME (Batches 3-5)	130.6

The waste oil derived FAME had a higher initial sodium concentration. Both FAME sources used similar catalyst (sodium methoxide) concentrations for the transesterification reaction (see Chapter 3, Section 3.1). However, the waste oil batches required additional sodium methoxide to neutralize the acid catalyst from the esterification pre-treatment. It is therefore reasonable that the waste oil FAME would have a higher initial sodium content.

5.3 Results and Discussion

5.3.1 Sodium Extraction

Figure 5.1 shows the final sodium concentration in the water phase after contacting

with the canola oil derived FAME with respect to the initial sodium concentration. The vertical distance between each data point and the 45° line represents the change in sodium concentration of the water phase which is equal to the quantity removed from the FAME. A linear trend is observed and the slope of the trendline is approximately equal to that of the parity line. This indicates that the quantity of sodium extracted from the FAME in each wash is nearly constant over the range tested.

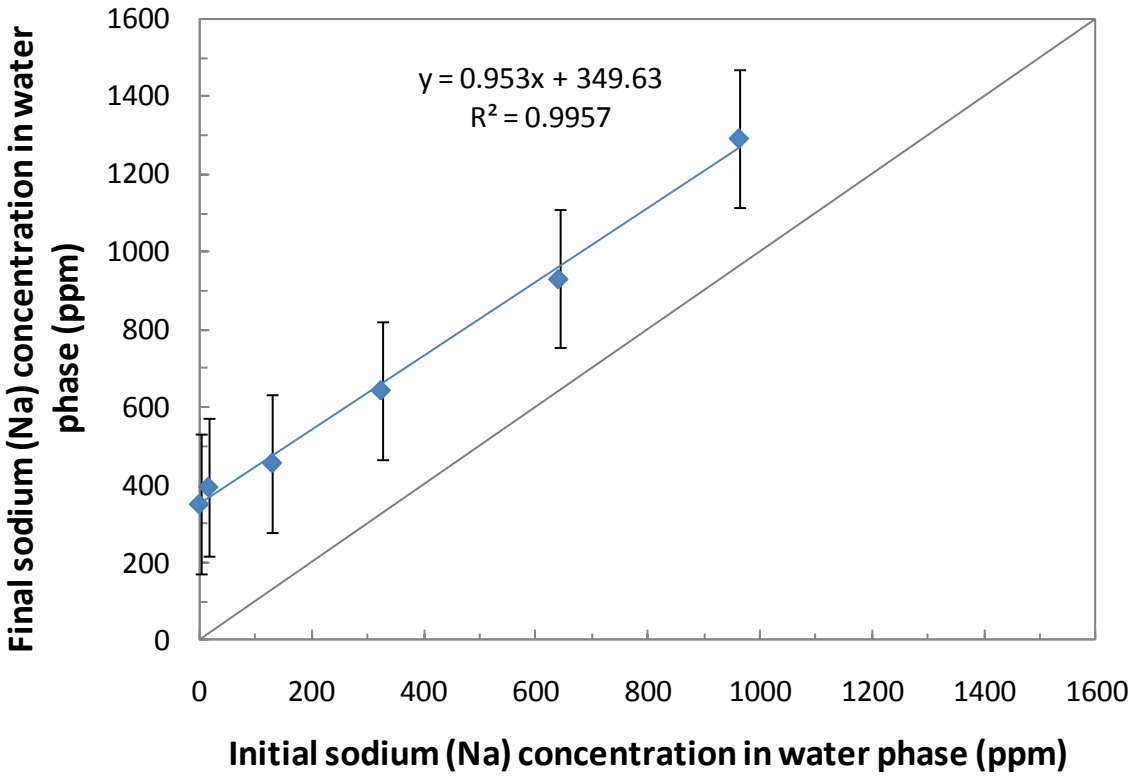

Figure 5.1 Initial and final sodium concentrations in the water phase for the canola oil derived FAME.

The same data for the waste oil derived FAME are shown in Figure 5.2. The data form a linear trend with a slope of approximately 0.69. The slope has a value less than 1, therefore there is a reduction in the amount of sodium extracted at high initial sodium concentrations compared to that at lower initial concentrations.

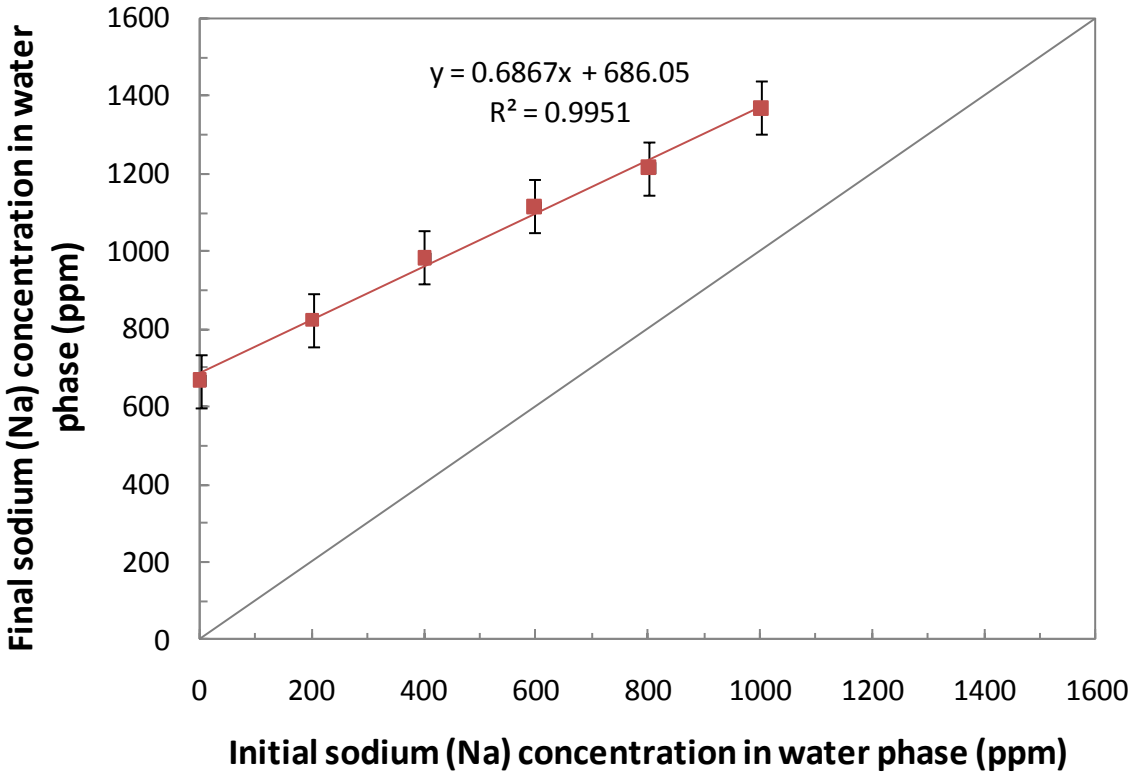

Figure 5.2 Initial and final sodium concentrations in the water phase for the waste oil derived FAME.

5.3.2 Distribution Coefficient

Figure 5.3 shows the final sodium concentrations in the canola oil derived FAME phase with respect to the final concentration in the water phase. The final sodium concentration in the FAME phase remains relatively constant. This indicates that the final concentration achieved by the washing is independent of the initial amount of sodium in the water phase over the range of concentrations studied.

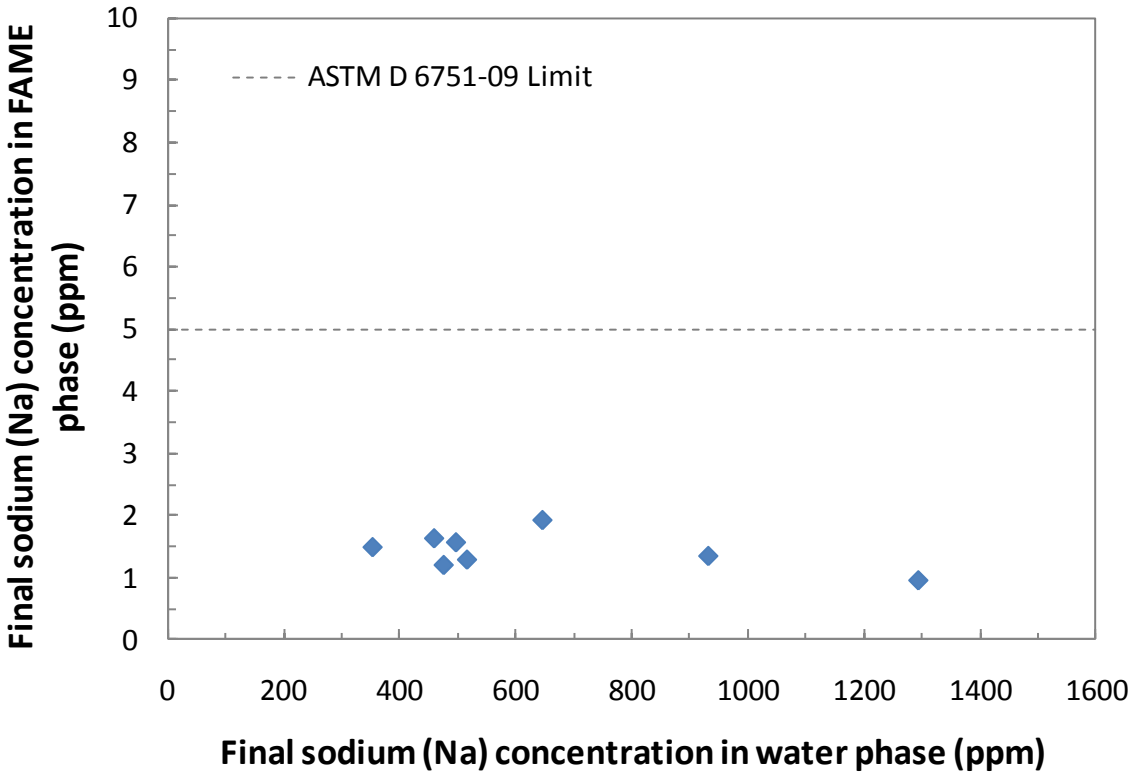

Figure 5.3 Final sodium concentrations in the canola oil derived FAME and water phases.

It should be noted that the ASTM limit for sodium (combined with potassium) is 5 ppm (ASTM D6751, 2009). This specification was therefore achieved, for the canola oil derived FAME, in a single washing step for the full range of concentrations tested. Similar results were also obtained by Gonzalo et al. (2010).

The data in Figure 5.3 can be used to determine the distribution coefficient (K) of sodium between the water and FAME phases. K can be defined as the ratio of the concentration of sodium in the water phase to the concentration in the FAME phase:

$$K = \frac{[Na]_{water}}{[Na]_{FAME}} \tag{5.1}$$

The values of the distribution coefficient as a function of concentration in the water phase are shown in Figure 5.4.

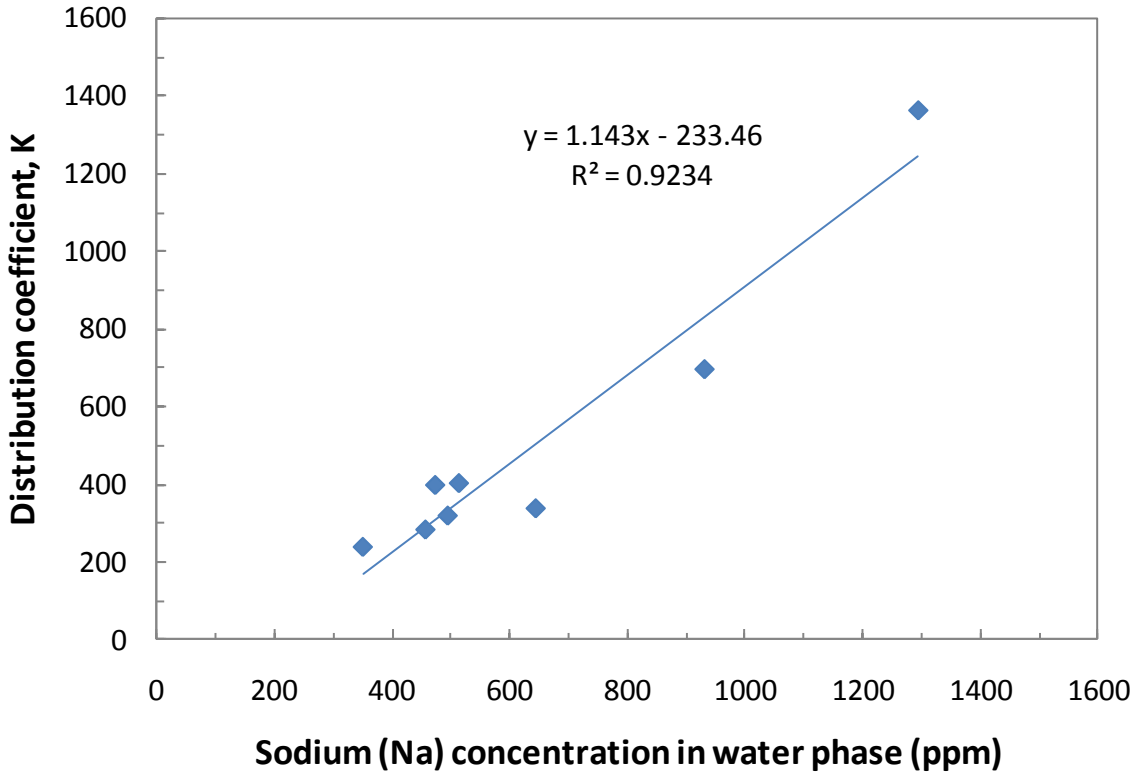

Figure 5.4 Distribution coefficient of sodium between the water and FAME phases for the canola oil derived FAME as a function of the concentration in the water phase.

The distribution coefficient was found to be very high, ranging from 238 to 1363. This is because the concentration of sodium in the FAME phase, as seen in Figure 5.3, was very low, with an average value of 1.4 ppm. Regardless of the total quantity of sodium in the system, almost all will partition into the water phase. Furthermore, because the concentration in the FAME phase is relatively constant, the trend in Figure 5.4 is approximately linear; this is because it depends primarily on the concentration in the water phase.

The high removal efficiency of sodium from FAME by water is due to the difference in relative permittivities of the two solvents. The relative permittivity of a solvent (ε_r), also referred to as the dielectric constant, is a relative measure of a solvent's polarity and influences the dissolution and dissociation of electrolytes (Izutsu, 2002). At 20°C, water has a relative permittivity of 80.20 (Dean, 1999) whereas methyl oleate, a common fatty acid methyl ester found in biodiesel, has a relative permittivity of only 3.211 (Gouw and Vlugter, 1964). For solvents with $\varepsilon_r<10$, the fraction of electrolytes dissociated into ions is small.

Conversely, in high-permittivity solvents with ε_r>40, electrolytes dissociate almost completely into ions (Izutsu, 2002). As a result, the sodium will transfer from the FAME phase to the water phase in the form of dissolved sodium sulfate salts.

Figure 5.5 shows the final sodium concentrations in the waste oil derived FAME phase with respect to the final concentration in the water phase. For comparison, the data for the canola oil derived FAME are also shown.

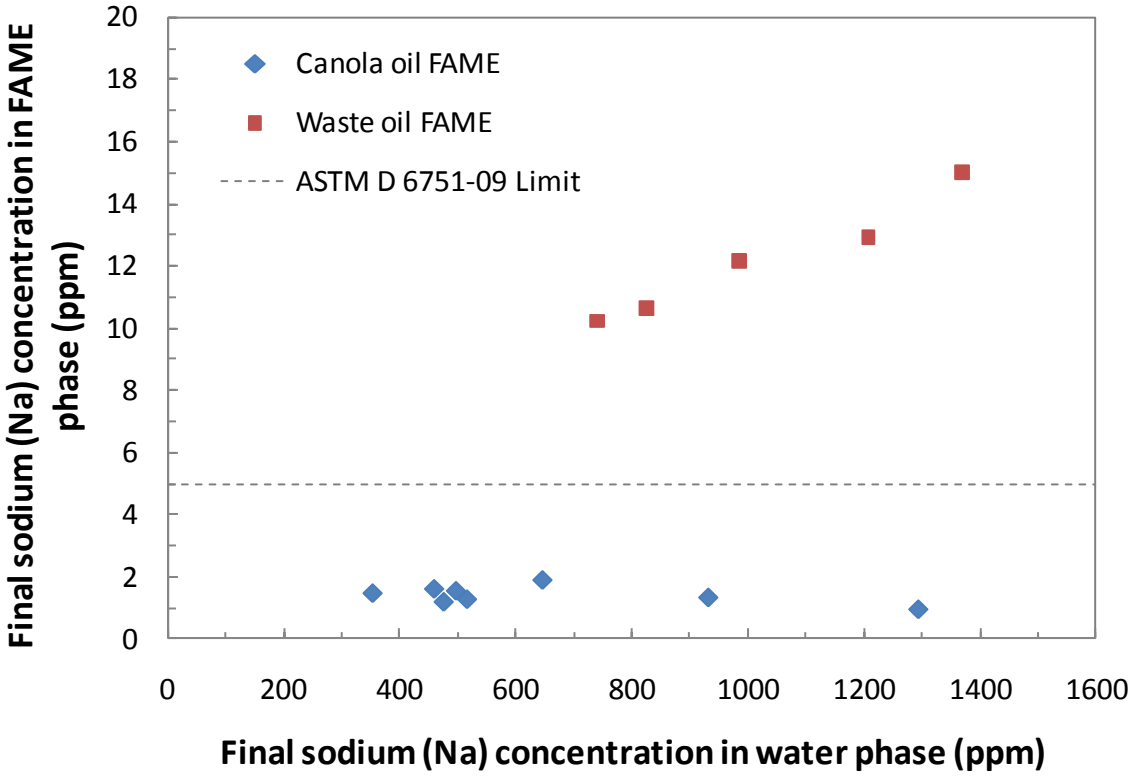

Figure 5.5 Final sodium concentrations in the waste and canola oil derived FAME and water phases.

The reduction in sodium extraction observed in Figure 5.2 is reflected in Figure 5.5. At higher initial sodium concentrations, less sodium is extracted to the water phase, resulting in a higher concentration in the FAME phase. As a consequence, it is not possible to extract all the sodium from the FAME phase in a single washing step. It was also observed that the specification for sodium (5 ppm) was not met for any of the runs for the waste oil derived

FAME. Therefore, multiple washes would be necessary to achieve the required level of purification.

The distribution coefficient (K) for the waste oil derived FAME is shown in Figure 5.6 along with the canola oil FAME data for comparison. The vales of K are found to range between approximately 72 to 93, much less than the values for the canola oil derived FAME.

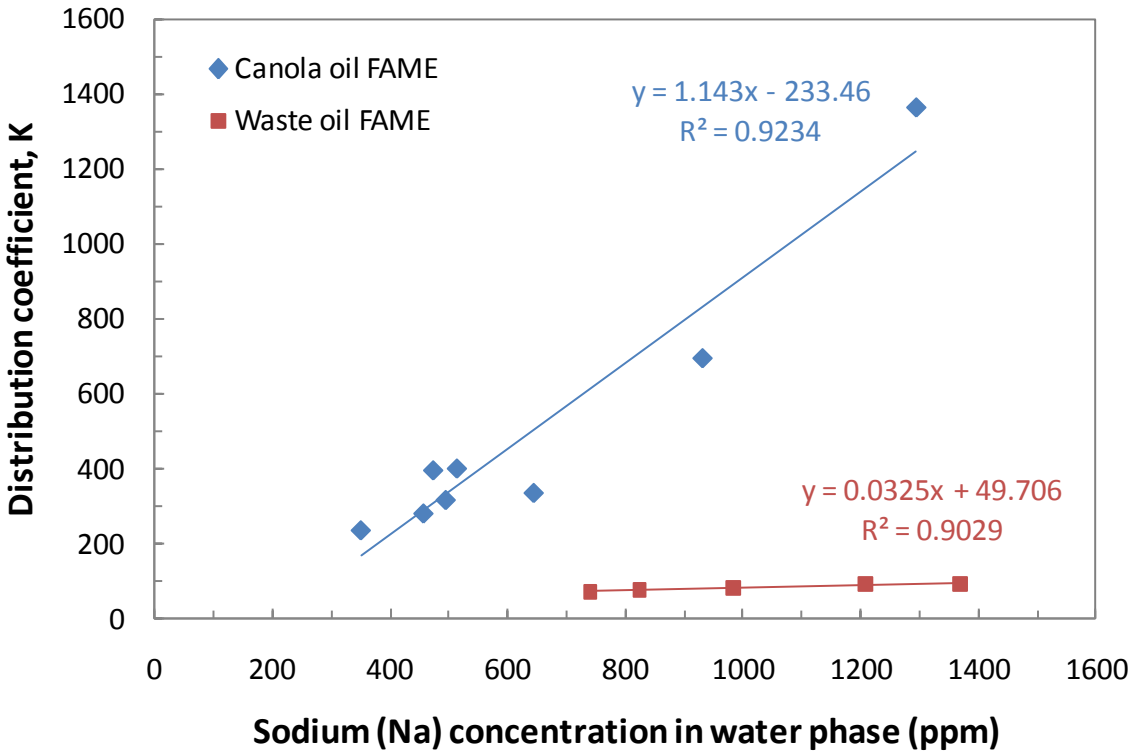

Figure 5.6 Distribution coefficient of sodium between the water and FAME phases for the waste and canola oil derived FAMEs as a function of the concentration in the water phase.

5.4 Free Fatty Acid (FFA) Extraction

Because the distribution coefficient for the waste oil derived FAME was found to be much lower than that of the canola oil derived FAME, it can be reasoned that there is an added factor affecting the removal of sodium. The difference in sodium removal can be attributed to the presence of FFA in the waste oil derived FAME, as described below.

For the waste oil derived FAME runs, the initial and final FFA concentrations were measured by titration (see Chapter 3, Section 3.4) to determine the amount of soap extracted

at each run condition. The initial FFA concentration in the FAME was measured to be (3552 ± 64) ppm which corresponds to a mass of (612 ± 11) mg. The final masses of FFA in both phases after washing are shown in Figure 5.7.

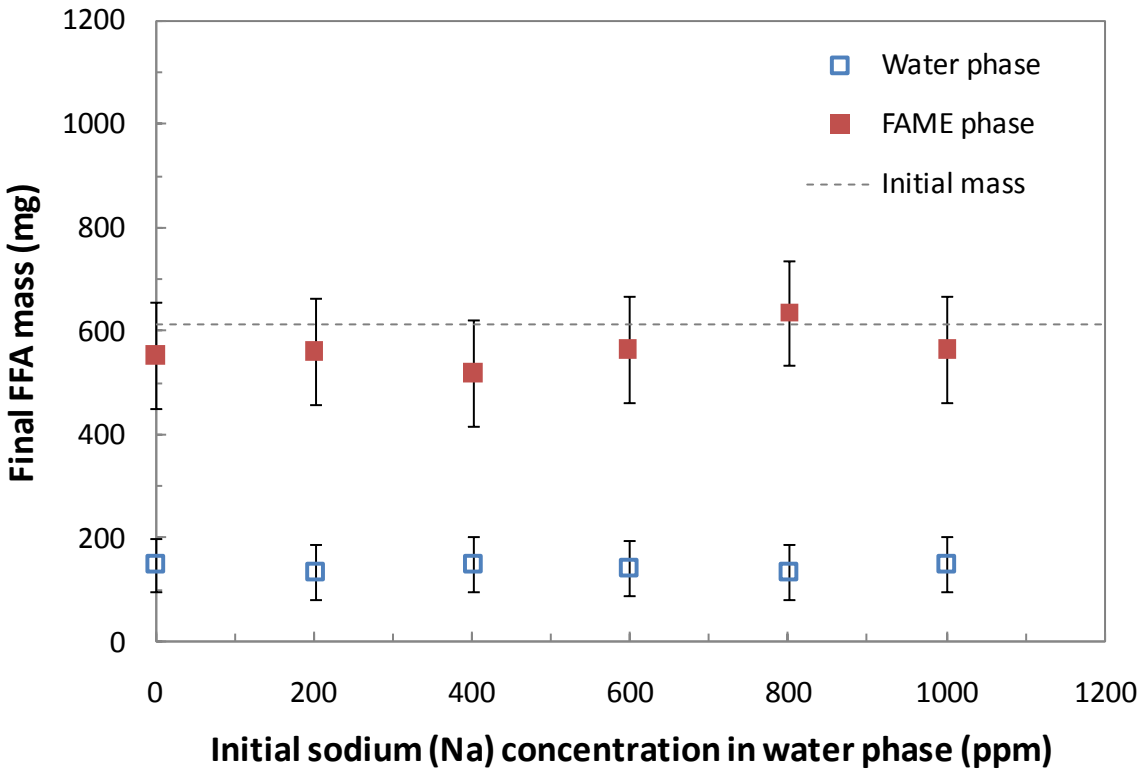

Figure 5.7 Final mass of FFA in the water and waste oil derived FAME phases with respect to initial sodium concentration in the water phase.

Figure 5.7 shows that FFA removal from the FAME phase was not significant. In fact, only 7% was removed, on average. The low quantity of FFA removed results from the use of acidic water, which is often recommended because it reduces foaming and the formation of emulsions. However, the acidic water shifts the equilibrium between FFA and soap toward the formation of FFA, which is not soluble in water. As a result, FFA removal was minimal over the full range of concentrations tested.

There is an apparent inconsistency in the mass balance of the system. The final amount of FFA measured in the water phase plus that in the FAME phase is greater than the initial measured mass, on average, by about 16%. Therefore, either the water measurements

are too high or the FAME measurements are too low. Since the titration method for measuring FFA is intended for biodiesel samples, it is possible that it is less accurate for water samples. Thus, it is possible that the measured FFA concentrations in the water phase are too high.

The concentrations of FFA in both phases are presented in Figure 5.8, along with the concentration measured at the interface between the two phases. Although the concentrations in the bulk phases remain relatively constant, there is an increase of FFA concentration at the interface for high initial sodium concentrations.

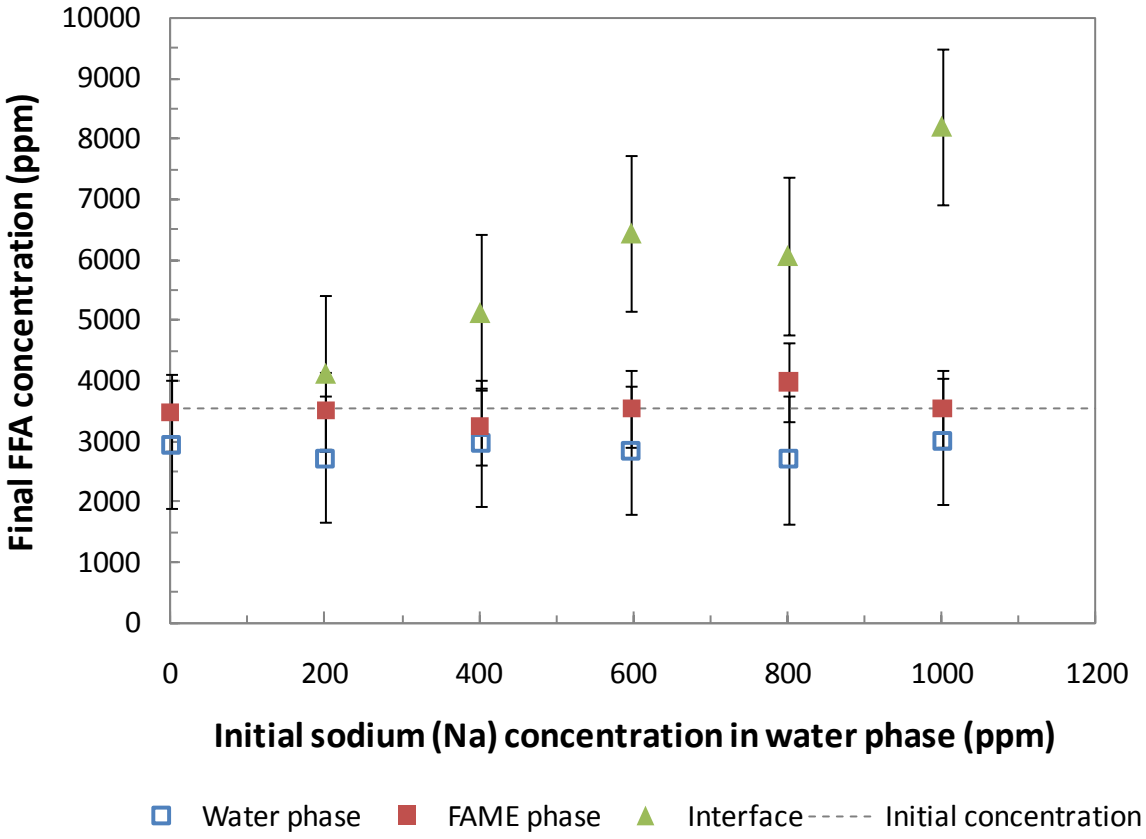

Figure 5.8 Final FFA concentration in the water and waste oil derived FAME phases with respect to initial sodium concentration in the water phase.

This accumulation of FFA at the interface explains the partitioning of sodium that was observed for the waste oil FAME washing runs (refer to Figure 5.5). The presence of FFA interacts with sodium removal by forming soap, as seen in Figure 5.9. Due to the

amphiphilic nature of soap, it acts as an emulsifier between the water and FAME phases. The hydrophilic head of the soap molecule interacts with the water phase while the hydrophobic tail interacts with the oil phase, creating an emulsion. After the washing process, the two phases were allowed to settle, during which time the soap molecules accumulated at the interface (Rosen, 2004).

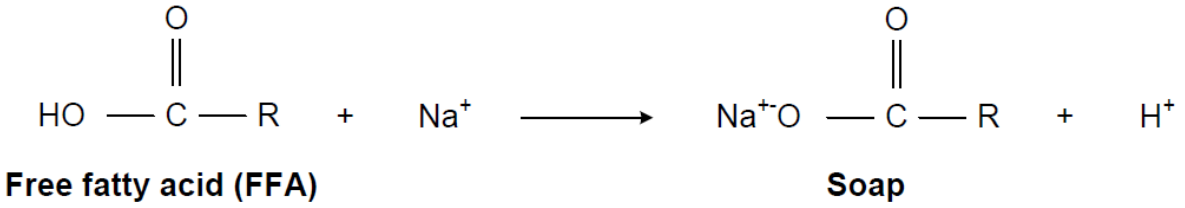

Figure 5.9 Reaction of FFA with sodium to form soap.

The results in Figure 5.8 indicate that with higher levels of sodium in the system, there is an increased amount of soap accumulation at the interface. This explains the observed partitioning of sodium in the FAME phase. When the phases were separated, the emulsified interface was kept with the FAME phase to avoid product loss. Keeping this interface influenced the concentration of sodium that was measured in the FAME phase.

5.5 Summary

FAME samples produced from both canola oil and waste frying oil were purified in a single water washing step. For the canola oil derived FAME, the specifications for sodium (5 ppm) were met within one washing step. The distribution coefficient for sodium was found to be high, ranging from approximately 238 to 1363. This indicates that sodium will almost completely partition into the water phase over the range of concentrations tested.

For the waste oil derived FAME, multiple washing stages would be necessary to achieve the 5 ppm specification. The incomplete extraction of sodium was caused by the presence of FFA in the FAME, which interacted with the sodium to form soap. The soap accumulated at the interface between the two phases, resulting in a distribution of sodium between the FAME and water phases. The distribution coefficient was found to range from approximately 72 to 93 over the range of concentrations studied.

The interaction of FFA in the removal of sodium stresses the need for complete

conversion of FFA in the acid esterification pre-treatment, and also the need for low concentrations of water in the transesterification mixture to reduce formation of FFA by saponification. The waste oil derived FAME used in these experiments was produced using an acid esterification pre-treatment followed by base transesterification. The initial level of FFA was approximately 3600 ppm (or 0.36 wt%). A lower FFA level would reduce the concentration of soap prior to the washing step. This would improve sodium extraction to the water phase because less would accumulate at the interface as soap.

The results show that sodium removal can still be accomplished in the presence of 0.36 wt% FFA, since a reduction in concentration was observed. However, in that case, multiple washes are required, resulting in high water use. Ensuring the FFA level is as low as possible will therefore help to reduce the amount of water required when purifying FAME produced with high FFA feedstocks such as waste frying oil.

FFA removal by water washing was not found to be significant when using acidic water. The alternative is to use basic or neutral water, which promotes the formation of emulsions leading to operational difficulties. Another option for FFA removal is to first remove any interface layer formed; however, this will represent a loss of product. This further highlights the complications that arise from the presence of FFA, and illustrates the need for reduced FFA levels when purifying FAME by water washing.

5.6 References

ASTM Standard D6751, "Standard specification for biodiesel fuel blend stock (B100) for middle distillate fuels," ASTM International, West Conshohocken, PA (2009).

Dean, J. A., "Section 5 - Physical Properties," in "Lange's Handbook of Chemistry ," J. A. Dean, Ed., McGraw-Hill, Inc., New York, NY (1999).

Gonzalo, A., M. García, J. L. Sánchez, J. Arauzo, and J. A. Peña, "Water cleaning of biodiesel. Effect of catalyst concentration, water amount, and washing temperature on biodiesel obtained from rapeseed oil and used oil," Ind. Eng. Chem. Res. 49, 4436-4443 (2010).

Gouw, T. H. and J. C. Vlugter, "Physical properties of fatty acid methyl esters. V. Dielectic constant," J. Am. Oil Chem. Soc. 41, 675-678 (1964).

Haas, M. J., A. J. McAloon, W. C. Yee, and T. A. Foglia, "A process model to estimate biodiesel production costs," Bioresource Technol. 97, 671-678 (2006).

Izutsu, K. “Electrochemistry in Nonaqueous Solutions,” Wiley-VCH, Weinheim, Germany (2002).

Rosen, M. J., “Surfactants and Interfacial Phenomena,” John Wiley & Sons, Inc., Hoboken, NJ (2004).

Chapter 6

Counter-Current Washing of Waste Oil Derived FAME

6.1 Introduction

As seen in Chapter 5, fatty acid methyl ester (FAME) produced from low free fatty acid (FFA) feedstock such as refined canola oil requires only one water washing step to reduce the concentration of sodium below the required limit of 5 ppm (ASTM D6751, 2009). Conversely, FAME produced from high FFA feedstocks such as waste frying oil will require multiple washing stages due to the interaction of FFA with sodium to form soap. In multistage liquid-liquid extraction, two common solvent contacting options, in this case water, are cross-current or counter-current, using either batch-wise or continuous operation (Frank et al., 2008).

In the current literature concerning water washing of biodiesel, samples are typically washed repeatedly with water, sometimes up to ten times (Predojević, 2008). This represents a cross-current contacting scheme and, on an industrial level, is not an efficient use of water. To conserve water and produce a more concentrated wastewater stream, a counter-current multiple-stage process should be used. As a result, less wastewater is produced, and less energy is required for downstream wastewater treatment. This will improve the overall energy efficiency and environmental impact of the biodiesel production process.

To reduce water use, Maliszewski et al. (2008) recommended recycling the spent wash water from biodiesel production and using a counter-current contacting scheme. However, experimental data from such a process have not yet been presented in the literature.

In this chapter, cross- and counter-current washing processes were simulated by solving the material balances for each process stage in conjunction with the equilibrium relationship obtained in Chapter 5. Experiments were also performed to compare sodium removal in a cross-current water washing scheme to that of a counter-current scheme and to evaluate the potential water reduction. The experiments were performed in a laboratory scale approximation of a counter-current contacting scheme, which employed repeated cross-current batch washing experiments. Finally, the simulation results were compared to the experimental data.

6.2 Simulations

To simulate the removal of sodium from FAME by multistage water extraction, equilibrium data for the distribution of sodium between the FAME and water phases are required. These data were previously obtained from the single stage experiments for the waste oil derived FAME (see Figure 5.5 in Chapter 5), and are shown again in Figure 6.1.

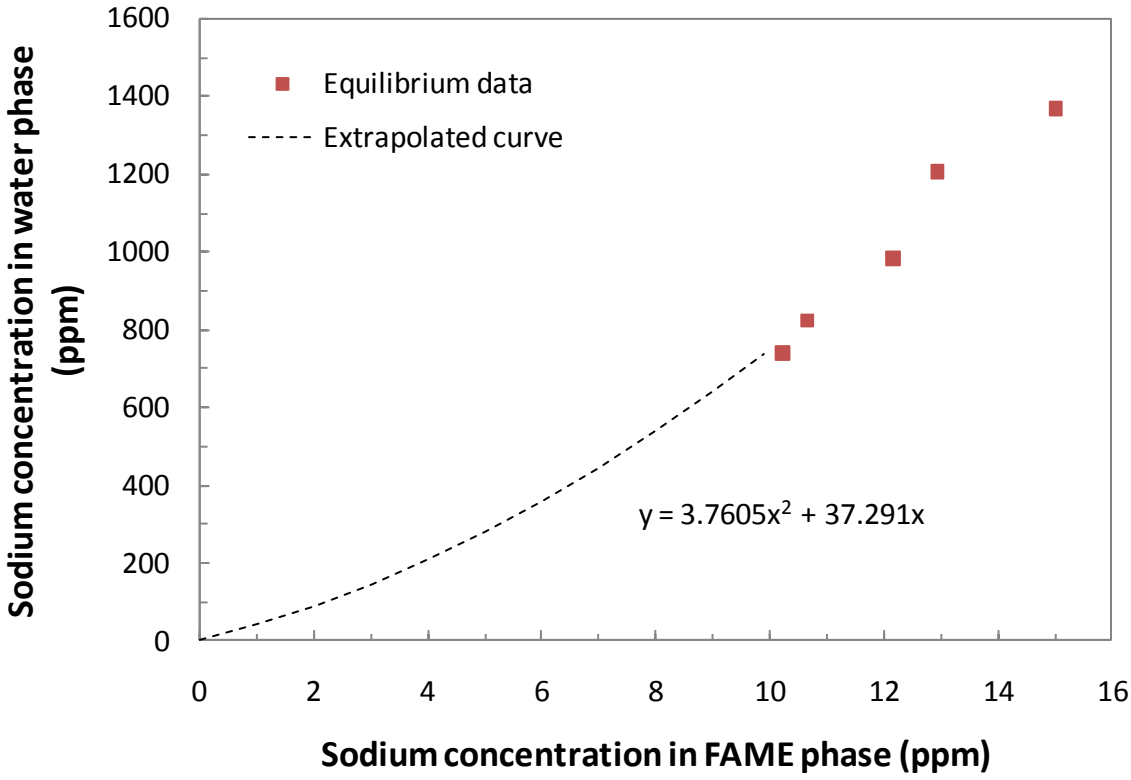

Figure 6.1 Equilibrium data for sodium distribution between FAME and water phases as determined from single stage washing experiments.

Unfortunately, there are no experimental data points in Figure 6.1 at very low concentrations in the FAME phase. The equilibrium was therefore estimated by extrapolating the curve to the origin. A second order polynomial was assumed for the extrapolation, due to lack of better information and because a linear equation would not cross the origin.

It is observed that there is a large difference in the scale of the two axes in Figure 6.1. Because sodium salts are more soluble in water in comparison to FAME, the partitioning of sodium will favour the water phase. As a result, a large quantity of sodium can be removed

from the FAME in one washing step. However, as concluded in Chapter 5, one water washing step was not sufficient to meet the ASTM limit of 5 ppm.

6.2.1 Cross-Current Washing

In a cross-current contacting scheme, shown in Figure 6.2, the crude FAME containing a high level of contaminants (F_0) is washed sequentially in multiple stages, each time using fresh water (W_0).

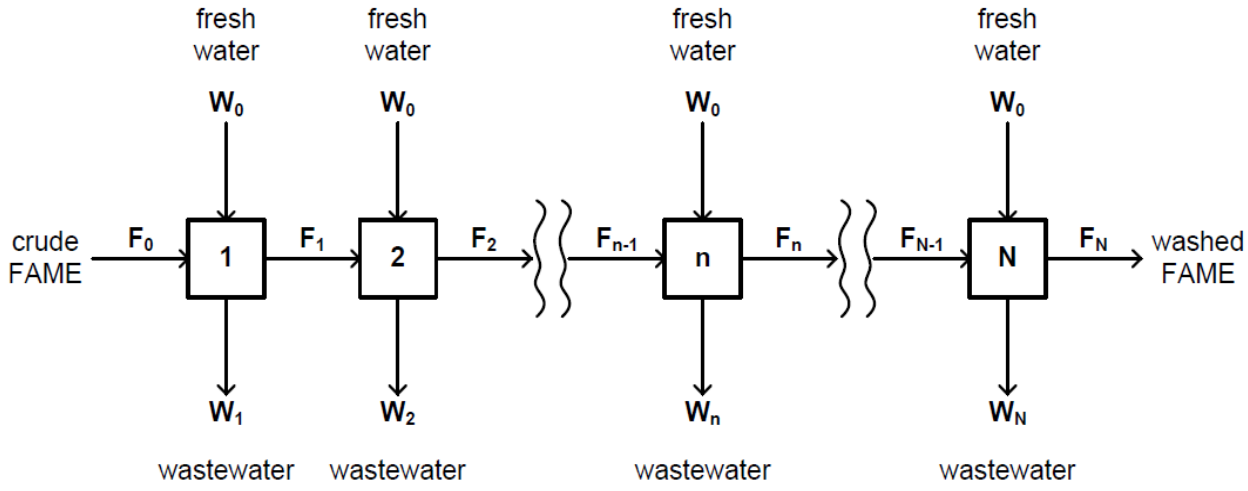

Figure 6.2 Cross-current multistage extraction process flow diagram.

Assuming that the water and FAME phases are immiscible, a mass balance on sodium around each stage can be used to determine the amount of sodium exchanged between the two phases:

$$F_{n-1}x_{n-1} + W_0y_0 = F_nx_n + W_ny_n \tag{6.1}$$

where F_n is the mass of FAME at stage n, W_n is the mass of water at stage n, x_n is the concentration of sodium in the FAME phase at stage n, and y_n is the concentration of sodium in the water phase at stage n. The units of mass for F_n and W_n represent batch-wise operation whereas units of flow (i.e., mass per unit time) would be required for continuous operation.

The concentration of sodium in the fresh water streams (y_0) is always equal to zero. Furthermore, the equilibrium relationship from Figure 6.1 can be used to replace one of the concentrations at stage n. Therefore, Equation (6.1) becomes:

$$F_{n-1}x_{n-1} = F_n x_n + W_n \cdot f(x_n) \tag{6.2}$$

where

$$f(x_n) = 3.7605\, x_n^2 + 37.291\, x_n \tag{6.3}$$

Note that all concentrations must be kept in units of ppm (µg/g) in order to use Equation (6.3).

Knowing the initial concentration of sodium in the feed FAME (x_0), Equation (6.2) was solved starting from the first stage and continuing until the concentration in the exiting FAME (x_N) was below the required limit of 5 ppm.

6.2.2 Counter-Current Washing

The counter-current process is depicted in Figure 6.3 with N number of stages (Geankoplis, 2003). The crude FAME containing a high level of contaminants (F_0) is contacted with fresh water (W_{N+1}) to produce FAME with a low level of contaminants (F_N).

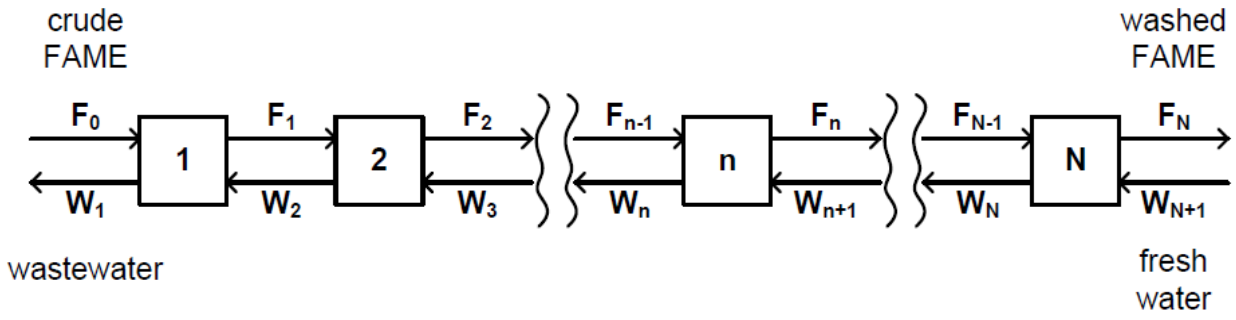

Figure 6.3 Counter-current multistage extraction process flow diagram.

Mass balances around each stage produce the following system of equations:

$$F_{n-1}x_{n-1} + W_{n+1}y_{n+1} = F_n x_n + W_n y_n \tag{6.4}$$

Substituting the equilibrium relationship, Equation (6.3), yields:

$$F_{n-1}x_{n-1} + W_{n+1} \cdot f(x_{n+1}) - F_n x_n - W_n \cdot f(x_n) = 0 \tag{6.5}$$

This leaves a system of nonlinear coupled equations. For small systems such as the one presented here, the system can be solved by minimizing the global sum of squares of the errors of the equations. This was done using the solver feature in Microsoft Excel.

6.2.3 Simulation Conditions

The conditions used for the simulations were the same as those used for the experimental work (discussed in Section 6.3) and are shown in Table 6.1. The initial sodium concentration of FAME Batches 6-9 (used for the experimental work) was determined by Inductively Coupled Plasma Optical Emission Spectroscopy (ICP-OES) to be 260 ppm.

Table 6.1 Simulation conditions.

Parameter	Value
Mass of FAME, F_0	172 g
Mass of water, W_0	40 g
Initial sodium concentration in FAME, x_0	260 ppm

It should be noted that the mass of the FAME and water phases did not remain constant for all the contacting stages for the experimental work. It was found in the first stage that on average there was a 7% reduction in mass due to methanol removal, and each subsequent stage experienced, on average, a 4% reduction in mass due to product loss to the water phase. This reduction in phase mass was taken into account when solving Equations (6.2) and (6.5). That is, the mass was not held constant in the simulations.

6.2.4 Simulation Results

For both cross-current and counter-current extraction schemes, the simulations required two washing stages to reach the ASTM limit for sodium of 5 ppm. These results are shown in Figure 6.4.

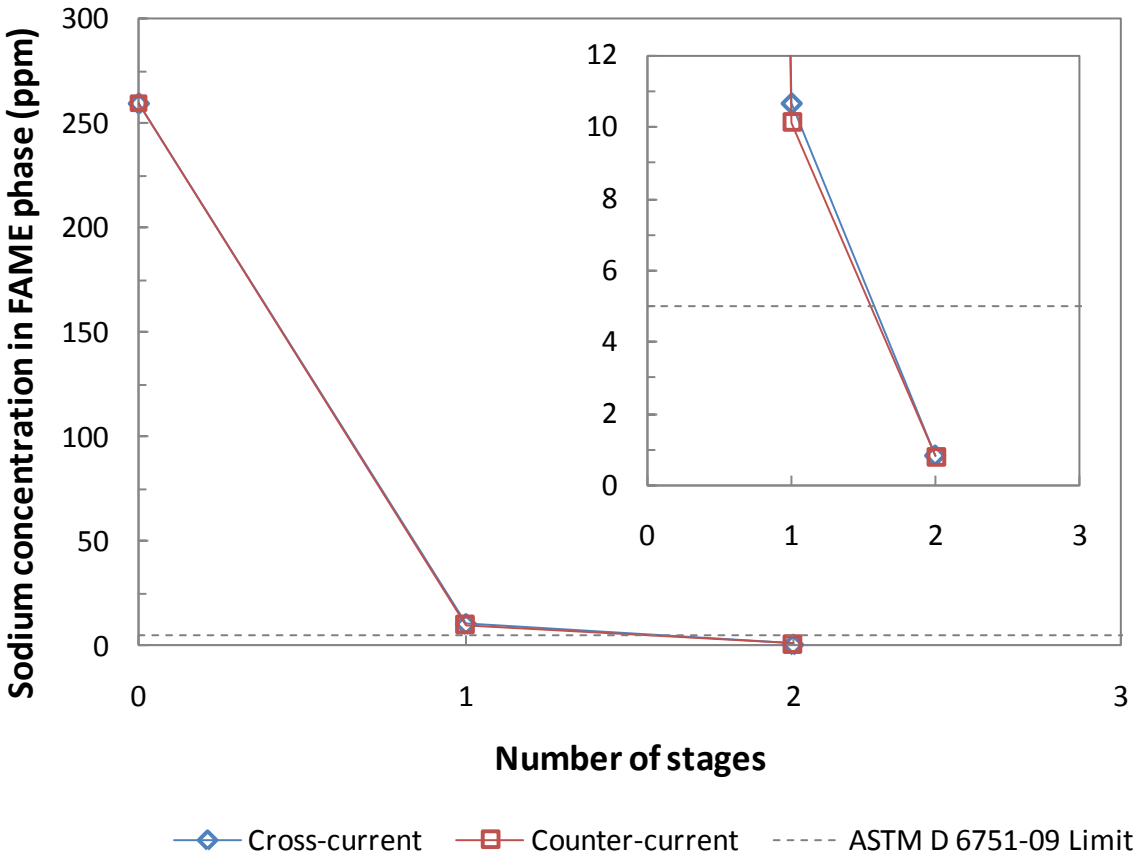

Figure 6.4 Concentration of sodium remaining in the FAME phase for the cross-current and counter-current simulations. The inset shows a close-up at concentrations close to 5 ppm.

Because sodium has a relatively high affinity for water in comparison to FAME, a large fraction of the sodium is removed in the first washing stage, reducing the concentration to about 10 ppm. However, a second stage is required to bring the concentration below 5 ppm. The final concentration reached is approximately 0.8 ppm.

The performance of both washing schemes is very similar. The cross-current scheme used a total of 80 mL of water, whereas the counter-current scheme used only 40 mL. This represents a 50% reduction of water use, thereby making the counter-current scheme the more efficient process.

6.3 Experimental Design

The following experiments used FAME produced from waste frying oil (Batches 6-9 combined) as described in Chapter 3, Section 3.1.2. The washing method was the same used

in the single stage water washing experiments (described in Chapter 3, Section 3.2) in a 5:1 FAME to water volume ratio (200 mL of FAME and 40 mL of water). After each wash, the phases were allowed to settle overnight before being separated. The conductivity of the water phase was then measured. The degree of sodium extraction was determined using a conductivity calibration curve determined from the single stage washing experiments (see Chapter 3, Section 3.3.2 for calibration curve).

6.3.1 Determination of Error

The error in the conductivity measurements was determined by repeating the measurements on separate occasions and was found to be approximately 25 μS/cm (two standard deviations). The errors in all subsequent calculations were determined using error propagation formulas. The error bars in all figures below represent two standard deviations, or a confidence interval of 95%.

6.3.2 Cross-Current Washing

The cross-current washing sequence is shown in Figure 6.5. The first step involved washing a single sample of FAME (200 mL) with fresh, deionized water (40 mL) in a separatory funnel. After the phases were separated, the conductivity of the water phase (W1A) was measured. The FAME was repeatedly washed each time using fresh water until the conductivity of the used water phase was low. This indicated that the majority of the salts, mainly sodium salts, had been removed. As seen in the results shown in Figure 6.8, five stages were required to reduce the conductivity below 10 μS/cm.

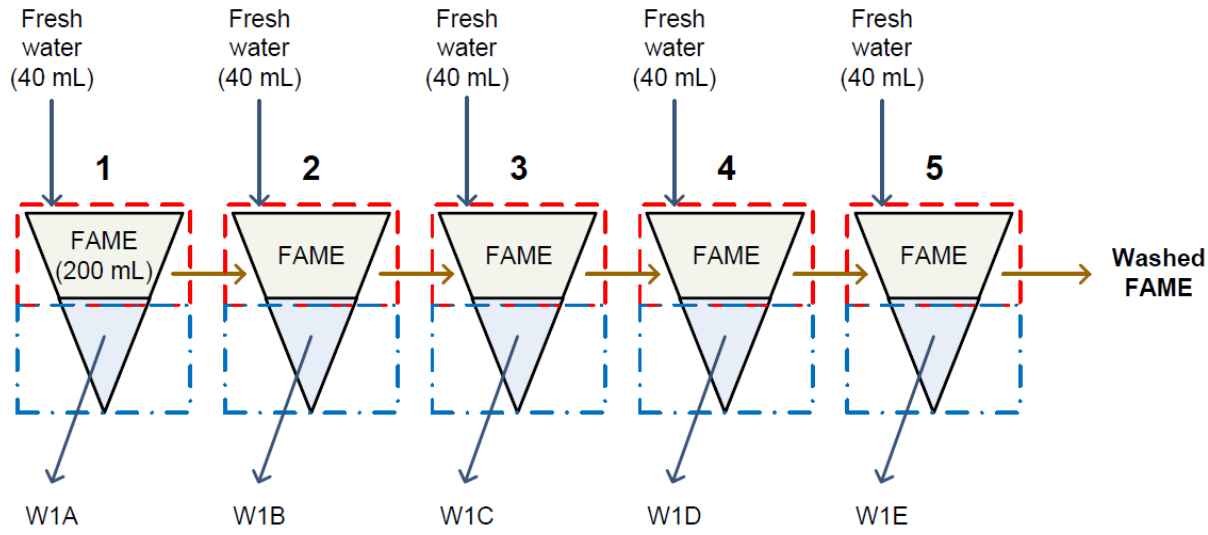

Figure 6.5 Cross-current washing sequence.

The measured conductivities (κ) were used to estimate the concentration of sodium in each of the water phases. The calibration curve, Equation (6.6), was determined using the results from the single stage washing experiments, where κ is the conductivity (µS/cm) and $C_{Na\ in\ water}$ is the concentration of sodium in the water phase (ppm).

$$\kappa = 2.159\ C_{Na\ in\ water} \tag{6.6}$$

The mass of sodium extracted ($m_{Na\ \ extracted}$) is then equal to the change in concentration of the water phase multiplied by the mass of the water phase (m_{water}):

$$m_{Na\ extracted} = \Delta C_{Na\ in\ water} \cdot m_{water} \tag{6.7}$$

For the cross-current sequence, the initial concentration was always equal to zero, therefore the change in concentration was equal to the final concentration.

It is assumed that essentially all of the sodium was extracted from the FAME over the five washing steps. Therefore the sum of the sodium extracted can be used to estimate the initial mass of sodium in the FAME:

$$m_{initial\ Na\ in\ FAME} = \sum_{i=1}^{5} m_{Na\ extracted\ at\ stage\ i} \tag{6.8}$$

The mass of sodium remaining in the FAME phase can then be calculated at each washing step by subtracting the amount extracted to the water phase:

$$m_{Na\ in\ FAME\ after\ stage\ n} = m_{initial\ Na\ in\ FAME} - \sum_{i=1}^{n} m_{Na\ extracted\ at\ stage\ i} \tag{6.9}$$

The concentration of sodium remaining in the FAME phase can then be calculated by dividing the mass of sodium by the mass of the FAME phase:

$$C_{Na\ in\ FAME\ after\ stage\ n} = \frac{m_{Na\ in\ FAME\ after\ stage\ n}}{m_{FAME\ after\ stage\ n}} \tag{6.10}$$

The error in each of the above calculations was determined by calculating the error propagation using the error from the conductivity and mass measurements.

6.3.3 Counter-Current Washing

It is difficult to perform a true counter-current washing sequence on a batch-wise laboratory scale since it requires continuous operation in order to reach steady-state. Therefore, a laboratory scale approximation to a counter-current extraction process was conceived. Similar experimental setups have been used before in order to test the feasibility of a counter-current extraction process (Haque et al., 1987; Masscheleyn et al., 1996).

Referring to Figure 6.6, the counter-current washing sequence started with a cross-current sequence. In the second series of washes, a second sample of FAME (FAME2) was contacted with water phase W1B from the previous series. Note that the letter in the water phase label represents the particular water phase and the number represents how many times the water has been used. Therefore, after the first wash in Series 2, the water phase is now labelled W2B and its new conductivity was measured. Following this wash, each of the remaining water phases from Series 1 was re-used (W1C, W1D, and W1E) to wash FAME2 and fresh water (W1F) was used in the final fifth stage.

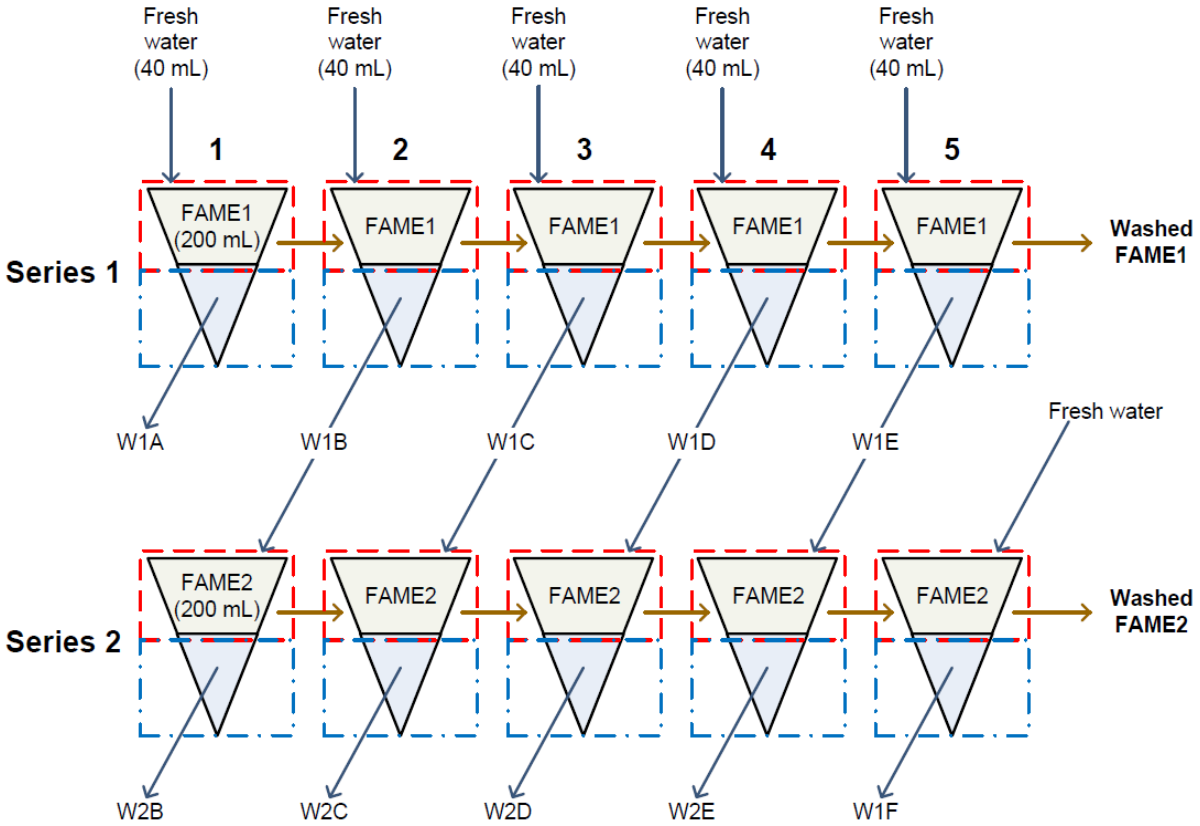

Figure 6.6 First two series of washes in the counter-current washing sequence.

This process was continued for Series 3, 4, and 5, as shown in Figure 6.7. The water phase that was used for the first stage of Series 5 had been used 5 times. At the second stage, the water had been used 4 times, and so on. This fifth series of experiments is assumed to approach a counter-current washing configuration.

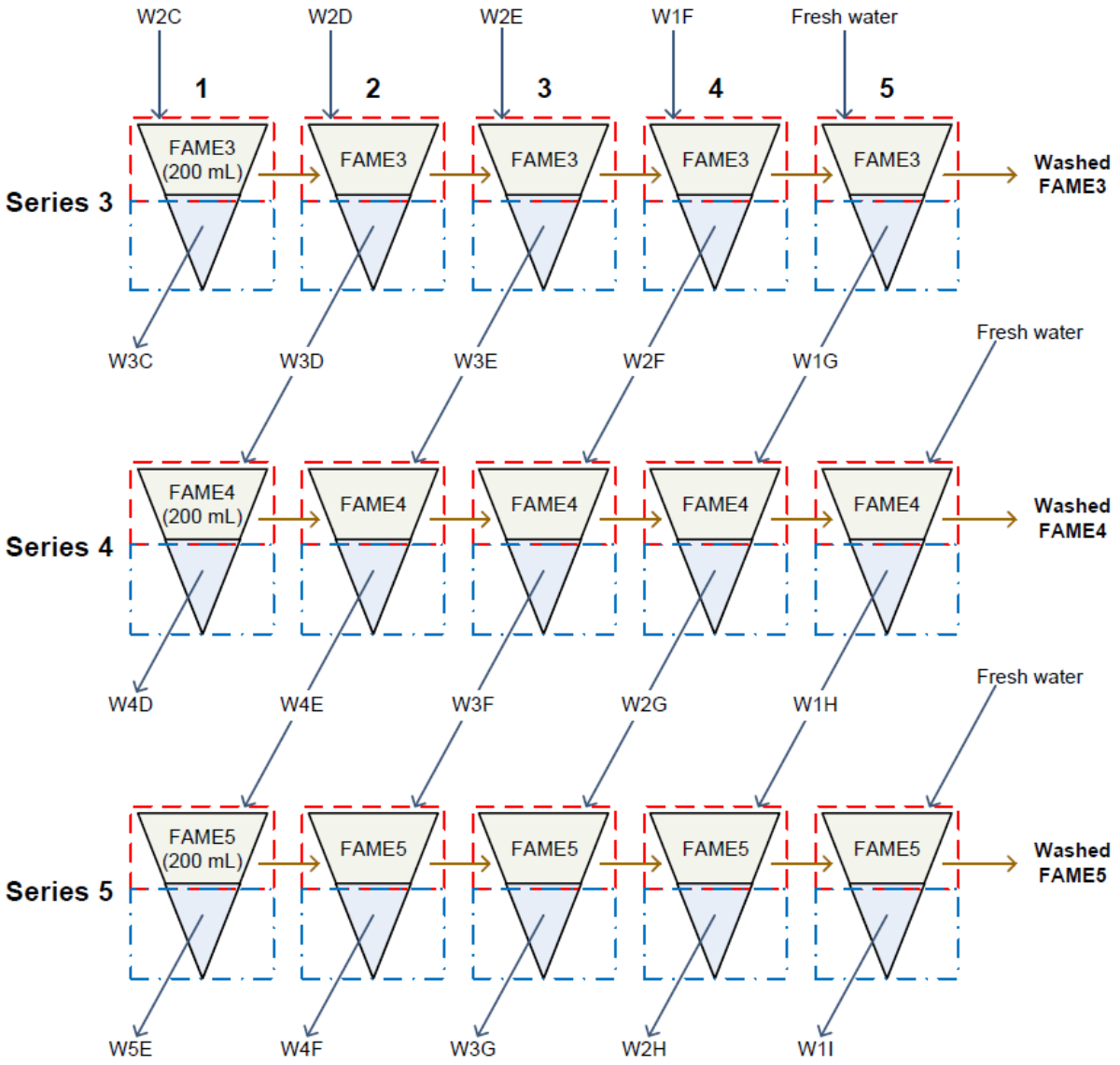

Figure 6.7 Final three series of washes in the counter-current washing sequence.

Although the process described only approximates a counter-current extraction scheme, the reduction in water use can still be evaluated by taking into account the amount of fresh water used for each series of washes. The water uses are shown in Table 6.2 along with the overall water to FAME ratio. In comparison to the cross-current sequence, the counter-current sequence reduced the water to FAME ratio from 1 to 0.36.

Table 6.2 Water use for each series in the counter-current washing experiments.

Series	Water used (mL)	Cumulative water used (mL)	Cumulative washed FAME (mL)	Water to FAME ratio
(1) Cross-current	200	200	200	1
(2)	40	240	400	0.60
(3)	40	280	600	0.47
(4)	40	320	800	0.40
(5) Counter-current	40	360	1000	0.36

6.4 Results and Discussion

6.4.1 Conductivity of Extracted Water Phases

The measured conductivities of the extracted water phases for each series of washes are shown in Figure 6.8.

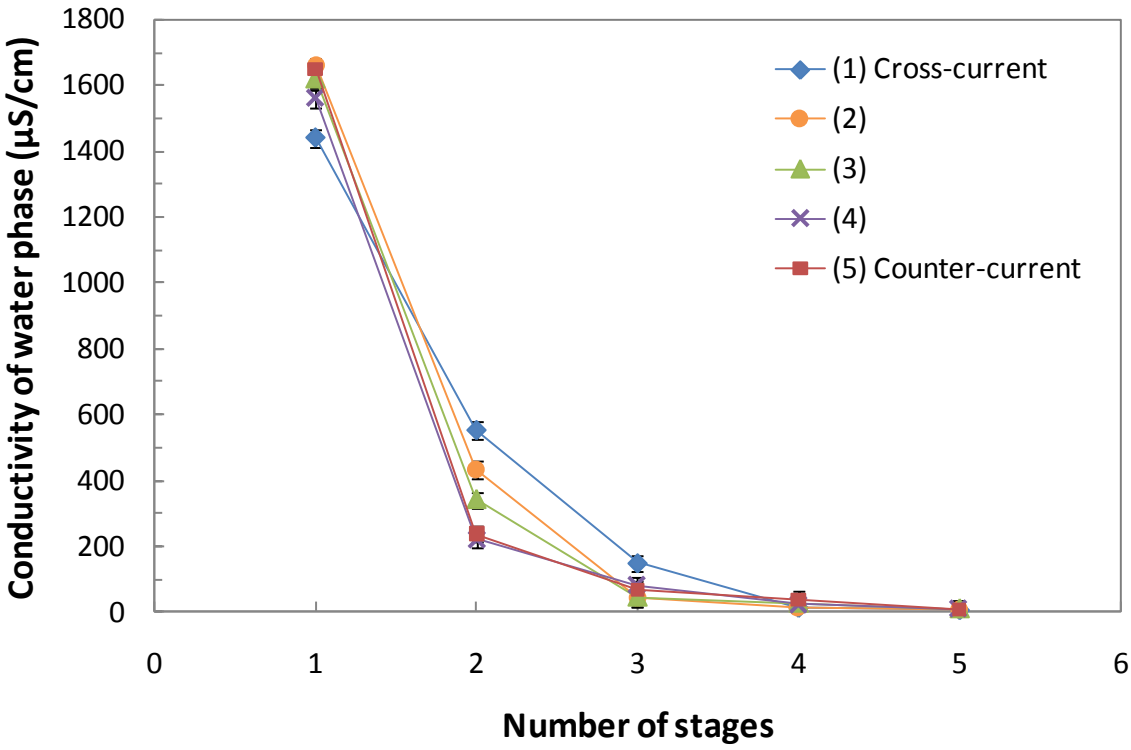

Figure 6.8 Conductivity of water phase after contacting with FAME for each washing series.

For each series, the largest amount of salt impurities was removed in the first stage. After a total of five stages, the conductivities of all the extracted water phases were below 10 µS/cm. This indicated that the concentration of salt remaining in the FAME phase was very low, and the washing process was complete.

The five series all behaved relatively the same, except for variations in the conductivity at the second stage. However, it is difficult to conclude with certainty whether these variations can be attributed to the difference in washing configuration or if it is due to experimental error. Since each series required the same number of stages to reduce the conductivity below 10 µS/cm, the variations between the series were most likely minimal.

6.4.2 Sodium Extraction by Cross-Current Washing

The concentration of sodium remaining in the FAME phase after each washing stage for the cross-current washing sequence is shown in Figure 6.9, along with the simulation data from Section 6.2.

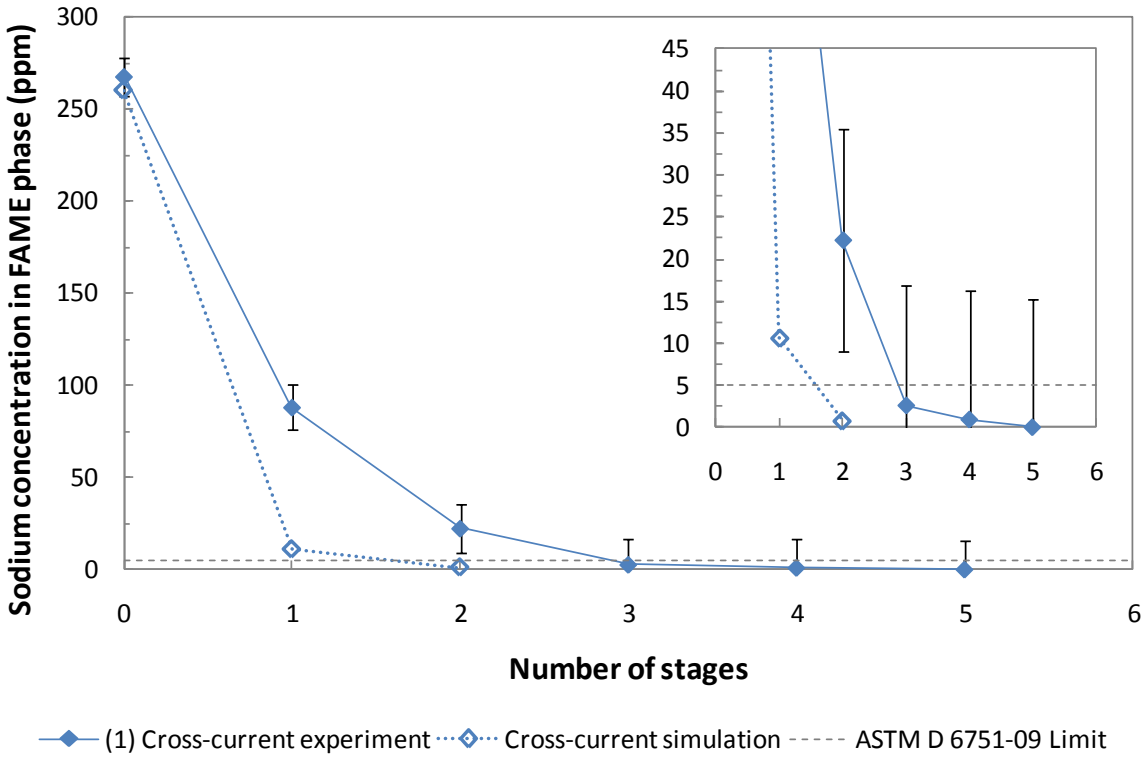

Figure 6.9 Concentration of sodium remaining in the FAME phase for the cross-current washing sequence. The inset shows a close-up at concentrations close to 5 ppm.

The ASTM limit for sodium (combined with potassium) is 5 ppm. The data in Figure 6.9 indicates that the ASTM limit for sodium is met after three washing steps, suggesting that the remaining two were not necessary. The error bars in Figure 6.9 are relatively large, indicating that the data at very low concentrations were beyond the limit that could be detected by conductivity. A sample of the FAME after the fifth wash was analyzed by ICP-OES and found to have a sodium concentration of 1.5 ppm. This suggests that although the absolute value of the concentration cannot be stated with absolute certainty, it is safe to assume that almost all of the sodium was extracted after five stages.

6.4.3 Sodium Extraction by Counter-Current Washing

Figure 6.10 shows the sodium concentration remaining in the FAME phase after each washing stage for the counter-current sequence. The simulation results are also included for comparison.

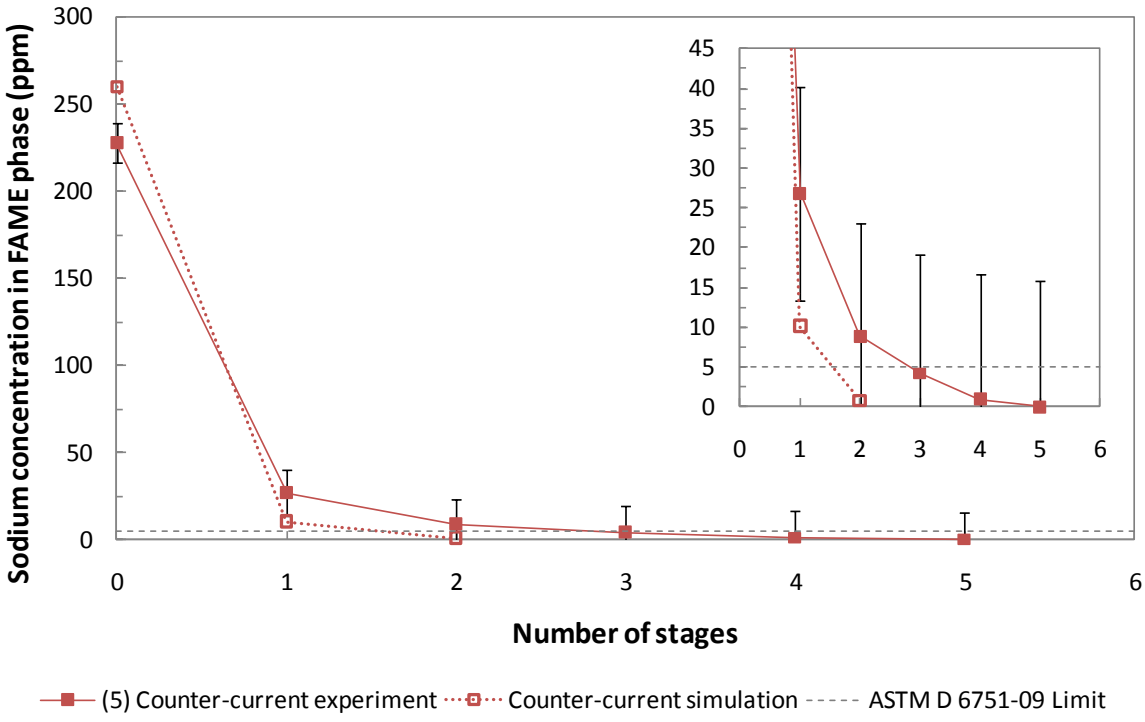

Figure 6.10 Concentration of sodium remaining in the FAME phase for the counter-current washing sequence. The inset shows a close-up at concentrations close to 5 ppm.

The counter-current experimental results follow the simulation results more closely than the cross-current experiments. However, a third stage was still required to meet the ASTM limit of 5 ppm.

6.4.4 Comparison with Simulation Results

There is a discrepancy between the number of stages predicted by the simulation and the experimental results. The simulation predicted that the sodium would be reduced below 5 ppm after 2 stages whereas the experiments required 3 stages. A source of error could be the extrapolation of the equilibrium curve. It is unknown how the presence of free fatty acids (FFA) observed in Chapter 5 may affect the distribution of sodium at lower concentrations.

6.4.5 Comparison of Experimental Results

Figure 6.11 shows a comparison between the experimental results for the cross-current (data from Figure 6.9) and counter-current washing sequences (data from Figure 6.10).

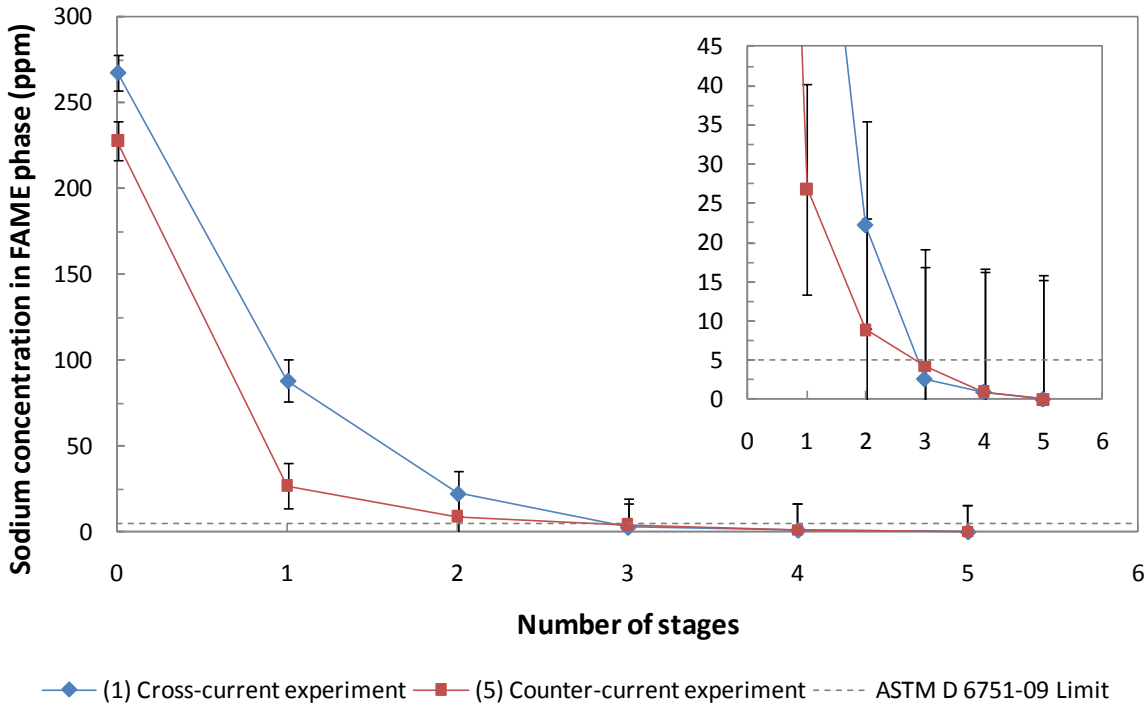

Figure 6.11 Concentration of sodium remaining in FAME phase wash for the counter-current washing sequences. The inset shows a close-up at concentrations close to 5 ppm.

The performance of the counter-current sequence is comparable to that of the cross-current sequence while only using a fraction of the water. The overall water to FAME ratio was reduced from 1 (200 mL of water to wash 200 mL of FAME) to 0.36 (360 mL of water to wash 1000 mL of FAME) while still maintaining the same level of purification. This represents a 64% reduction in water use.

6.5 Summary

FAME produced from refined vegetable oils such as canola oil does not typically require extensive washing to reach required purification levels. In particular, the removal of sodium can be achieved in one washing step using a FAME to water volume ratio of 5:1. Conversely, FAME made from high FFA feedstock such as waste frying oil will require multiple washes. FFA in the FAME will interact with sodium removal such that it cannot be reduced to the required limit in one washing step. Therefore, the use of two multistage extraction processes, cross- and counter-current, were investigated for the removal of sodium from FAME made from waste oil.

The removal of sodium by cross- and counter-current water washing was simulated using an extrapolated model from equilibrium data obtained from previous experiments. The simulation results suggest that the sodium level can be reduced below the ASTM limit in two cross- or counter-current washing stages. Both washing configurations performed similarly, with the exception that the counter-current sequence used 50% less water.

The two washing configurations were also compared experimentally. The first involved washing a 200 mL sample of FAME in a five-stage cross-current washing sequence, using 40 mL of fresh water at each stage for an overall water to FAME volume ratio of 1. The second configuration was an approximated counter-current washing sequence which used 360 mL of water to wash 1000 mL of FAME, for an overall water to FAME ratio of 0.36. The results indicated that sodium was reduced to the ASTM limit after three washing stages. The two washing sequences performed similarly, however the counter-current sequence used only a fraction of the water. It represented a 64% reduction in the amount of water used.

The results indicate that when purifying FAME, the use of a counter-current water contacting scheme results in a more efficient use of water while achieving the same level of

purification for sodium compared to cross-current contacting. This would result in a more concentrated wastewater stream, thereby reducing the energy load of downstream waste treatment operations and improving the overall energy efficiency of the biodiesel production process.

In addition, both washing schemes required the same number of stages to accomplish the required level of purification for sodium. This indicates that the same number of extraction units would be required and both washing schemes would have the same capital cost.

6.6 References

ASTM Standard D6751, "Standard specification for biodiesel fuel blend stock (B100) for middle distillate fuels," ASTM International, West Conshohocken, PA (2009).

Frank, T. C., L. Dahuron, B. S. Holden, W. D. Prince, A. F. Selbert, and L. C. Wilson, "Liquid-Liquid Extraction and Other Liquid-Liquid Operations and Equipment," in "Perry's Chemical Engineers' Handbook," D. W. Green and R. H. Perry, Eds., McGraw-Hill Companies, Inc., New York, NY (2008).

Geankoplis, C. J., "Transport Processes and Separation Process Principles," Pearson Education, Inc., Upper Saddle River, NJ (2003).

Haque, K. E., J. J. Laliberté, and J. Pruneau, "Batch and counter-current acid leaching of uranium ore," Hydrometallurgy 17, 229-238 (1987).

Maliszewski, T. A., D. L. Bunning, D. J. Schreck, L. A. Kapicak, and N. L. Balmer, "Biodiesel production with reduced water emissions," Patent No. WO 2008/091944 A2 (2008).

Masscheleyn, P. H., F. M. Tack, and M. G. Verloo, "Feasibility of a counter-current extraction procedure for the removal of heavy metals from contaminated soils," Water, Air, Soil Pollut. 89, 317-335 (1996).

Predojević, Z., "The production of biodiesel from waste frying oils: A comparison of different purification steps," Fuel, 87, 3522-3528 (2008).

Chapter 7

Ion Exchange of Biodiesel Wastewater

7.1 Introduction

The wastewater from a biodiesel production plant typically contains various components including methanol, glycerol, soap, dissolved and suspended solids, free fatty acids (FFA), and fatty acid methyl ester (FAME or biodiesel) (Boornazian and Smith, 2008). As seen in Table 7.1, the specific properties of the wastewater will vary from process to process, but it will generally contain high amounts of oil and grease and a high COD (chemical oxygen demand). It therefore may require treatment prior to discharge to a water treatment facility. To improve the overall efficiency and reduce the negative environmental impact, this water should be recovered and recycled back to the process.

Table 7.1 Typical properties of biodiesel wastewater.

Source	pH	COD (mg/L)	BOD (mg/L)	O&G (mg/L)	Conductivity (µS/cm)
Chavalparit and Ongwandee (2009)	8.9	30,980	np	6020	350
Berrios and Skelton (2008)	6.7	18,362	np	np	1119
Jaruwat et al. (2010)	9.3-10.8	312,000	168,000	18,000	np
Banerjee et al. (2009)	9	684-792	np	1433-1640	np

COD: chemical oxygen demand; BOD: biochemical oxygen demand; O&G: oil and grease
np: not provided

The recovery processes recommended in the literature include distillation and membrane separation (Haas et al., 2006; Maliszewski et al., 2008). However, distillation operations are energy intensive, and the complexity and variability of the wastewater could make membrane systems difficult to use. Another option for removing ionic components from the wastewater prior to reuse is ion exchange.

Ion exchangers are solid materials that carry exchangable cations or anions. When in contact with an electrolyte solution, the ions on the exchanger can be exchanged with an equivalent amount of other ions of the same charge from the solution (Helfferich, 1962). This

property makes ion exchange useful in wastewater treatment operations such as demineralization, dealkalization, and water softening (Hardland, 1994).

Figure 7.1 shows the water treatment process first introduced in Chapter 4. After the water washing step, ion exchange is used to reduce the salt content of the wastewater so that it can be recycled back to the process. After methanol removal by distillation, the ion exchange operation would involve the use of both cation and anion exchange resins to remove cations and anions, respectively. The use of the two resins can either be performed simultaneously in a mixed bed or by passing the wastewater sequentially through two separate columns (LeVan and Carta, 2008). The cleaned water can then be recycled directly back to the washing process. Furthermore, since ion exchange is an inherently dynamic process, both resins would need to be regenerated periodically in an industrial operation.

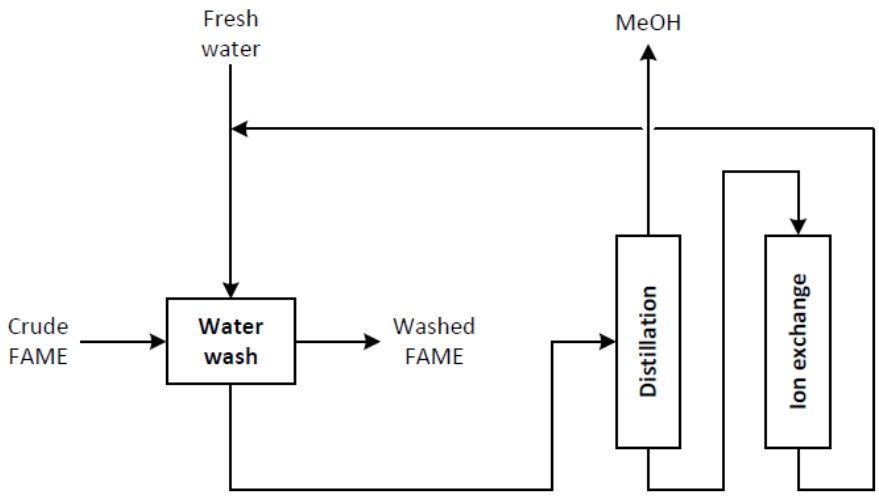

Figure 7.1 Treatment of biodiesel wastewater by ion exchange for recycle.

The potential use of ion exchangers for biodiesel wastewater recovery was evaluated in the following experiments. Biodiesel wastewater samples with known sodium concentrations obtained from previous water washing experiments (see Chapter 5) were contacted with a cation exchange resin in batch equilibrium experiments. The amount of sodium removed was calculated and used to plot isotherms to characterize the performance of the resin. The results were also compared to data obtained using prepared pure

water/sodium salt solutions of the same initial concentrations to determine the potential effect of other components in the wastewater.

7.2 Ion Exchange Theory

Ion exchange resins are insoluble materials that contain exchangeable ions attached to permanently bound functional groups of opposite charge. Most ion exchangers for commercial applications consist of a bed of synthetic polymer beads, with particle diameters most commonly ranging from 0.15 to 1.2 mm (Crittenden et al., 2005). In general, cation exchange resins contain bound sulfonic acid groups and anion exchange resins contain quaternary ammonium groups or other amino groups. The polymeric beads are usually polystyrene cross-linked with divinylbenzene.

Figure 7.2 shows a schematic of a cation exchanger initially in the "A" form that is placed in an electrolyte solution of ions of the "B" form, where "A" and "B" represent ions of the same charge. Because there is a difference in concentration between the resin phase and the solution phase, an ion exchange reaction takes place in which the ions are redistributed by diffusion. The ion exchange resin releases replacement ions, "A", into the solution. To maintain electroneutrality within both the resin and solution, the "B" ions diffuse into the resin to replace the "A" ions. This reaction is reversible and is completed when a state of equilibrium is attained (Zagorodni, 2007).

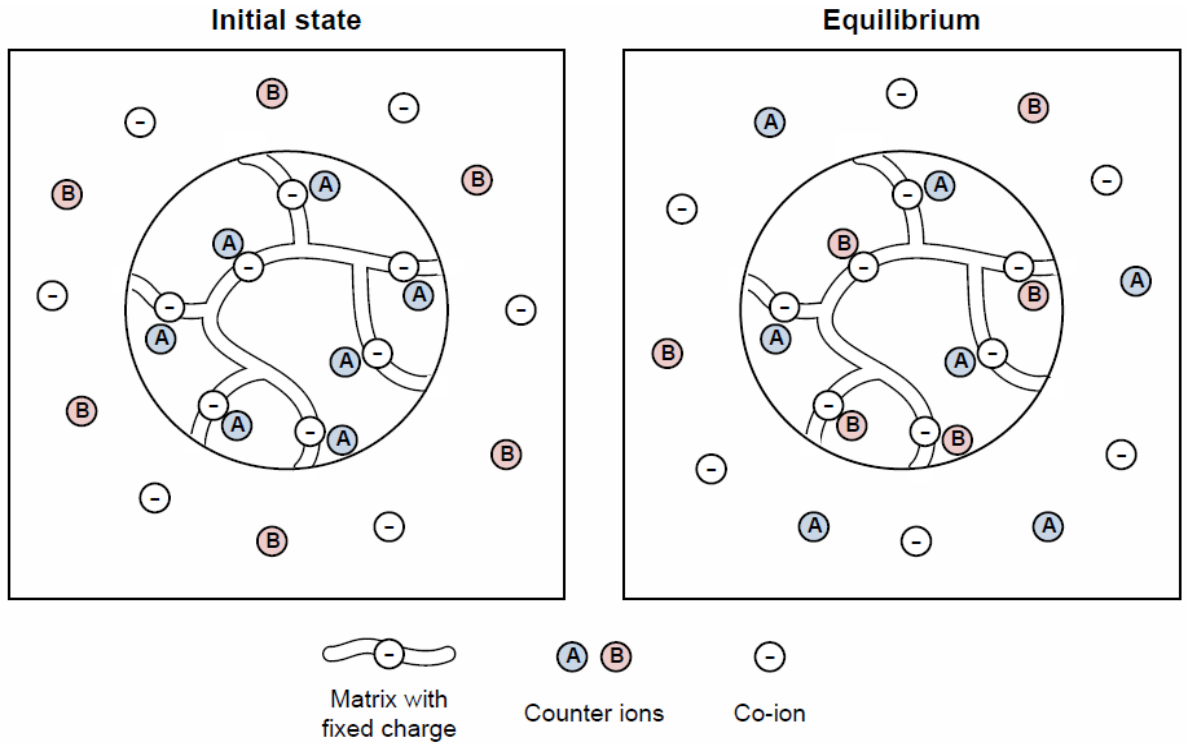

Figure 7.2 Cation exchanger initially in the "A" form (left) in solution with counter ion "B". The counter ions are redistributed by diffusion until equilibrium is attained (right). Figure adapted from Helfferich (1962).

The equilibrium reaction between an ion exchange resin initially in the "A" form that is placed in an electrolyte solution with counter ion "B" is given by the following equation:

$$z_B\overline{A} + z_A B \leftrightarrow z_B\overline{B} + z_A A \tag{7.1}$$

where A and B are the ions in the solution, $\overline{A}$ and $\overline{B}$ are the ions in the resin, and z_A and z_B are the charges of ions "A" and "B", respectively.

The concentration ratio of the two competing counter ions in the ion exchanger is usually different from that in the solution due to the preference of the ion exchanger for one species over the other. This concentration ratio can be expressed as the distribution coefficient (λ) for each species:

$$\lambda_i = \frac{\overline{C_i}}{C_i} \tag{7.2}$$

where $\overline{C_i}$ and C_i are the concentrations of species i in the resin and solution, respectively.

The preference of the ion exchanger for ion "B" over ion "A" can be expressed as the ratio of the two distribution coefficients:

$$\alpha_A^B = \frac{\lambda_B}{\lambda_A} \tag{7.3}$$

The value in Equation (7.3) is called the separation factor. If ion "B" is preferred, $\alpha_A^B > 1$, and if ion "A" is preferred, $\alpha_A^B < 1$. The separation factor is usually not constant, but depends on the total concentration of the solution, the temperature, and the equivalent fraction of one of the components (Zagorodni, 2007).

The equilibrium concentrations in an ion exchange system can be represented by an equilibrium isotherm. For adsorption or ion exchange processes[5], the isotherm is a graphical representation of the distribution of the adsorbed material between the adsorbed phase and the solution phase at equilibrium. The basic difference between adsorption and ion exchange is that while there is only one isotherm at a specified temperature for adsorption, more than one isotherm can exist at a specified temperature for different normalities of the solution. The influence of normality on the isotherm is more pronounced for the exchange of ions with different valences (i.e., $z_A \neq z_B$) but is still observed for systems where the valences are equal (i.e., $z_A = z_B$) (Barrer and Klinowski, 1974). This dependence on normality is due to the change in preference by the ion exchanger for one species over the other. The concentrations of ions in the external solution will affect the equilibrium in Equation (7.1). This occurs because the two counter ions are effectively competing for binding sites on the ion exchange resin (Rood, 1995).

Because the ion exchange reaction is reversible, the resin can be regenerated and reused. After the resin has been exhausted such that essentially all of the useable exchange sites are in the "B" form, the resin is contacted with a solution with a high concentration of the "A" ion. This shifts the equilibrium in Equation (7.1) to the left side, returning the resin to its original form. As a result, the regeneration solution will be highly concentrated with the "B" ion.

[5] Adsorption and ion exchange share many common features in regard to application as they both involve the transfer and resulting distribution of one or more solutes between a fluid phase and particles.

7.3 Experimental Design

Three wastewater samples (~40 mL each) were selected from the single stage washing experiments presented in Chapter 5 to be used in the ion exchange trials. The initial sodium concentrations, as measured by Inductively Coupled Plasma Optical Emission Spectroscopy (ICP-OES), of these samples are shown in Table 7.2. In order to provide a comparison, the same experiments were conducted using pure water-NaCl solutions that were prepared to have sodium concentrations similar to that of the wastewater samples (also shown in Table 7.2).

Table 7.2 Initial sodium concentrations of wastewater and pure water-NaCl samples.

Wastewater sample	Wastewater Na concentration		Pure water Na concentration	
	(ppm)	(mmol/L)	(ppm)	(mmol/L)
Run 7	1369	57	1415	59
Run 4	1092	46	1011	42
Run 9	668	28	606	25

In the ion exchange reaction, sodium ions in the solution are exchanged with hydrogen ions from the resin. This results in a change in concentration of hydrogen ions in the solution and thus a change in solution pH. By adding known amounts of resin to each of the solutions and measuring the change in pH, the change in sodium concentration was estimated. The experiments and calculation procedures are discussed in further detail below.

The pH meter used was the Corning pH/ion Analyzer 350 with a Mettler Toledo InLab Science Pro probe.

7.3.1 Ion Exchange Resin

The ion exchange resin selected for this study was the strong acid cation exchange resin GF404, produced by Lanxess Lewatit (Birmingham, NJ). Some key properties of this resin are shown in Table 7.3.

Table 7.3 Properties of strong acid ion exchange resin (GF404)

Property	Units	Value
Ionic form as shipped	-	Neutral (H^+)
Functional group	-	Sulfonic acid
Structure	-	Macroporous
Total capacity	eq/L	1.6
	mmol/g	2.16
Mean bead diameter	mm	0.67
Bulk density	g/L	740
Density	g/mL	1.24

Although the resin was already shipped in the appropriate neutral form (i.e., in the form of exchangeable hydrogen ions), materials as shipped by manufacturer can give irreproducible results and it is recommended that resins be conditioned prior to testing. A batch of resin (~100 g) was treated according to recommended regeneration procedures. This involved washing the resin with about 250 mL of a strong acid solution (4% hydrochloric acid) to ensure that the resin was in the neutral form (H^+). The mixture was stirred for 30 min and repeated with another 250 mL of acid. The resin was then rinsed with 250 mL of deionized water to remove any remaining acid. The rinsing was repeated (about five times) until the pH of the water was neutral, indicating that all of the acid had been removed.

7.3.2 Pure Water-NaCl Solutions

A known amount of resin (shown in Table 7.4) was added to approximately 20 g of each of the three solutions of normalities 25, 42, and 59 mmol/L, as well to 20 g of deionized water. The samples were shaken for about 10 seconds and left overnight to achieve equilibrium. The following day, the samples were shaken again for about 10 seconds and the pH of the water was measured.

Table 7.4 Amounts of resin added to the pure water-NaCl solutions.

Amount of resin (g)	Amount of resin per mass of sample (g/g)
0	0
0.1	0.005
0.25	0.0125
0.5	0.025
0.65	0.0325
0.8	0.04
1	0.05

7.3.3 Wastewater Solutions

A procedure similar to that used for the pure water-NaCl solutions was followed for the three wastewater samples. Two samples of approximately 20 g were used for each solution with normalities of 28, 46, and 57 mmol/L for a total of six samples.

After the initial pH of each solution was measured, approximately 0.01 g resin was added to each of the six samples. The samples were shaken for about 10 seconds and given at least three hours to equilibrate, shaking occasionally. After the pH was measured again, another known amount of resin was added. The process was repeated for resin additions ranging from 0.01 to 5 g, shown in Table 7.5. The final amount of resin added was increased to 5 g since it was noticed from the pure water-NaCl results that 1 g was not sufficient to completely remove the sodium. The change in mass after each pH measurement was also recorded.

Table 7.5 Amounts of resin added to the wastewater solutions.

Amount of resin (g)	Amount of resin per mass of sample (g/g)
0	0
0.01	0.0005
0.1	0.005
0.25	0.0125
0.5	0.025
1	0.05
5	0.25

7.3.4 Determination of Error

The error in the pH measurement was estimated to be ±0.09 (two standard deviations) as determined from repeated measurements. The error bars displayed in the figures in this chapter all represent two standard deviations as calculated from error propagation equations.

7.3.5 Determination of the Change in Sodium for the Pure Water-NaCl Solutions

For the pure water-NaCl solutions, the change in sodium concentration in the water phase was equated to the change in hydrogen ion concentration, as measured by pH:

$$[Na^+]_{change} = [H^+]_{final} - [H^+]_{initial} \tag{7.4}$$

where

$$[H^+] = 10^{-pH} \tag{7.5}$$

therefore,

$$[Na^+]_{change} = 10^{-pH_{final}} - 10^{-pH_{initial}} \tag{7.6}$$

The final sodium concentration in the water was therefore equal to the initial concentration minus the change in concentration:

$$[Na^+]_{final\ in\ water} = [Na^+]_{initial\ in\ water} - [Na^+]_{change} \tag{7.7}$$

A mass balance was then used to determine the concentration in the resin phase, since the mass of sodium lost by the water phase must equal the mass gained by the resin phase:

$$[Na^+]_{final\ in\ resin} = \frac{[Na^+]_{change} \cdot m_{sample}}{\rho_{sample} \cdot m_{resin}} \tag{7.8}$$

where m_{sample} is the mass of the sample (~20 g), ρ_{sample} is the density of water (1000 g/L), and m_{resin} is the amount of resin added. $[Na^+]_{final\ in\ resin}$ represents the concentration of sodium ions in the resin phase and has units of mmol/g.

The isotherm for each sample was then plotted using the values calculated by Equations (7.7) and (7.8).

7.3.6 Determination of the Change in Sodium for the Wastewater Solutions

It was noticed that the wastewater samples behaved as a buffered system at low additions of resin. This was due to the presence of FFA in the wastewater, which are weak acids. Although the samples contained a mixture of different FFAs, oleic acid is usually present in the highest quantity. The equilibrium relation for oleic acid is:

$$C_{17}H_{33}COOH \leftrightarrow C_{17}H_{33}COO^- + H^+ \tag{7.9}$$

Upon addition of resin, sodium ions were exchanged with hydrogen ions, which were released into the solution. The buffered system resisted a change in pH by shifting the equilibrium in Equation (7.9) toward the left (i.e., toward the formation of non-ionized oleic acid molecules). Because these hydrogen ions were bound to the FFA, they did not influence the pH of the solution. Therefore, Equation (7.6) used to model the pure water-NaCl system was not appropriate for the wastewater solution.

To model the wastewater system, the equilibrium of oleic acid in water was taken into consideration. The acid dissociation constant, K_a, for the equilibrium in Equation (7.9) is defined as:

$$K_a = \frac{[C_{17}H_{33}COO^-][H^+]}{[C_{17}H_{33}COOH]} \tag{7.10}$$

K_a is often represented as:

$$pK_a = -\log K_a \tag{7.11}$$

or

$$K_a = 10^{-pK_a} \tag{7.12}$$

The pK_a for oleic acid is 9.85 (Kanicky and Shah, 2002). It was noted that this value is larger than that of short-chain fatty acids which have pK_a values of about 4.8. As described by Kanicky and Shah (2002), with increasing chain length, there is an increase in van der Waals interactions between the chains of adjacent molecules. This packs the carboxylic acid groups closer together, shielding the hydrogen atom and resulting in a higher pK_a value.

The total amount of FFA in each sample was measured using the titration method described in Chapter 3, and are shown in Table 7.6.

Table 7.6 Initial concentrations of FFA in the wastewater solutions.

Wastewater sample	Initial Na concentration (mmol/L)	FFA concentration, C_0 (mmol/L)
Run 7	57	10
Run 4	46	9.2
Run 9	28	8.2

The total concentration of FFA (C_0) is equal to the sum of the ionized and non-ionized species in the solution:

$$C_0 = [C_{17}H_{33}COOH] + [C_{17}H_{33}COO^-] \tag{7.13}$$

Substituting Equations (7.12), (7.13), along with the definition for hydrogen ion concentration in terms of pH, Equation (7.5), into Equation (7.10) and rearranging for the concentration of non-ionized oleic acid species gives the following expression:

$$[C_{17}H_{33}COOH] = \frac{C_0 \cdot 10^{-pH}}{10^{-pH} + 10^{-pKa}} \tag{7.14}$$

When calculating the change in sodium concentration, the change in the concentration of non-ionized oleic acid must also be taken into account since it contains bound hydrogen ions that have been exchanged with sodium ions:

$$[Na^+]_{change} = 10^{-pH_{final}} - 10^{-pH_{initial}} + [C_{17}H_{33}COOH]_{initial} - [C_{17}H_{33}COOH]_{final} \quad (7.15)$$

The concentrations of sodium in the resin and water phases were calculated using Equations (7.7) and (7.8) for determination of the isotherms.

7.4 Results and Discussion

The pH with respect to the mass of resin per mass of sample for deionized water, water-NaCl solutions, and wastewater solutions is shown in Figure 7.3. The initial pH measurements for each solution are shown in Table 7.7. To distinguish the differences between the sets of data, the same data are shown on a log scale in Figure 7.4.

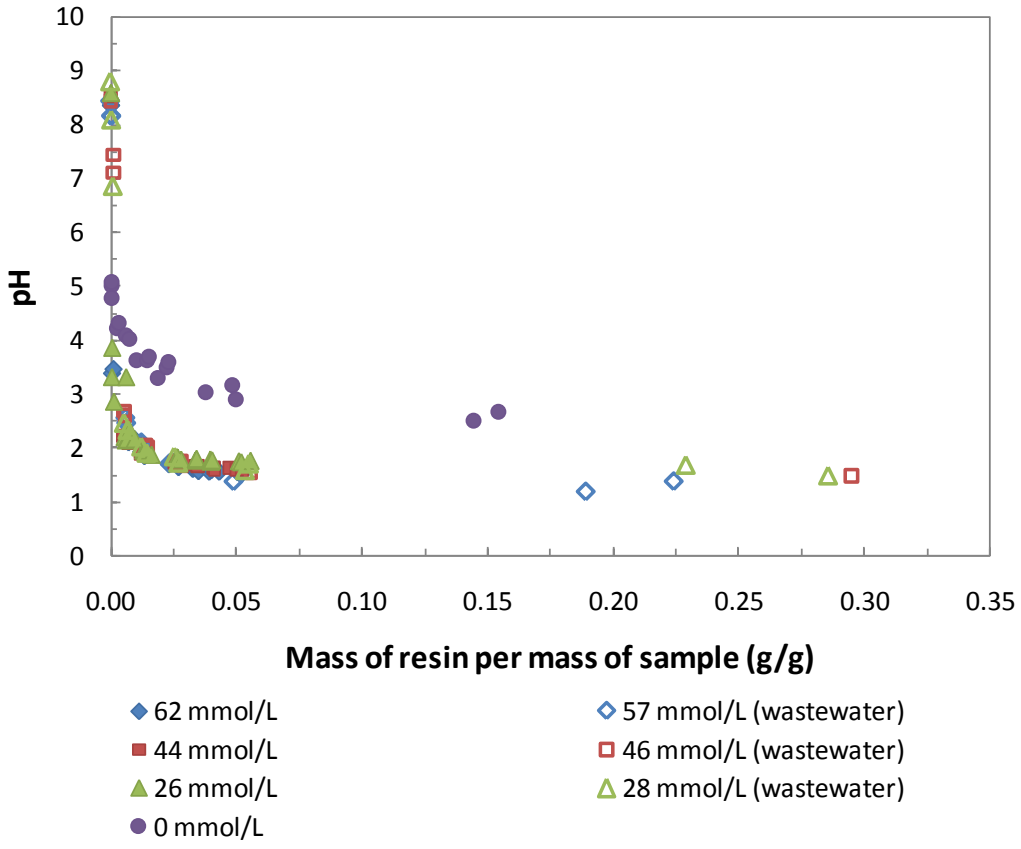

Figure 7.3 pH with respect to the ratio of the mass of resin to the mass of sample.

Table 7.7 Initial pH of samples prior to adding resin.

Sample	Initial Na concentration (mmol/L)	Initial pH
Water-NaCl	62	8.353
Water-NaCl	44	8.538
Water-NaCl	26	8.603
Deionized water	0	5.009
Wastewater	57	8.450
Wastewater	46	8.452
Wastewater	28	8.818

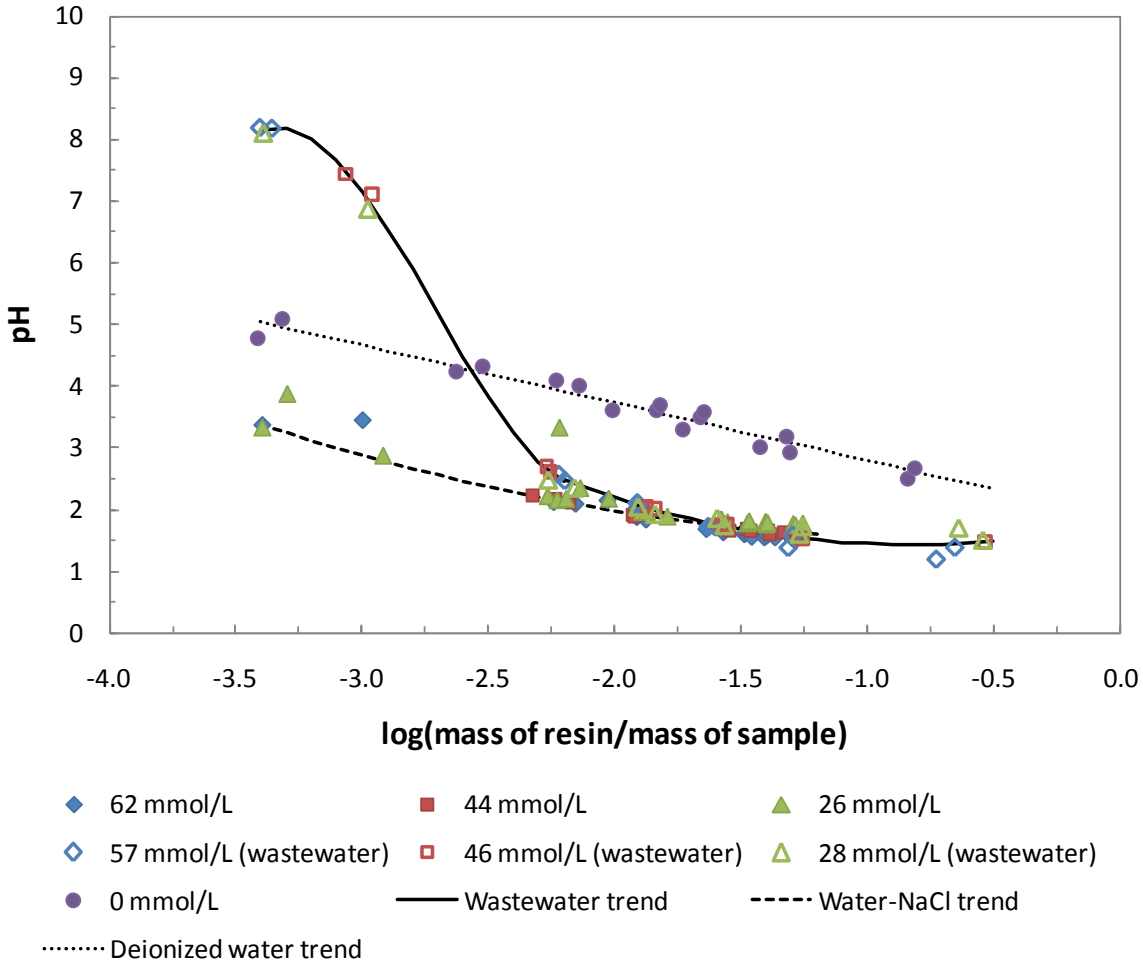

Figure 7.4 pH with respect to the log of the ratio of the mass of resin to the mass of sample.

The deionized water samples showed a decrease in pH with added resin. It is possible some hydrochloric acid remained within the pores of the resin from the regeneration process described in Section 7.3.1. This implies that for each addition of resin, there was a proportional amount of hydrogen ions released into the water solution that did not participate in the exchange with sodium ions. This could have affected the results since the change in sodium concentration was calculated using the change in pH. To determine the magnitude of this effect, the change in hydrogen ion concentration in the water phase was calculated by Equation (7.6) (note that the change in sodium ion concentration is equal to the change in hydrogen ion concentration). The values for the deionized water samples along with those of the water-NaCl solutions are shown in Figure 7.5.

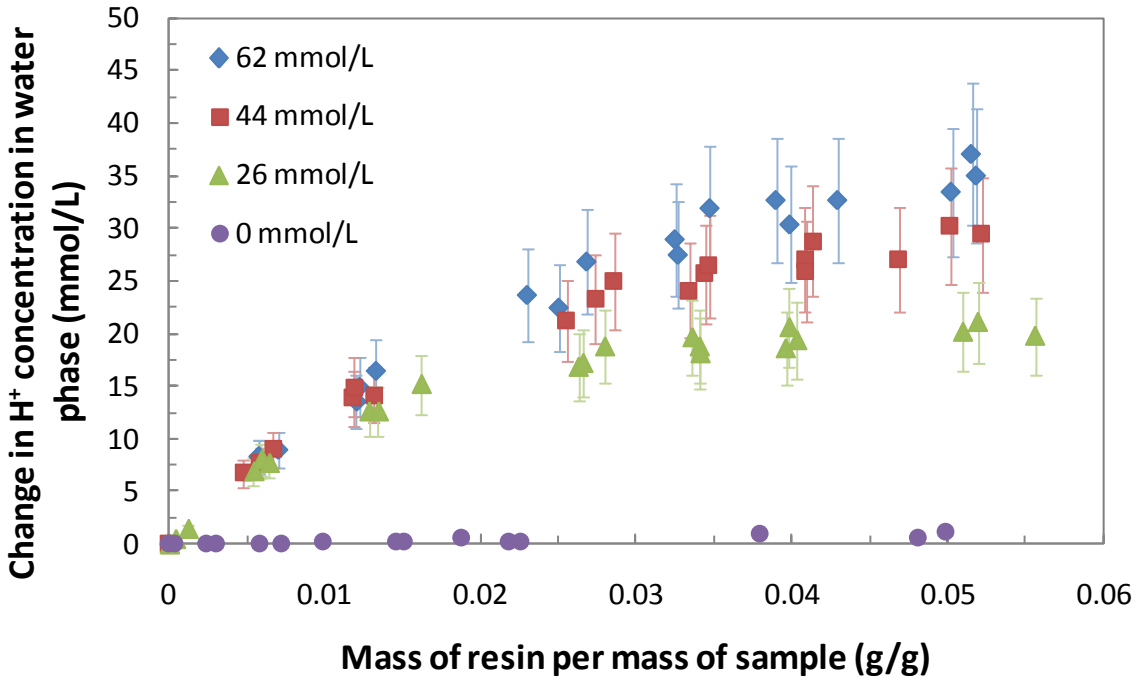

Figure 7.5 Change in hydrogen ion concentration of water phase with respect to the ratio of the mass of resin to the mass of sample for deionized water samples and water-NaCl solutions.

Although the change in pH for the deionized water seems relatively large in Figure 7.4, the change in hydrogen ion concentration in the water phase is less significant than for the water-NaCl solutions. This suggests that any hydrochloric acid released by the resin from the regeneration process did not significantly impact the calculation for change in sodium.

Referring to Figure 7.4, there was a larger initial decrease in pH for the water-NaCl solutions in comparison to the deionized water samples (see Table 7.7 for initial pH values). This is due to the presence of sodium ions, which were exchanged with the hydrogen ions on the resin. This exchange thus decreased the pH of the solution.

For the wastewater solutions, the initial drop in pH at low amounts of resin was not as significant in comparison to the water-NaCl solutions (see Table 7.7 for initial pH values). This is caused by the presence of FFA in the wastewater. Because FFA is a weak acid, it formed a buffered system which resisted changes to pH. However, with increasing resin additions, the buffer equilibrium reached a point where it was completely shifted toward the formation of non-ionized FFA. After this point, the pH of the wastewater changed similarly to that of the water-NaCl samples.

7.4.1 Sodium Removal from Water-NaCl Solutions

The equilibrium isotherms at ambient temperature for the water-NaCl solutions as calculated by Equations (7.7) and (7.8) are shown in Figure 7.6.

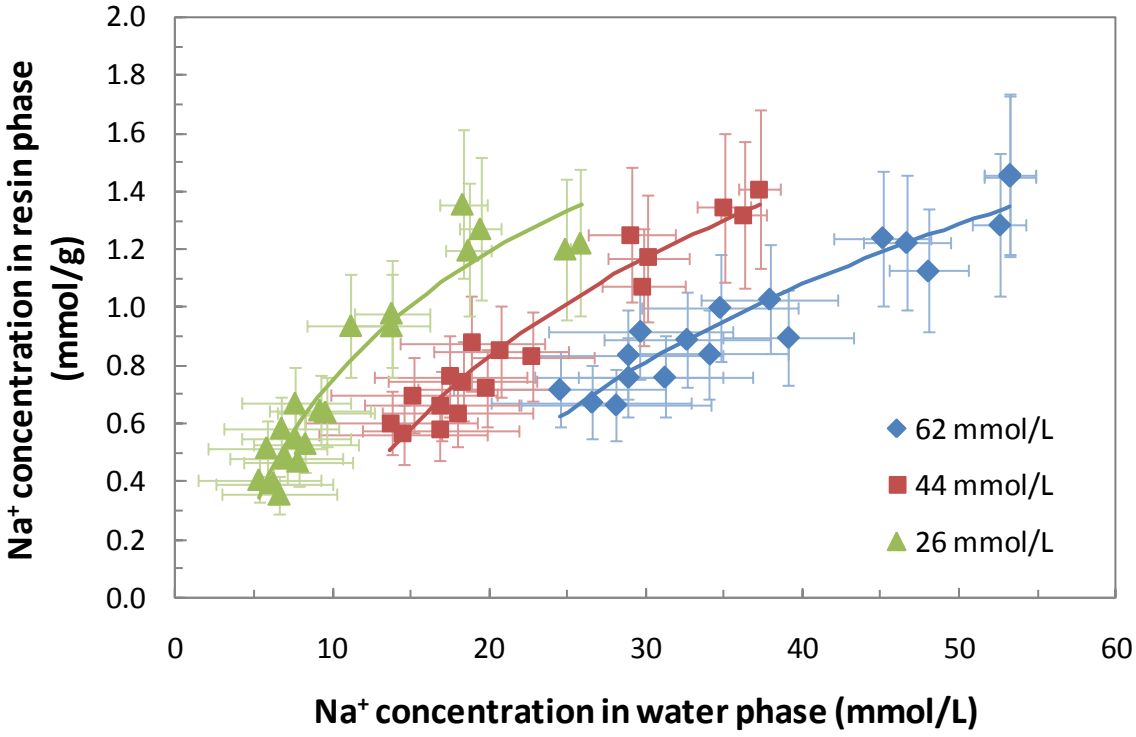

Figure 7.6 Isotherms for the water-NaCl solutions at ambient temperature.

The variability in the concentrations was found to be larger at low concentrations of sodium in the water phase and at high sodium concentrations in the resin phase. This is due to the error propagation from the pH measurement, which was used to calculate the change in sodium ion concentration with Equation (7.6). As a result, it may be more appropriate to use other analytical techniques under these conditions. Nonetheless, the trends observed are consistent with what is expected in ion exchange; that is, the solutions of different normalities produced three different isotherms. This was due to the varying quantities of hydrogen ions competing with sodium for the binding sites on the resin. With each resin addition, more hydrogen ions were present in the solutions with higher total normalities. Thus, there was more competition for the binding sites and the selectivity for sodium decreased. To verify this observation, the separation factors for each data point in the isotherm were calculated using Equation (7.3). The results are shown in Figure 7.7 with respect to the amount of resin per sample.

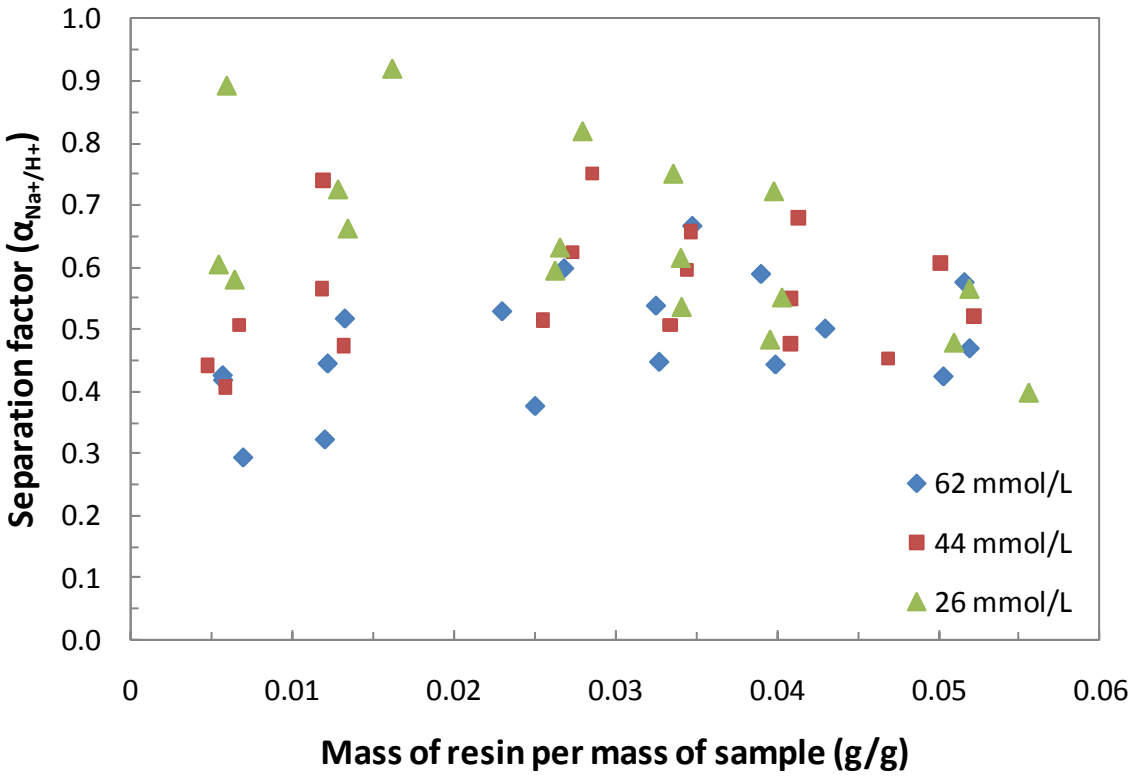

Figure 7.7 Separation factors for sodium with respect to the ratio of the mass of resin to the mass of sample.

The general trend in Figure 7.7 shows that the preference by the resin for sodium decreases with increasing solution normality. This supports the result in Figure 7.6 that isotherms depended on solution normality.

The initial and final sodium concentrations along with the percent sodium removal are shown for each solution in Table 7.8 using the data from Figure 7.6. For a resin addition of approximately 0.05 grams per gram of solution, the percent removal of sodium ranged from 48.4 to 66.3%. Therefore, in order to approach a lower level of sodium closer to that of deionized water, a greater quantity of resin would be required.

Table 7.8 Percent sodium removal from water-NaCl solutions.

Initial Na concentration (mmol/L)	Average amount of resin added per gram of sample (g/g)	Average final Na concentration (mmol/L)	Percent removal (%)
62	0.051	32	48.4
44	0.050	19	56.0
26	0.053	8.9	66.3

7.4.2 Sodium Removal from Wastewater Samples

The equilibrium isotherms at ambient temperature for the wastewater solutions as calculated using Equations (7.15), (7.7), and (7.8) are shown in Figure 7.8. The trends for the pure water-NaCl data from Figure 7.6 are also included for comparison.

Unfortunately, the data in Figure 7.8 are quite scattered, especially at either end of the x-axis. Similar to the pure water-NaCl results, the error arises from using the pH measurements to calculate the sodium removal. Additionally, the calculations for the wastewater samples had an extra source of error from the concentration of FFA in Equation (7.14). From the results in Chapter 5, the titration method for determination FFA concentration was found to have a relatively high degree of error. However, these measurements provided the best estimate of FFA concentration.

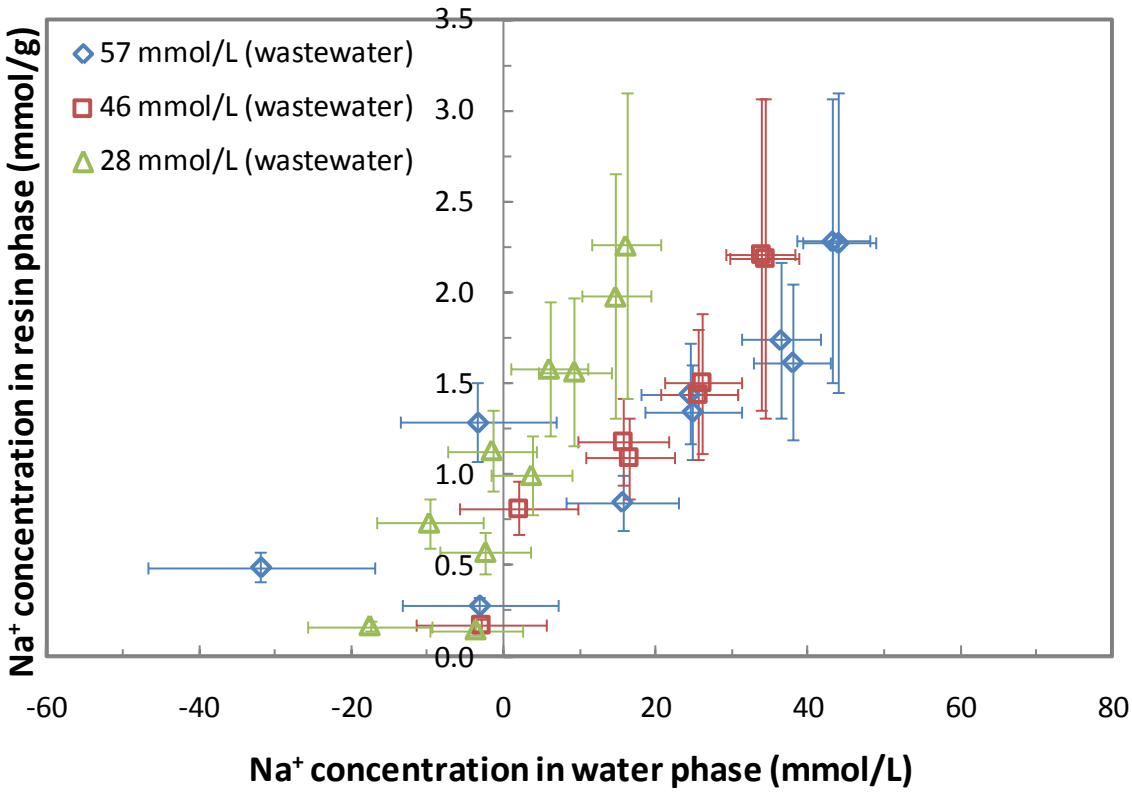

Figure 7.8 Isotherms for the wastewater samples at ambient temperature.

At low resin additions (i.e., at high sodium concentrations for each isotherm), the system was in the buffered region of FFA. Therefore, the data points here are highly dependent on the value for the pK_a used in Equation (7.14). The pKa of oleic acid is 5.02 (Riddick et al., 1986), and this value was used since it is the fatty acid present in the highest quantity. However, in reality there is a mixture of different FFAs. Due to this variability and uncertainty of the exact value of the pK_a for the wastewater, the data in the buffered region is less reliable.

The wastewater samples had the added potential error that the resin was consecutively added to the same sample, whereas for the pure water-NaCl solutions a new sample was used for each amount of resin added. After each pH measurement, some sample was lost due to wetting of the probe. Although this change in mass was measured before adding more resin, the change may have had an effect on the equilibrium of the system, thereby providing another source of error to the results.

Because a resin addition of about 5 g for the 20 g sample was added, the data for the wastewater solutions extends relatively close to the origin in Figure 7.8. However, due to the large degree of error, the exact amount of sodium removed cannot be determined from the data. Instead, the initial and final conductivities were measured. Assuming conductivity is proportional to concentration, the percent removal was determined, and these results are shown in Table 7.9. Note that prior to measuring the final conductivity, an anion exchange resin was added to each sample until the pH was neutral. This removed the excess chlorine ions since they would also contribute to the conductivity.

Table 7.9 Percent sodium removal from wastewater samples.

Sample	Initial Na concentration (mmol/L)	Initial Conductivity (µS/cm)	Resin added per gram of sample (g/g)	Final Conductivity (µS/cm)	Percent removal (%)
1	57	3000	0.19	863	71.2
2	57	3000	0.22	340	88.7
4	46	2360	0.29	192	91.9
5	28	1440	0.29	171	88.1
6	28	1440	0.23	128	91.1

Results for sample 3 were not possible due to a spill.

In comparison to the pure water-NaCl solutions, the wastewater contained other components such as oil compounds, methanol, and glycerol. The presence of these compounds did not seem to have a pronounced effect on the sodium removal efficiency by ion exchange since the results are similar to that of the pure water-NaCl solutions. In fact, because the solution became more acidic with each addition of resin, the equilibrium of FFA in Equation (7.9) was shifted to the left side, or to the formation of non-ionized FFA which is not soluble in water. This created a more distinct interface between the oil and water in the wastewater, which may make separation of the two phases easier in an industrial operation.

The percent sodium removal ranged from 71.2 to 91.9% for the wastewater solutions. This indicates that the majority of sodium can be removed from solutions in this range of initial concentrations by adding between approximately 0.2 and 0.3 grams of resin per gram of solution.

7.5 Summary

The ability of a cation exchange resin to remove sodium ions from biodiesel wastewater was evaluated by adding known amounts of resin to samples and measuring the change in pH. The results were compared to pure water-NaCl solutions of similar sodium concentrations.

For the pure-water NaCl solutions, three separate isotherms were determined for three solutions with normalities of 26, 44, and 62 mmol/L. The results suggested that selectivity by the resin for the sodium ion over the hydrogen ion decreased with increasing normality. By adding approximately 0.05 grams of resin per gram of solution, the percent of sodium removed was 66.3, 56.0, and 48.4% from the 26, 44, and 62 mmol/L solutions, respectively.

For the wastewater solutions, the data calculated from pH measurements were found to be less reliable at low amounts of resin (or high concentrations in the water phase) due to the creation of a buffered system by the presence of FFA. Outside the buffering capability of FFA, the data was found to follow that of the pure water-NaCl solutions more closely. This indicates that ion exchange resins can be effectively used to remove sodium ions from the wastewater, and the behaviour of the system tends to follow that of a purely aqueous system. For the wastewater solutions, the percent of sodium removed ranged between 71.2 to 91.9% by adding between 0.2 and 0.3 grams of resin per gram of solution.

The results verify that an ion exchange resin can effectively remove sodium ions from wastewater solutions in a batch contacting process. In an industrial setting, the contacting would be performed in a column containing a bed of cation exchange resin followed by a column containing anion exchange resin, or the two resins can be combined in a mixed bed operation. Therefore, the next step for investigation would be to conduct experiments in a column operation and also include the removal of anion contaminants such as chloride and sulphate ions.

Another area of investigation would involve the effect of other components in the wastewater. It is promising that the wastewater and pure water systems were found to behave similarly on a small scale batch process. However, on a larger scale operation, non-ionic components, such as FFA, methanol, and glycerol, could potentially interact with the ion exchange process by blocking the resin pores and thereby reducing performance.

Determining the effect of these non-ionic components on the long term operability of the resin is therefore an important next step.

Once these issues have been addressed and long term column operability has been demonstrated, the process presented in Figure 7.1 could prove to be an effective and energy efficient way to recover biodiesel wastewater for reuse.

7.6 References

Barrer, R. M. and J. Klinowski, "Ion-exchange selectivity and electrolyte concentration," J. Chem. Soc. Farad. T. 1, 70, 2080-2091 (1974).

Boornazian, L. Y. and M. T. Smith, "Applicability of Effluent Guidelines and Categorical Pretreatment Standards to Biodiesel Manufacturing," United States Environmental Protection Agency, Office of Water Management, Washington, D.C. (2008).

Crittenden, J. C., R. R. Trussell, D. W. Hand, K. J. Howe, and G. Tchobanoglous, "Water Treatment: Principles and Design," John Wiley & Sons, Inc., Hoboken, NJ (2005).

Haas, M. J., A. J. McAloon, W. C. Yee, and T. A. Foglia, "A process model to estimate biodiesel production costs," Bioresource Technol. 97, 671-678 (2006).

Harland, C. E., "Ion Exchange: Theory and Practice," The Royal Society of Chemistry, Cambridge, UK (1994).

Helfferich, F., "Ion Exchange," McGraw-Hill Book Company Inc., New York, NY (1962).

LeVan, M. D., G. Carta, "Adsorption and Ion Exchange," in "Perry's Chemical Engineers' Handbook," D. W. Green and R. H. Perry, Eds., McGraw-Hill Companies, Inc., New York, NY (2008).

Maliszewski, T. A., D. L. Bunning, D. J. Schreck, L. A. Kapicak, and N. L. Balmer, "Biodiesel production with reduced water emissions," Patent No. WO 2008/091944 A2 (2008).

Riddick, J. A., W. B. Bunger, T. K. Sakano, and A. Weissberger, "Organic Solvents: Physical Properties and Methods of Purification," Wiley, New York, NY (1986).

Rood, D., "The Use of Solid Phase Extraction for Environmental Samples," in "Quality Assurance in Environmental Monitoring: Instrumental Methods," G. Subramanian, Ed., VCH Publishers, New York, NY (1995).

Zagorodni, A. A., "Ion Exchange Materials: Properties and Applications," Elsevier, Amsterdam, The Netherlands (2007).

Chapter 8

Conclusions and Recommendations

There is increasing global concern surrounding the depletion of fossil fuel resources and the impact that their combustion has on the environment. Renewable fuels, such as biodiesel, are therefore receiving increased attention as potential alternatives. Unfortunately, biodiesel production requires the use of large amounts of water for purification, especially when the biodiesel is produced from waste feedstocks such as used frying oils. This reduces the overall energy efficiency of biodiesel since wastewater treatment is typically achieved through distillation, which requires large amounts of energy.

In this thesis, the effect of the amount of water and the choice of water treatment options in biodiesel production was investigated. In addition, the removal of sodium from crude biodiesel (i.e., fatty acid methyl ester or FAME) was studied in both single stage and multistage washing configurations. Preliminary results for an alternative water treatment process involving the use of ion exchange resins were also presented. The main conclusions from these studies are stated below. Recommendations for future work are also discussed.

8.1 Conclusions

8.1.1 Chapter 4 – Simulation of Biodiesel Wastewater Treatment Processes

The purification of biodiesel by water washing was simulated using Aspen HYSYS simulation software. A comparison was made between conventional wastewater treatment by distillation and the use of ion exchange resins. Typically, about one litre of wastewater is generated per litre of biodiesel produced. Under these conditions, 3.12 MJ of energy are required to purify the wastewater per litre of biodiesel using distillation. An alternative process using ion exchange resins to treat the wastewater was estimated to require only 0.978 MJ of energy per litre of biodiesel. This represented an energy reduction of 69% in comparison to distillation. These results indicate that ion exchange has the potential to be used to improve the efficiency of the wastewater treatment process.

The effect of the amount of water used on the energy requirements was also evaluated. In both processes, the energy required was shown to decrease linearly with

decreasing amount of water used in the washing step. This showed that reducing the amount of water can result in capital cost savings and also improve the overall energy efficiency of the process.

8.1.2 Chapter 5 – Sodium Distribution between Water and FAME Phases

The removal of sodium from crude FAME was investigated. FAME derived from both refined canola oil (low free fatty acid (FFA) feedstock) and used frying oil (high FFA feedstock) were washed in a single water washing step in a 5:1 FAME to water volume ratio. For the canola oil derived FAME, the required specification for sodium content of <5 ppm was met with one washing step. The distribution coefficient was found to be high and ranged from approximately 238 to 1363.

On the contrary, multiple washing stages would be necessary for the waste oil derived FAME to meet the 5 ppm specification. The FAME contained 0.36 wt% FFA which was found to interfere with sodium removal. Soap was found to accumulate at the interface between the FAME and water phases. This lowered the distribution coefficient in comparison to the canola oil derived FAME, and was found to range between approximately 72 and 93.

Because FFA was shown to interfere with sodium removal, it is important to ensure the concentration of FFA is as low as possible. This requires that the acid esterification pre-treatment reaction proceeds as close to completion as possible and that water is removed prior to the transesterification reaction. Another option is to remove the interface layer that is formed between the two phases. Unfortunately, this would result in product loss.

8.1.3 Chapter 6 – Counter-Current Washing of Waste Oil Derived FAME

It was found that multiple washing steps would be required to reduce the sodium concentration in waste oil derived FAME within required specifications. Therefore, two multi-stage contacting schemes were compared: cross- and counter-current. The required limit of sodium was achieved within three water washing steps. The two washing configurations behaved similarly, however the counter-current sequence required only a fraction of the water. This represented a 64% reduction in the amount of water used.

The results suggest that using a counter-current contacting scheme can still achieve the same level of purification for sodium while using the water more efficiently. As a result,

a more concentrated wastewater stream is produced which reduces the load on downstream waste treatment operations. Therefore, if multiple washing stages are required, it should be completed in a counter-current washing configuration to reduce the amount of wastewater produced. Reducing the amount of water was seen to have a strong positive impact on the energy required by downstream treatment operations.

8.1.4 Chapter 7 – Ion Exchange of Biodiesel Wastewater

The removal of sodium from biodiesel wastewater samples by ion exchange was evaluated for three different initial sodium concentrations. Percent removal ranged between 71 and 92% for the three solutions when adding between 0.2 and 0.3 grams of resin per gram of solution. Preliminary results indicated that the purification was not affected by the presence of other compounds in the wastewater.

8.2 Recommendations

Because distillation is an energy intensive process, other water treatment options should be further investigated to help improve the energy efficiency of the biodiesel purification process. The preliminary work presented in this thesis shows that ion exchange is a viable alternative to distillation. Further work would be required to verify that the ion exchange resin can effectively and efficiently remove salt impurities in a conventional column operation and in the presence of other impurities. Also, the limit to which glycerol can be allowed to accumulate in the recycle stream, since it is not removed by the ion exchange resin, must also be determined.

When reviewing the literature on water washing, it can be seen that there is a large variability in the water washing conditions used to purify various qualities of FAME. In this work, a FAME to water volume ratio of 5:1 was chosen based on the results of previous studies. For the waste oil derived FAME, it was found that three washing stages were required to purify the FAME using this water to FAME ratio. However, it is unknown if the amount of water used could be further reduced using other washing conditions. This presents an opportunity to optimize the washing process based on the level of contaminants (i.e., FFA, methanol, glycerol, sodium, etc.) present in the crude FAME. Knowing the best washing

ratio and number of washes required could help biodiesel producers achieve the required standards, while minimizing the amount of wastewater produced.

Appendix A

Raw Data

A.1 Wastewater Treatment Process Simulations

Table A.1 Simulation data for design of distillation column T-102 for water treatment by distillation process (Figure 4.1).

	Water to FAME volume ratio (m^3/m^3)					
	1.0	**0.8**	**0.6**	**0.4**	**0.2**	**0.1**
Mass flow of Water wash stream (kg/h)	1154	914	694	454	234	114
Mole fraction of methanol in feed to T-102	0.0534	0.0668	0.0867	0.1287	0.2323	0.4158
Vapour-liquid distribution coefficient, K_{water}	0.965	0.957	0.945	0.921	0.865	0.763
Vapour-liquid distribution coefficient, $K_{methanol}$	6.65	6.40	6.04	5.37	4.16	3.02
Relative volatility of feed stream, α_F	6.89	6.69	6.40	5.83	4.81	3.96
Relative volatility of distillate, α_D	2.48	2.48	2.48	2.48	2.48	2.48
Relative volatility of bottoms, α_B	7.75	7.75	7.75	7.75	7.75	7.75
Average relative volatility, $\alpha_{average}$	5.10	5.04	4.97	4.82	4.52	4.24
Minimum number of stages, N_{min}	8	8	8	9	9	9
Number of stages, N	16	17	17	17	18	19
Reflux ratio, R	24.6	19.5	14.9	9.67	4.95	2.32

Table A.2 Energy stream data for water treatment by distillation process (Figure 4.1).

	Water to FAME volume ratio (m^3/m^3)					
	1.0	**0.8**	**0.6**	**0.4**	**0.2**	**0.1**
Heating streams						
T-101 Reboiler energy stream, R1 (kW)	852.9	681.7	524.6	353.1	196.3	110.7
T-102 Reboiler energy stream, R2 (kW)	137.2	114.5	92.46	62.98	38.36	23.39
Cooling streams						
Cooling stream, E1 (kW)	91.14	71.78	54.03	34.63	16.91	7.166
Cooling stream, E2 (kW)	13.49	10.62	7.994	5.109	2.43	0.9004
T-102 Condenser energy stream, C2 (kW)	879.7	706.9	547.1	367.2	204.7	114.3

Table A.3 Simulation data for design of ion exchange operation for water treatment by ion exchange process (Figure 4.2).

	Water to FAME volume ratio (m^3/m^3)					
	1.0	**0.8**	**0.6**	**0.4**	**0.2**	**0.1**
Volume flow of wastewater fed to ion exchange operation (L/h)	1138	897.8	657.4	437.1	216.7	96.4
Water treated by SAC (L water/L resin)	155.4	122.6	89.8	59.7	29.6	13.2
Water treated by SBA (L water/L resin)	86.32	68.10	49.87	33.16	16.44	7.31
Regenerant solution for SAC (L regenerant/L resin)	1.477	1.477	1.477	1.477	1.477	1.477
Regenerant solution for SBA (L regenerant/L resin)	1.543	1.543	1.543	1.543	1.543	1.543
Wastewater effluent for SAC (L/h)	36.45	36.45	36.45	36.45	36.45	36.45
Wastewater effluent for SBA (L/h)	79.63	79.63	79.63	79.63	79.63	79.63
Total wastewater effluent (L/h)	116.1	116.1	116.1	116.1	116.1	116.1

Table A.4 Energy stream data for water treatment by ion exchange process (Figure 4.2).

	Water to FAME volume ratio (m^3/m^3)					
	1.0	**0.8**	**0.6**	**0.4**	**0.2**	**0.1**
Heating streams						
T-101 Reboiler energy stream, R1 (kW)	51.13	51.13	51.13	51.13	51.13	51.13
T-102 Reboiler energy stream, R2 (kW)	176.4	176.4	176.4	176.4	176.4	176.4
Ion exchange effluent (kW)	82.73	82.73	82.73	82.73	82.73	82.73
Cooling streams						
Cooling stream, E1 (kW)	96.55	96.55	96.55	96.55	96.55	96.55
T-102 Condenser energy stream, C2 (kW)	75.33	75.33	75.33	75.33	75.33	75.33

A.2 Single Stage Washing Experiments

Table A.5 Raw data from single stage washing of canola oil derived FAME.

Run	FAME Batches	Initial mass of FAME phase (g)	Initial mass of water phase (g)	Initial concentration of Na_2SO_4 in water phase (ppm)	Initial concentration of Na in water phase (ppm)
1	1-7	175.73	39.64	0	0
10	8-12	175.37	40.09	0	0
2	1-7	174.72	40.09	50	16.2
6	1-7	175.77	39.83	50	16.3
3	1-7	174.85	40.36	99	32.1
5	1-7	175.21	40.01	200	64.7
4	1-7	174.54	39.79	402	130
7	1-7	175.38	40.04	1001	324
8	1-7	175.03	40.49	1980	641
11	8-12	174.33	40.52	1984	642
9	1-7	174.05	40.51	2975	963

Table A.5 Raw data from single stage washing of canola oil derived FAME (continued).

Run	Conductivity before washing (µS/cm)	Conductivity after washing (µS/cm)	Final concentration of Na in water phase by ICP-OES (ppm)	Final concentration of Na in FAME phase by ICP-OES (ppm)
1	0	1070	396	1.54
10	0	1057	308	1.41
2	83.9	1187	595	1.32
6	85.7	1295	396	1.79
3	159	1208	475	1.19
5	321	1299	515	1.28
4	624	1636	458	1.62
7	1491	2392	645	1.91
8	2752	3316	927	2.36
11	2714	3323	935	0.320
9	3945	4332	1293	0.949

Table A.6 Raw data from single stage washing of waste oil derived FAME.

Run	Initial mass of FAME phase (g)	Initial mass of water phase (g)	Initial concentration of NaCl in water phase (ppm)	Initial concentration of Na in water phase (ppm)	Mass of FAME phase after washing (g)	Mass of water phase after washing (g)
1	173.56	40.05	0	0	156.52	54.83
9	171.60	40.63	0	0	161.97	47.83
2	171.71	40.04	510	201	164.38	44.83
3	172.31	40.06	1020	401	160.60	49.53
8	172.71	40.12	1503	591	157.79	53.03
4	172.54	40.11	1536	604	159.08	51.20
6	171.63	40.07	2035	801	160.87	48.79
5	172.86	40.07	2037	802	159.90	50.62
7	172.12	40.07	2545	1001	157.20	53.34

Table A.6 Raw data from single stage washing of waste oil derived FAME (continued).

Run	Conductivity before washing (µS/cm)	Conductivity after washing (µS/cm)	Final concentration of Na in water phase by ICP-OES (ppm)	Final concentration of Na in FAME phase by ICP-OES (ppm)
1	10.1	2520	1199	12.5
9	11.2	1440	668	nm
2	832	1730	825	10.7
3	1630	2030	984	12.2
8	2290	2520	1140	24.1
4	2410	2360	1092	16.2
6	3130	1630	740	10.2
5	3160	2680	1216	13.4
7	3910	3000	1369	15.0

nm: not measured

Table A.7 Titration of FAME and water samples for determination of FFA concentration.

	Sample	Mass of sample (g)	Volume of 0.01 N KOH in isopropanol added (mL)	Volume of 0.01 N HCl in isopropanol added (mL)	Concentration of FFA (ppm)
Initial FAME	FAME Batches 3-5	2.53	2.50	3.2	3851
	FAME Batches 3-5	2.88	2.90	3.6	3806
	FAME Batches 6-9	2.59	2.65	3.2	3762
	FAME Batches 6-9	2.84	3.25	3.7	3966
	FAME Batch 9	2.73	2.95	3.7	4126
FAME phase	Run 1	2.69	3.35	3.3	3735
	Run 2	2.69	3.30	3.4	3848
	Run 2	1.96	2.40	2.4	3728
	Run 3	2.69	3.20	3.1	3509
	Run 4	2.69	3.20	3.4	3848
	Run 4	1.73	2.05	2.1	3696
	Run 5	2.64	3.40	3.4	3921
	Run 5	1.84	1.40	3.4	5626
	Run 6	2.66	3.20	3.3	3777
	Run 6	1.90	2.35	2.4	3846
	Run 7	2.64	3.10	3.4	3921
	Run 7	2.05	2.45	2.5	3713
	Run 8	2.66	3.25	3.4	3891
Interface	Run 2	3.67	2.20	5.2	4314
	Run 2	3.46	2.00	5.2	4576
	Run 3	3.25	1.65	5.9	5527
	Run 4	3.58	1.80	7.5	6378
	Run 4	1.74	1.55	3.3	5774
	Run 5	3.61	2.20	7.7	6494
	Run 5	1.73	2.15	2.2	3872
	Run 6	3.86	2.65	8.1	6389
	Run 6	2.12	1.50	4.7	6750
	Run 7	3.13	2.10	9.1	8851
	Run 7	1.87	2.25	2.6	4233
	Run 8	3.19	2.55	9.1	8685
Water phase	Run 1	0.97	0.50	1.2	3766
	Run 2	0.94	0.25	0.9	2915
	Run 3	0.95	0.40	1.0	3205
	Run 4	0.94	0.30	0.9	2915
	Run 5	0.94	0.30	1.0	3239
	Run 6	0.95	0.35	0.8	2564
	Run 7	0.94	0.30	1.0	3239
	Run 8	0.94	0.25	1.0	3239
	Run 9	0.94	0.30	0.8	2591

A.3 Counter-Current Washing Experiments

Table A.8 Raw data from counter-current washing of waste oil derived FAME.

Series	FAME sample name	Water sample name	Initial mass of FAME phase (g)	Initial mass of water phase (g)	Conductivity of water phase before washing (µS/cm)	Mass of water phase after washing (g)	Conductivity of water phase after washing (µS/cm)	Final mass of FAME phase (g)
1	FAME1	W1A	171.6	39.9	11.2	47.8	1440	
		W1B		40.7	9.50	41.3	553	
		W1C		39.8	1.62	44.6	149	
		W1D		40.5	nm	39.4	14.2	
		W1E		40.7	2.38	39.7	7.42	145.6
2	FAME2	W2B	170.8	42.4	562	52.4	1660	
		W2C		42.4	202	44.4	434	
		W2D		36.7	nm	35.4	43.2	
		W2E		38.2	nm	38.0	13.9	
		W1F		41.6	0.930	39.3	6.01	
		na[6]		42.1	1.06	40.5	8.31	133.4
3	FAME3	W3C	173.1	41.2	nm	43.4	1620	
		W3D		33.5	100	34.4	341	
		W3E		36.3	nm	35.5	44.3	
		W2F		40.1	9.78	40.3	25.9	
		W1G		37.9	1.50	37.8	8.85	127.5
4	FAME4	W4D	174.3	40.7	404	45.9	1560	
		W4E		40.0	37.2	41.8	221	
		W3F		40.1	23.3	38.8	81.2	
		W2G		38.2	nm	37.7	23.8	
		W1H		40.6	1.24	39.2	8.41	118.0
5	FAME5	W5E	178.7	39.7	nm	54.8	1650	
		W4F		40.1	75.4	41.4	238	
		W3G		38.4	21.5	37.8	68.4	
		W2H		40.1	8.10	38.9	37.2	
		W1I		41.2	2.04	40.4	8.24	154.3

nm: not measured
na: not applicable

[6] A sixth wash of FAME2 was conducted to verify that the conductivity of the extracted phase was at a minimum.

A.4 Ion Exchange Experiments

Table A.9 Raw data for ion exchange of deionized water samples.

Sample	Sample mass (g)	Mass of added resin (g)	Resin per sample (g/g)	Initial pH	Final pH
1	14.404	0.000	0	5.009	5.009
2	20.743	0.008	0.0004	5.009	4.783
8	20.645	0.010	0.0005	5.009	5.087
14	21.161	0.050	0.0024	5.009	4.225
15	20.821	0.063	0.0030	5.009	4.316
3	21.762	0.128	0.0059	5.009	4.096
9	20.348	0.147	0.0072	5.009	4.019
16	20.741	0.204	0.0098	5.009	3.624
10	20.445	0.299	0.0146	5.009	3.617
4	20.766	0.312	0.0150	5.009	3.701
17	21.254	0.399	0.0188	5.009	3.295
5	20.294	0.443	0.0218	5.009	3.509
11	21.330	0.482	0.0226	5.009	3.593
18	20.336	0.771	0.0379	5.009	3.026
6	20.261	0.974	0.0481	5.009	3.177
12	21.767	1.087	0.0499	5.009	2.918
13	21.215	3.063	0.1444	5.009	2.510
7	21.259	3.283	0.1544	5.009	2.676

Table A.10 Raw data from ion exchange of pure water-NaCl samples.

Sample	Initial Na concentration (mmol/L)	Sample mass (g)	Mass of added resin (g)	Resin per sample (g/g)	Initial pH	Final pH
58	26.3	19.579	0	0	8.603	8.603
1	26.4	22.083	0	0	8.603	8.603
60	26.3	19.846	0.008	0.0004	8.603	3.324
59	26.3	19.754	0.010	0.0005	5.664	3.868
61	26.3	19.785	0.024	0.0012	8.603	2.867
40	26.4	19.677	0.107	0.0054	8.603	2.211
2	26.4	20.723	0.123	0.0059	8.603	2.147
63	26.3	19.823	0.120	0.0061	5.664	3.323
22	26.4	19.764	0.127	0.0064	8.603	2.166
64	26.3	19.814	0.145	0.0073	5.664	2.342
62	26.3	19.704	0.187	0.0095	5.664	2.170
23	26.4	19.716	0.253	0.0128	8.603	1.959
41	26.4	18.980	0.255	0.0134	8.603	1.959
3	26.4	19.579	0.317	0.0162	8.603	1.880
42	26.4	19.673	0.517	0.0263	8.603	1.837
24	26.4	19.484	0.518	0.0266	8.603	1.828
4	26.4	19.621	0.549	0.0280	8.603	1.791
5	26.4	19.851	0.667	0.0336	8.603	1.772
25	26.4	19.344	0.659	0.0341	8.603	1.791
43	26.4	19.932	0.680	0.0341	8.603	1.806
44	26.4	20.027	0.793	0.0396	8.603	1.795
6	26.4	19.857	0.791	0.0398	8.603	1.752
26	26.4	19.859	0.801	0.0403	8.603	1.778
27	26.4	20.003	1.020	0.0510	8.603	1.761
7	26.4	19.809	1.029	0.0519	8.603	1.742
45	26.4	19.740	1.098	0.0556	8.603	1.769
8	44.0	19.703	0	0	8.538	8.538
28	44.0	19.736	0.094	0.0048	8.538	2.224
46	44.0	19.839	0.116	0.0058	8.538	2.165
9	44.0	19.748	0.132	0.0067	8.538	2.101
29	44.0	19.110	0.226	0.0118	8.538	1.919
10	44.0	19.736	0.235	0.0119	8.538	1.888
47	44.0	19.814	0.261	0.0132	8.538	1.910
48	44.0	19.783	0.505	0.0255	8.538	1.739

Table A.10 Raw data from ion exchange of pure water-NaCl samples (continued).

Sample	Initial Na concentration (mmol/L)	Sample mass (g)	Mass of added resin (g)	Resin per sample (g/g)	Initial pH	Final pH
30	44.0	19.738	0.540	0.0274	8.538	1.700
11	44.0	19.217	0.549	0.0286	8.538	1.669
49	44.0	19.761	0.660	0.0334	8.538	1.685
31	44.0	19.829	0.683	0.0344	8.538	1.659
12	44.0	19.664	0.682	0.0347	8.538	1.646
32	44.0	19.783	0.808	0.0408	8.538	1.637
50	44.0	19.847	0.811	0.0409	8.538	1.654
13	44.0	19.745	0.816	0.0413	8.538	1.610
51	44.0	19.818	0.929	0.0469	8.538	1.636
14	44.0	19.600	0.983	0.0502	8.538	1.590
33	44.0	19.573	1.021	0.0522	8.538	1.601
15	61.6	19.696	0	0	8.353	8.353
65	61.6	6.350	0	0	8.353	8.353
66	61.6	19.872	0.008	0.0004	8.353	3.382
67	61.6	19.924	0.020	0.0010	8.353	3.460
34	61.6	20.147	0.115	0.0057	8.353	2.133
16	61.6	19.885	0.114	0.0057	8.353	2.133
52	61.6	19.932	0.139	0.0070	8.353	2.102
68	61.6	19.936	0.186	0.0093	8.353	2.159
53	61.6	19.956	0.240	0.0120	8.353	1.928
35	61.6	20.085	0.245	0.0122	8.353	1.887
17	61.6	20.056	0.266	0.0133	8.353	1.846
36	61.6	20.102	0.462	0.0230	8.353	1.693
54	61.6	20.141	0.504	0.0250	8.353	1.715
18	61.6	20.065	0.538	0.0268	8.353	1.640
37	61.6	20.096	0.653	0.0325	8.353	1.608
55	61.6	20.004	0.654	0.0327	8.353	1.630
19	61.6	19.977	0.694	0.0347	8.353	1.567
20	61.6	20.134	0.785	0.0390	8.353	1.557
56	61.6	19.957	0.796	0.0399	8.353	1.588
38	61.6	20.090	0.863	0.0430	8.353	1.557
57	61.6	19.954	1.003	0.0503	8.353	1.547
21	61.6	20.072	1.035	0.0516	8.353	1.504
39	61.6	20.180	1.047	0.0519	8.353	1.528

Table A.11 Raw data from ion exchange of wastewater samples.

Sample	Initial Na concentration (mmol/L)	Sample mass (g)	Mass of added resin (g)	Resin per sample (g/g)	Initial pH	Final pH
1	57.2	20.000	0	0	8.450	8.450
1	57.2	20.376	0.009	0.0004	8.450	8.168
1	57.2	20.350	0.130	0.0064	8.450	2.461
1	57.2	20.279	0.251	0.0124	8.450	2.099
1	57.2	20.730	0.490	0.0236	8.450	1.713
1	57.2	20.664	1.013	0.0490	8.450	1.375
1	57.2	20.567	3.886	0.1889	8.450	1.186
2	57.2	20.215	0.008	0.0004	8.450	8.179
2	57.2	20.185	0.122	0.0060	8.450	2.559
2	57.2	20.151	0.251	0.0125	8.450	2.031
2	57.2	20.068	0.502	0.0250	8.450	1.721
2	57.2	19.983	1.019	0.0510	8.450	1.574
2	57.2	19.853	4.445	0.2239	8.450	1.377
3	45.6	20.000	0	0	8.452	8.452
3	45.6	18.533	0.016	0.0009	8.452	7.442
3	45.6	18.479	0.103	0.0056	8.452	2.610
3	45.6	18.454	0.248	0.0134	8.452	2.046
3	45.6	18.387	0.486	0.0264	8.452	1.748
4	45.6	18.175	0.020	0.0011	8.452	7.108
4	45.6	18.151	0.098	0.0054	8.452	2.692
4	45.6	18.113	0.261	0.0144	8.452	2.025
4	45.6	18.030	0.501	0.0278	8.452	1.766
4	45.6	17.935	0.998	0.0556	8.452	1.535
4	45.6	17.815	5.250	0.2947	8.452	1.479

Table A.11 Raw data from ion exchange of wastewater samples (continued).

Sample	Initial Na concentration (mmol/L)	Sample mass (g)	Mass of added resin (g)	Resin per sample (g/g)	Initial pH	Final pH
5	27.9	20.000	0	0	8.818	8.818
5	27.9	18.973	0.020	0.0011	8.818	6.875
5	27.9	18.922	0.131	0.0069	8.818	2.348
5	27.9	19.056	0.275	0.0144	8.818	1.922
5	27.9	18.973	0.514	0.0271	8.818	1.738
5	27.9	18.891	1.013	0.0536	8.818	1.600
5	27.9	18.791	5.366	0.2856	8.818	1.501
6	27.9	19.675	0.008	0.0004	8.818	8.109
6	27.9	19.630	0.107	0.0055	8.818	2.477
6	27.9	19.585	0.242	0.0124	8.818	2.039
6	27.9	19.499	0.495	0.0254	8.818	1.856
6	27.9	19.433	1.073	0.0552	8.818	1.722
6	27.9	19.348	4.430	0.2290	8.818	1.698